DRUG DELIVERY SOLUTIONS FOR THE

POTENTIAL TREATMENT OF CHILDHOOD OCULAR CONDITIONS

DRUG DELIVERY SOLUTIONS FOR THE POTENTIAL TREATMENT OF CHILDHOOD OCULAR CONDITIONS

By FRANCES LASOWSKI, B.Eng.Biosciences

A Thesis Submitted to the School of Graduate Studies in Partial Fulfilment of the Requirements for the Degree Doctor of Philosophy

Doctor of Philosophy (2019) McMaster University

Chemical Engineering Hamilton, Ontario

TITLE: Drug Delivery Solutions for the Potential Treatment of Childhood Ocular Conditions

AUTHOR: Frances Lasowski, B.Eng.Biosciences (McMaster University)

SUPERVISOR: Professor Heather Sheardown

NUMBER OF PAGES: xxii, 178

Lay Abstract

Sustained ocular drug delivery is critical to minimize side effects, maximize compliance and improve the clinical outcomes experienced by the patient. This is particularly true in pediatric applications, such as retinoblastoma and myopia. The objective of this thesis is to create drug delivery systems that could be used to treat these childhood conditions, with a focus on non-invasive delivery technologies.

In this project, contact lenses are explored as drug delivery vehicles for two drugs which can be used to treat retinoblastoma and myopia. Multiple materials and drug loading are explored to create a sustained drug delivery system that meets the needs of these conditions. This is then expanded into examining systems that fit within current commercial manufacturing practices, creating a delivery system that meets the demands of the disease and industry.

Alternative delivery systems that could be utilized as inserts are also explored. A lipid based system, whose materials are native to the body, are explored as a unique system capable of delivering drugs in a controlled fashion under specific hydration and temperature conditions. Alternatively, a silicone-based system is explored, whose unique chemistry eliminates many of the prohibitive biological side effects seen with these materials, allowing for a sustained drug delivery system for these ocular conditions.

Abstract

Ocular drug delivery remains a challenge due to the anatomical and physiological barriers of the eye. Topical drops have poor penetration and side effects, and injections are highly invasive; an alternative approach is transscleral delivery. Sustained drug release systems utilizing this delivery pathway are non-invasive yet provide extended treatment periods with single doses. Specifically, such systems would be beneficial for treating pediatric populations for diseases such as retinoblastoma and myopia. A chemo-preventative treatment for retinoblastoma, a childhood ocular cancer, has been proposed utilizing CdK inhibitors such as roscovitine and R547. Myopia, a more common, chronic condition in children, can be treated with atropine, though the dosing must be tightly controlled. Three novel delivery systems have been developed in this work to deliver these drugs, generating potential treatment platforms for these conditions.

Contact lenses have been investigated previously to deliver various therapeutics, as they act as a slow, equilibrating reservoir, and the prolonged corneal residence time improves bioavailability. Silicone lenses, with their ability for continuous wear, have been explored looking at various material compositions and drug loading levels and techniques to confirm the feasibility of this system for these conditions (Chapter 2). This work has been extended to include covalent tethers for roscovitine, ensuring that it is able to survive a more commercially-relevant synthesis and providing additional ways to tailor the drug release profiles (Chapter 3).

Alternatively, amphiphiles, which can self-assemble in the presence of excess water, have been explored for their drug delivery potential. Novel materials consisting of oleoylethanolamide and linoleoylethanolamide were developed to exhibit cubic phase transitions at physiologically relevant conditions, and their subsequent drug release characteristics were explored (Chapter 4). Silicone-based materials have broad usages as biomaterials, and a novel approach of incorporating PEG into the material without the use of metal catalysts were explored (Chapter 5). These exhibited a significant reduction in protein fouling, and material compositions were further iterated on, and their subsequent drug delivery capabilities were examined (Chapter 6). Overall, these three approaches have been able to successfully delivery roscovitine, R547 and atropine in non-invasive manners that have the potential to be an appropriate treatment for the childhood conditions they are intended to treat.

Acknowledgements

The list of people to thank over this long (yet wonderful) journey are far too numerous to list without this becoming the most prolific part of my thesis. I am grateful to all of you, as I would not have been able to get through the many (many) years without all of your love, support and encouragement, and I will be forever grateful.

First and foremost, I would like to thank my supervisor, Dr. Heather Sheardown. I feel very fortunate to have had such a positive, supportive supervisor and I am grateful for the guidance, advice and the freedom to pursue my varied interests (both within and outside the lab). I am very grateful for the many exceptional opportunities I was afforded in your lab over my degree, and am thrilled to continue to work with you toward our common passion to improve vision for patients. As I've often said, I would not have been able to finish a PhD with any other supervisor (though even you may have started to question the timing!).

Thank you to my committee members, Dr. Lyndon Jones and Dr. Judy West-Mays. I appreciate your helpful suggestions throughout my degree and for challenging me to think about my research in different ways. I think I enjoyed my committee meetings far more than the average student, and thank you for that. Lyndon I'm ticking the box! Thank you to Sharon and Minoo for supervising me in Australia- working with you was an enriching experience and I learned a great deal. It was a wonderful way to start my graduate education. Thank you to Kirk Green for tolerating my many LCMS samples and troubles!

I would like to thank all of the Sheardown group members I have had the pleasure of working with over the years. We have had so much fun and you have all made my time in graduate school and in the lab enjoyable and memorable. Specifically to Scott, Marta and Laura- I learned how to do research from you, and am grateful for that sound education every day. Thank you to Lina for always taking the time to help me (both in and out of the lab) and keep everything in the lab functioning- we are all grateful. I realize now I have learnt from the best (Bahram I am by far the most diligent HPLC user our lab has) and am so grateful to have had that opportunity. Vida, I am happy that our work together has book ended your time in the lab, starting as a volunteer and ending as a post-doc, all while I've been working on my PhD. I have loved working with you and am excited we can be baby buddies together. Myrto, Giuliano, Ivana, Alysha, Megan- coming through grad school with you guys has been a joy, and I appreciate you walking me off the ledge many times. To my summer students, thank you for your enthusiasm and help. Ben, we have been here together the longest, and I am grateful for your friendship, understanding and patience. You are a wonderful travel companion and gate builder, and we are lucky to have you and Natasha as friends. I am excited to continue to work with you knowing that you're always up for anything I need (including running ill-fated races). Talena, I am thrilled to have been

able to collaborate with you during our PhDs (and during your post-doc!) and could not be happier to share an office with such a great friend. Your willingness to always lend a hand is appreciated (both in the lab and with our little ones), proving good help can be found (but it is tough!). You have proven this over and over to the very end ☺

I am so grateful to all the friends I have made at McMaster over my time in graduate studies. Ashley, Steve, Aaron, Kyla, Daryl (and all the others I can't list because it's getting long!), it has been a fun 10 years and you helped make graduate school an unforgettable experience, thank you for always being there to talk (or go to the Phoenix) when needed! Special thanks to Steve, Megan and Sumo- despite me still being in school long after we graduated, our time together has saved me a lot of therapy. I love you all and I couldn't be happier to see where our lives have ended up over the last decade. Thank you to Michelle, Tina, Jess (and Jill) who have always checked in and helped in any way they could- I could not ask for better friends.

Thank you to my parents, Frank and Rosanne, for all of the love and support, for always inspiring me to reach for the stars and for always believing in me (even when you're not sure what I do). I have been privileged to have you as parents and am eternally grateful for all of the opportunities you have given me (and continue to be for all of the time you watch Charlee even as I finish this thesis). You can finally stop asking when I will get a real job. Thank you to Joseph and Olivia- while I'm sure you've questioned many times how I'm still in school, I appreciate your endless love, support and encouragement. Special thanks to my extended family, for always being willing to help with Charlee to allow me to finish work or drop off eyeballs with cookies (Coici B!)- it is a blessing to be part of this group.

Last but certainly not least, all my love to my husband Kyle. Your support, quasi patience and understanding have meant the world to me. Your willingness to help, even when you're not sure what will help, and for being understanding when I am busy or have taken over part of the house/apartment has meant so much (especially during my comps). I know you have always listened to me and let me vent, and I am blessed to have you in my life. You help me strive to be the best version of myself and I am grateful to be married to someone who encourages me to follow my passion and dreams. I love you with all my heart and soul. While neither of us run the show anymore, I could not have asked to parent with a better partner, and appreciate all of your help with Charlee as I've worked to finish my degree. Charlee, you've taught me patience and the ability to multitask even against all odds, and I have borrowed a page out of your stubbornness guide to finish this up. Kyle I am thrilled for our little cashew of joy on the way, providing that extra motivation to finish my degree (this time). Super excited to meet you in February Baby Lake 2!

Table of Contents

List of Figures

List of Tables

List of Abbreviations and Symbols

ANOVA	Analysis of variance
BSA	Bovine serum albumin
CuAAC	Copper catalyzed azide-alkyne click
$CDCl_3$	Deuterated chloroform
CdK	Cyclin-dependent kinase
CYC202	Roscovitine
D_2O	Deuterated water
D_4	1,1,3,3,5,5,7,7-Octamethylcyclotetrasiloxane
DCM	Dichloromethane
DMA	N,N-dimethylacrylamide
DIC	diisopropyl carbodiimide
DLS	Differential light scattering
DMAP	4-dimethylaminopyridine
DMSO	Dimethylsulfoxide
DSC	Differential scanning calorimetry
EGDMA	ethylene glycol dimethacrylate
EWC	Equilibrium water content
G’	Storage modulus (elastic modulus)
G’’	Loss modulus (viscous modulus)
^{1}H NMR	Proton Nuclear Magnetic Resonance Spectroscopy
HCl	Hydrochloric Acid
HEL	Hen egg lysozyme
HPLC	High-performance liquid chromatography
IPA	Isopropyl alcohol
IR	Infrared spectroscopy
Lac0/Lac0x	Zero unit lactide spacer
Lac2/Lac2x	Two unit lactide spacer
Lac10/Lac10x	10 unit lactide spacer
LEA	Linoleoylethanolamide
LC/MS	Liquid chromatography mass spectrometry
LVE	Linear viscoelastic
MeOD-d4	Deuterated methanol

mol	Mole
Mn	Number average molecular weight
MTT	3-(4,5-dimethylthiazol-2-yl)-2,5-diphenyltetrazolium bromide
MW/MWt	Molecular weight
Mw	Weight average molecular weight
NaOH	Sodium hydroxide
NMR	Nuclear magnetic resonance
OEA	Oleoylethanolamide
PBS	Phosphate Buffered Saline
PDI	Polydispersity index
PDMS	Polydimethylsiloxane
PEG	Poly(ethylene glycol)
PEGMA	Poly(ethylene glycol) methacrylate
PEO	Poly(ethylene oxide)
Pt	Platinum
RB	Retinoblastoma
Ros	Roscovitine
RTV	Room-temperature vulcanization
SAXS	Small angle x-ray scattering
Suc	Succinic anhydride
TBA	Tert-butanol
TEM	Transmission electron microscopy
TRIS	3-methacryloxypropyltris (trimethylsiloxy)silane
TRIS-OH	3-(3-methacryloxy-2-hydroxypropoxy) propylbis(trimethylsiloxy)methylsilane
UV	Ultraviolet
w/w	Weight percent by weight
wt	Weight

Declaration of Academic Achievement

Published Manuscripts

1. Fitzpatrick, S.D.; Mazumder, M.A.J.; **Lasowski, F**., Fitzpatrick, L.E., Sheardown, H. "PNIPAAm-Grafted-Collagen as an Injectable, In Situ Gelling, Bioactive Cell Delivery Scaffold," *Biomacromolecules*, **2010**, 11, 2261-2267.

2. Wells, L.A.; **Lasowski, F**.; Fitzpatrick, S.D.; Sheardown, H. "Responding to Change: Thermo- and Photoresponsive Polymers as Unique Biomaterials," *Critical Reviews in Biomedical Engineering*, **2010**, 38, 487-509.

3. Rambarran, T.; Gonzaga, F.; Brook, M.A.; **Lasowski, F.**; Sheardown, H. *"*Amphiphilic Elastomers from Metal-Free, Click Crosslinking of PEG-Grafted Silicone Surfactants,*" Journal* of *Polymer Science Part A: Polymer Chemistry*, **2015,** 53, 1082-1093.

4. **Lasowski, F.**; Sheardown, H. "Atropine and Roscovitine Release from Model Silicone Hydrogels," *Optometry and Vision Science*, **2016**, 93, 404-411.

5. Princz, M.A.; **Lasowski, F.**; Sheardown, H. "Chapter 16- Advances in intraocular lens materials." *Biomaterials and Regenerative Medicine in Ophthalmology (Second Edition)*, 2016, 401-417.

Preface

In accordance with the guidelines for the preparation of a doctoral thesis set forth by the McMaster University School of Graduate Studies, this work has been prepared as a sandwich thesis. The majority of the work described in this thesis was conducted, interpreted, and written by the author of this thesis. On the first page of each body chapter, a footnote contains a breakdown of each author's contribution to the multi-authored chapters. The work for the five body chapters was completed between 2009 and 2018, over the course my graduate degree. With the exception of Chapter 5, I led the investigations described in these chapters, performed most of the experimental work, wrote the first draft of all of the work and helped with editing and responding to reviewers' comments. With the exception of Chapter 5, I was first author on all of the published work and will be first author on the remaining work when submitted that is included in this thesis. Chapter 5 is an exception, as I am a fourth author, and is included in the thesis to support Chapter 6, which is a continuation of the work in Chapter 5. Co-authors were acknowledged when they helped or conducted an experiment that contributed to the research project, for helpful discussion or for being in a supervisory role.

1. Introduction

There is a current need for novel, non-invasive ophthalmic treatments to treat a variety of ocular ailments. While some new treatments will come in the form of new therapeutics, there is an opportunity to improve therapies and clinical outcomes by creating drug delivery systems that work together with the therapeutic to treat the condition. While all patients would benefit from these products, pediatric patients who suffer from diseases such as retinoblastoma and myopia would be particularly aided, as current treatments are unable to effectively treat their conditions.

1.1. Retinoblastoma

Retinoblastoma (RB) is the most common intraocular malignancy in children, affecting about 1 in 20,000 children [Brantley 2001, Pacal 2006] before the age of 5. [Bremner 2014] RB appears as a yellow-white mass in the retina, often surrounded by dilated blood vessels. The primary factors believed to contribute significantly to RB are the mutations on the Rb gene, which results in a dysfunctional or compromised Rb protein, and additional mutations in other regulatory proteins. Combined, these two conditions result in an improper exit from the cell cycle and ultimately improper terminal differentiation. [Pacal 2006, Chen 2004, DiCiommo 2000] While the retinal cells are the most common target for RB, it is possible to have tumour cell growth into the vitreous cavity, choroid, optic nerve and even the anterior of the eye. [Harbour 2001]

RB is often described by two genetic forms, referred to as somatic/non-heritable RB and germline/heritable RB. About 40% of RB cases are heritable, indicating the presence of a "null" retinoblastoma (Rb) allele that requires only one additional mutation for tumour development. [Brantley 2001, DiCiommo 2000] These patients often develop bilateral, multifocal tumours, transmit the defect to their offspring in an autosomal-dominant fashion [Harbour 2001] and tend to succumb to subsequent malignant neoplasms [Brantley 2001, Yu 2009] since all of their cells have this deficiency. It is this population that the proposed therapy aims to treat, as only 1% of the children who carry the mutation do not develop retinoblastoma tumours. [Dimaras 2012]

Based on a postulated "two hit" hypothesis stemming from the work of Knudsen [1971] and Comings [1973], the genetic mutation creates an environment whereby retinal cells are unable to terminally differentiate at the appropriate time. While the molecular interactions that control this progression are complex, they ultimately rely on activating E2fs [Wu 2001] and CdK1 or CdK2 [Santamaria 2007]. Despite the complex crosstalk between the axes, activation of only one axis provides limited ectopic division, as E2f and Cdk2 activity are both required for sustained division; this was demonstrated in Drosophilia [Buttitta 2007]. Limited pharmacological options make the reduction of the E2f axis difficult, however many Cdk inhibitors are currently in clinical trials. [Stadler 2000] This could be used to lower this axis and prevent the formation of the RB pathology, though an inhibitor must be chosen carefully due to complex biological substitutions.

The Bremner group at the University of Toronto has been exploring options for an appropriate Cdk inhibitor, which could be used as a chemopreventative agent, and have suggested roscovitine (CYC202) and R547 as agents for further exploration. [Bremner 2010, Sangwan 2012] This treatment protocol requires a local drug delivery system to minimize systemic exposure to the drugs, as they would have highly detrimental impacts to developing infants. However, it remains uncertain what the exact human dosing requirements would be. Furthermore, a minimally invasive approach is preferred, as the children will be very young when treated and intravitreal injections are used cautiously in these populations due to fears around tumour seeding. [Brantley 2001, Shields 2012]

1.2. Myopia

Another clinical disease with profound impacts in children is myopia. A much more common condition than retinoblastoma, this can affect over 85% of some populations, and in high myopia, there is an increased risk of visual impairment and blindness. [Ganesan 2010] While the cause of myopia is not understood, it is believed to have both genetic and environmental influences. [Ostrow 2010] Atropine has been studied since the 1970s as a pharmacologic means to arrest the disease. It is believed that atropine has a biochemical effect on the retina or sclera that causes remodeling of the sclera associated with eye growth, [Chia 2009] thus allowing it to exude an effect on the overgrowth associated with myopia. While this therapy shows some success, concentrations must be tightly controlled to reduce side effects. [Shih 1999] These side effects are typically associated with dilated pupils, resulting in the children having light sensitivity and impaired vision for periods of time; this greatly affects their lives and limits who is

willing to use this treatment. Additional complications, such as growth upon treatment completion, [Ostrow 2010] further limit its effectiveness. Recently, low dose atropine has been demonstrated to also be effective. [Chia 2012] This suggests that a delivery system capable of delivering small amounts of atropine, which would substantially reduce side effects experienced by patients, could help minimize the burden associated with this disease. Again, this system would have to be minimally invasive and capable of sustained release over a long period of time to facilitate patient compliance for this chronic condition.

1.3. Ocular Drug Delivery

Ocular drug delivery is challenging due to the anatomical and physiological barriers of the eye, as well as patient barriers, such as comfort and compliance. As with most drug delivery, the aim is to create a system that allows for the controlled release of the drug within the therapeutic window, while eliminating the periods of under-dosing and overdosing shown in Figure 1.1. This minimizes side effects while ensuring a sufficient therapeutic amount of drug for the treatment of the disease, and simultaneously reduces the number of doses required to increase compliance.

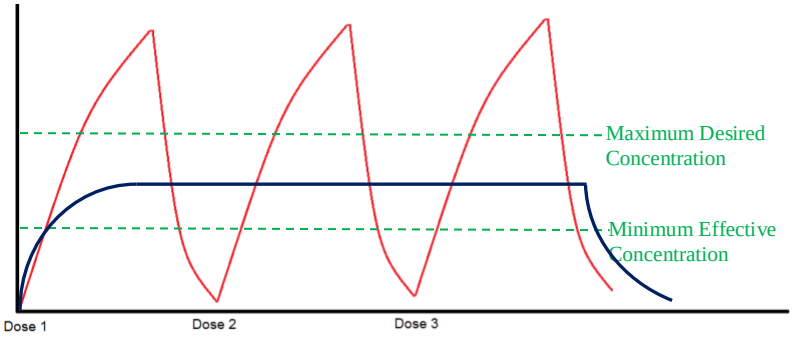

Figure 1.1: Controlled drug release with one dose, shown by the blue line, contrasted with traditional multi-dose drug delivery shown in the red line.

Currently, topical ocular delivery treatments are preferred for many applications, as they are regarded as safe, convenient, non-invasive and able to be self-administered. However, they suffer from challenges due to both anatomical and patient barriers and are particularly challenging for posterior eye applications. For instance, much of the drug is eliminated upon installation due to drainage. In particular, the cul-de-sac typically holds 7-10µL but a typically drop is about 30µL. [Mitra 1996] Even if topical applications reach therapeutic concentrations in the anterior segment, the posterior segment shows substantially less efficient penetration. [Shah 2010] This is due to the complex pathway for penetration, which is shown in Figure 1.2.

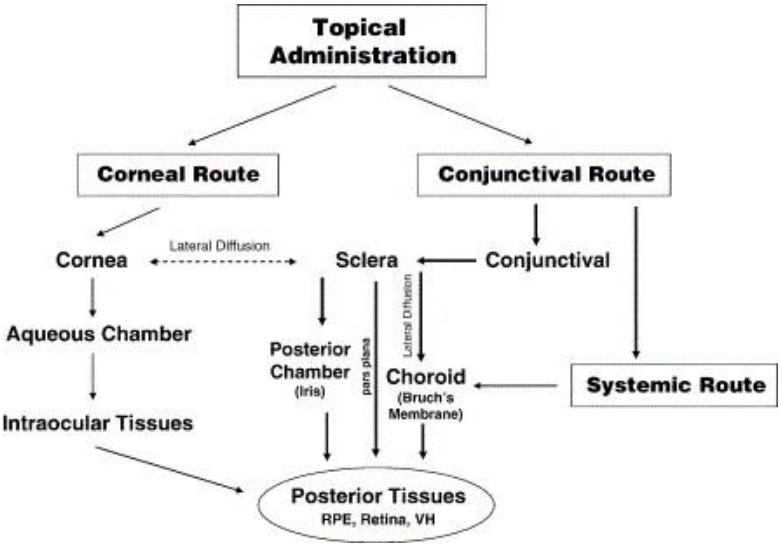

Figure 1.2: Drug distribution pathways following topical administration [Taken from Hughes 2005].

Drugs must penetrate the tight junctions of the cornea and avoid elimination by the vascularized conjunctiva. [Sasaki 2009, Mitra 1996] Drugs can penetrate the eye through transcellular or paracellular routes, determined predominantly by their hydrophilicity or lipophilicity and their size. While transcellular transport mechanisms include simple diffusion, facilitated diffusion, active transport or endocytosis, paracellular transport is passive and limited by the size and charge of the intercellular space. [Mitra 1996] The conjunctiva tissues were shown to be more permeable to various MW PEGs and less dependent on molecular size than the cornea, owing to its larger pores and greater pore density. [Hamalainen 1997] Furthermore, the penetration for each tissue differs substantially for different molecules, [Hughes 2005] suggesting that modelling is a complex endeavour. It is known that many epithelial and endothelial cells contain tight junctions which restrict the paracellular movement of small hydrophilic compounds, and

the retinal pigmented epithelium prevents the movement of polar molecules from the choroid. [Hughes 2005] As is relevant for therapeutics like roscovitine, R547 and atropine, the RPE-choroid has been suggested to be the rate-limiting barrier, followed by the conjunctiva or sclera, for passive transcellular transport of hydrophobic drugs. [Hughes 2005]

Given these challenges, many different delivery systems have been developed for ocular applications. Viscosifying agents have been added to topical liquid applications to increase their ocular surface conjunctival cul-de-sac residence time, [Lee 1986, Trueblood 1975] though these have had limited success alone; however their pairing with mucoadhesive agents have yielded increased penetration and efficacy. [Greaves 1993, Saettone 1999] Similarly, emulsions can provide a slower release rate but often cause blurred vision for the patients. [Dave 2012] Vesicle-based delivery systems, such as micelle, liposomal and niosomal formulations, have been explored, though they are known to be expensive, difficult to produce and have limited loading. [Dave 2012] However, niosomes are showing to be more stable and more economical. [Kaur 2004, Pham 2012] Particulate systems, such as nano- and microparticles, have been synthesized from a range of polymers to entrap or bond drugs, though they can easily be washed away without being paired with a mucoadhesive polymer [Dave 2012] or within another delivery system like gel or suspension. [Choy 2008] In situ gelling systems can also increase the residence time of drugs on the ocular surface. [Rathore 2010] While these topical-based systems have potential for numerous applications, they still require

relatively frequent dosing and may not be able to reliably deliver low doses; this is not favourable for conditions like retinoblastoma or myopia.

Alternatively, ophthalmic inserts are another method of drug delivery within the eye. These can include degradable and non-degradable systems, such as contact lenses, punctal plugs, scleral plugs, devices placed in conjunctival cul-de sac and intravitreal implants, and allow controlled release over a long period of time, limiting the number of applications required. [Ghate 2006, Dave 2012] While intravitreal injections are common in clinical settings, allowing a higher dose to reach the target site with a single treatment, it is highly invasive and carries significant risks. This has rendered it inappropriate for retinoblastoma and myopia treatments.

These limitations have led to transscleral delivery, which utilizes the avenues of retrobulbar, peribulbular, sub-Tenon's, subconjunctival or conjunctival cul-de-sac delivery. [Shah 2010, Gaudana 2010] Although normally requiring an injection, this does not necessarily penetrate the globe and a sustained device on the scleral surface could also be considered. Transscleral delivery is attractive, as the large scleral surface area and relatively high permeability, compared to the cornea, make it attractive for compounds which may have to enter the back of the eye. [Lee 2004] While many barriers still exist with transscleral delivery, such as the permeability and clearance of the drug, with the appropriate therapeutic, this method could provide successful sustained delivery with infrequent or single dosing, without the complications or invasiveness associated with intravitreal injections. Furthermore, based on the location of the device, such as

conjunctival compared to peribulbar placement, the systemic absorption could also be controlled. [Geroski 2001] Therefore, this has been the avenue explored within this thesis.

1.3.1. Contact Lens Delivery

Contact lenses have been investigated previously to deliver various therapeutics, [Peng 2012, Bajgrowicz 2015, Phan 2016, Dixon 2018] as they act as a slow, equilibrating reservoir and the prolonged corneal residence time improves bioavailability. [Schultz 2011, Gupta 2012] This is important, as many drugs delivered as eye drops have only about a 5 minute residence time, and thus only 1-5% of the drug penetrates ocular tissue. [Kim 2008] The lenses themselves should be capable of sufficient drug loading, zero order release and stability. [Schultz 2011] As well, with the advent of silicone extended wear lenses, whose oxygen permeability is sufficient to be worn overnight and up to 30 days, and the increased prevalence of these lenses in the market, [Morgan 2011] the option to use contact lenses for continuous drug delivery is emerging. This is particularly relevant for the applications of retinoblastoma and myopia, where continuous drug release is needed.

The advantage of drug loaded contact lenses stems from the drug's increased residence time on the eye and improved safety profile. Specifically, a drug loaded lens placed on the cornea allows diffusion of the therapeutic to both the post-lens tear film and the pre-lens tear film, and the use of soft contact lenses has been shown to prevent mixing of these two layers, slowing the drainage of the tear fluid trapped beneath the lens that is in contact with the corneal surface. [Creech 2001, McNamara 1999]. These two factors

increase the residence time of the drug with the corneal surface and maintain a high concentration gradient driving diffusion into the tissue, which has been shown to substantially boost drug bioavailability [Li 2006, Peng 2012]. Given these benefits, the amount of drug required for a therapeutic effect is substantially reduced, [Peng 2012] lowering the amount of drug that enters systemic circulation and presumably minimizing side effects. Additionally, patience compliance would be improved with a lens-based system, as they do not require frequent dosing. All of these factors would work well in a treatment regime for retinoblastoma or myopia.

Contact lenses for drug delivery have historically been limited by insufficient loading or release, due to the limits of drug solubility and partitioning, or the lack of controlled release, often presenting with a burst release profile and short release duration. [White 2010] However, through greater understanding of polymer networks, the rational design of hydrogels is possible, which are better able to control release kinetics and capacity. These can include diffusional barrier incorporation [Kim 2010], molecular imprinting [Guidi 2014], particle entrapment [Gulsen 2005], functionalized monomer with drug affinity [Alvarez-Rivera 2018] and the incorporation of wetting agents [Korogiannaki 2015]. Furthermore, various methods to load the drug and various material components can also contribute to improved drug delivery profiles. [Hui 2008] These various techniques can be explored and optimized for the specific delivery of roscovitine and atropine.

1.3.2. Other Materials Used in Ocular Drug Delivery

While contact lenses, either as conventional or silicone hydrogels, are one type of material used for ocular drug delivery, there are numerous other options. This is true even within transscleral delivery systems specifically. While all of these materials have advantages and disadvantages, self-assembling amphiphilic materials and silicone-based materials were chosen for exploration within this thesis and further introduced here. This selection was primarily based on the available expertise within the Sheardown lab and its collaborators, though many other groups are exploring the same material types for various drug delivery applications.

1.3.2.a. Self-Assembling Amphiphilic Materials

Amphiphiles are molecules which contain both hydrophilic and hydrophobic domains, allowing them to self-assemble into aggregates, generally in an attempt to minimize the hydrophobic components' interaction with the water solvent. [Kaasgaard 2006] While the phase behaviour and self-assembly of these molecules has historically been examined to understand their role in biomembranes, more recently their role in controlled drug delivery, particularly from the bicontinous cubic phase, has been explored. [Sagnella 2009, Huang 2018] While there are numerous types of amphiphiles that demonstrate this behavior, materials derived from endogenous unsaturated monoethanolamide lipids [Sagnella 2010A] were of particular interest for ocular drug delivery applications, as variations of these materials exhibited cubic phase formation

around physiological conditions and similar materials had shown low toxicity in in vitro cell studies [Sagnella 2010B].

These materials are attractive for drug delivery for a variety of reasons. First, due to the amphiphilic nature of the lipids that make up these materials, it is possible to encapsulate hydrophilic, hydrophobic and amphiphilic therapeutics, including bioactive species such as proteins. [Tyler 2015] Specifically, hydrophilic therapeutics are accommodated within the aqueous pores, hydrophobic therapeutics within the lipid bilayer and amphiphilic therapeutics at the interface. [Conn 2013, Huang 2018] Additionally, these are highly ordered structures which contain a large surface area of the lipid/water interface, [Angelov 2003] allowing for adjustable parameters for subsequent drug release, and a material structure that can partially adapt to accommodate therapeutics, like proteins, which can prevent them from denaturing [Conn 2013]. Furthermore, these bicontinous cubic phases can be dispersed into sub-micro particles, known as cubosomes, which can be used with stabilizers to both stabilize the particle and limit immunogenic responses. [Conn 2013]

The phase behaviour of these materials is affected by many factors, including temperature, pH, light and water content; therefore, drug delivery can be also be controlled by altering these factors. [Kaasgaard 2006] Specifically drugs are most quickly released from lamellar phases, then cubic phases, then hexagonal phases and finally micellar cubic phases. [Huang 2018] While some drug release has shown to conform to Higuichi diffusion kinetics, the release rate of solubilized drugs are related to many factors, such as the polarities of the drug, molecular weight of the drug and the internal

structure of the material; it has been shown theoretically and experimentally that drug diffusion kinetics depend in a complex way on the geometry. [Huang 2018] Therefore, both the material and drug must be considered together to create a feasible drug delivery system.

1.3.2.b. Silicone-based Materials

Silicones have been widely used in medical applications owing to their excellent biocompatibility and biodurability in many applications. This is a consequence of their unique properties; particularly their flexibility, high gas permeability, low surface tension and good chemical stability, which make them excellent candidates for biomaterials. [Colas 2013] Given their low glass transition temperature, silicones are stable during high-temperature sterilization and their permeability is beneficial for both wound healing and drug delivery; this is apparent in their increased usage as a contact lens material.

While silicones are incredibly versatile, their high surface hydrophobicity makes them, like all hydrophobic implants, susceptible to being quickly coated in protein upon contact with the body and biological fluids, [Chen 2008] which can compromise their drug delivery performance or cause device failure. This failure is commonly seen in biosensing applications, where drug delivery of corticosteroids has been used with moderate success to prolong the life of biosensors, [Norton 2007] such as dexamethasone release from a silicone gel. [Ward 1999] Therefore, modifications are necessary to improve protein interactions, including passivating the surface to minimizes non-specific protein binding. This is often accomplished by the presence of wetting agents, such as

poly-ethylene glycol (PEG), which are used to increase the hydrophilicity of the surface, reducing protein adhesion. However, in order to adhere PEG to PDMS, the PDMS, modification methods must be developed, as pure PDMS does not have a functional group handle present to easily modify the surface.

A variety of techniques to modify PDMS have been developed. For example, PEO was grafted to the surface with one step chemistry using hydroxyl-modified PDMS (PDMS-OH) by Chen et al. [2004]. However, this resulted primarily in a surface modification, and bulk modifications are also required to have a positive impact for drug delivery applications. Furthermore, many of these modifications require the use of a metal catalyst or have the potential for side reactions, which results in additional processing to remove these impurities. [Jankowiak 2005] Therefore, simple modifications methods which are able to improve the properties of silicone materials while minimizing protein fouling would be of great interest for drug delivery applications in the eye.

1.4. Thesis Objectives

The objective of this work is to create a sustained ocular drug delivery system that could be useful in treating childhood conditions such as retinoblastoma and myopia. In order to treat these conditions, three therapeutics will be examined. For retinoblastoma, the CdK inhibitors roscovitine and R547 will be used. Atropine will be used for myopia. The structures of these drugs are shown in Figure 1.3. It is known that a low dose is needed for all of these compounds, as the CdK inhibitors have chemotherapeutic properties at higher doses and atropine use, even at conventional doses, lead to vision-

impairing side effects such as light sensitivity. Therefore, the delivery system must be capable of delivering low, consistent doses that ideally cannot be adversely impacted by patient/caregiver error.

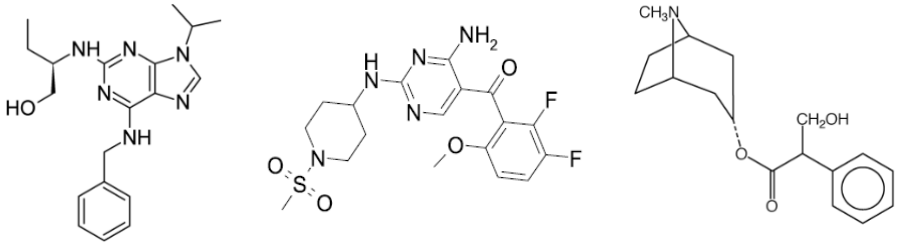

Figure 1.3. Structure of molecules: Roscovitine (cyc202) on left, R547 in middle, Atropine on right.

Since this treatment is intended for use in infants (for retinoblastoma) and children (for myopia), the delivery system must be appropriate for use with this type of population. Specifically, frequent repeated dosing would be difficult, so a sustained delivery system capable of multiple day or week delivery would be preferred. However, minimally invasive systems would be necessary, given the pediatric population, and particularly the risk of tumour seeding in retinoblastoma and the need for chronic treatment in myopia. Given these limitations, it is unlikely that a topical application, such as an eye drop, would be effective nor would an intravitreal injection be warranted or desired. However, a transscleral approach could meet all of these requirements. This would allow for extended drug delivery from a material reservoir that could be placed in a minimally-invasive fashion by a physician or caregiver, depending on the nature of the device. Given the device's known release kinetics, the patient dosing would not be subjected to compliance issues and could exert the greatest therapeutic benefit with the fewest side

effects. However, it is critical to completely understand these release kinetics to ensure patient safety, as both of these therapies will have side effects if extra drug is given.

Therefore, the hypothesis is that understanding the hydrophilic/hydrophobic interface is critical to the creation of an appropriate sustained release system. This stems from the belief that the drug will interact with the material, and that interaction will dictate the drug loading, release kinetics and ultimately determine the success or failure of the system. Given the varied characteristics of the drugs explored for these conditions, it is expected that they will interact differently with the materials, however, most of this interaction will occur at the interfaces of the materials or its internal domains. For this reason, experiments that are able to determine which variables exert the greatest impact on these interfaces and how this subsequently impacts the drug release profiles are necessary.

Given this hypothesis, two aims came from this work. The first was to investigate silicone hydrogel materials as a potential drug delivery system, determining the ideal parameters for the release of these therapeutics. The second aim was to explore other potential materials that could be used as a transscleral delivery system, evaluating their potential for this pediatric application.

1.4.1. Thesis Aim I: Ideal Parameters for Silicone Hydrogel

Given the expertise in the Sheardown lab with model contact lenses and drug delivering lenses, exploring silicone hydrogels for this application was a natural initial starting system. Contact lenses, or contact lens-like materials, which could also be fit as

scleral lenses or used in the cul-de-sac, could be fit on patients and remain in place for numerous weeks, providing a continuous dose of drug. Since they would be placed on the ocular surface for weeks at a time, the risk of contamination would be minimized. For retinoblastoma particularly, given the young age of the children and the lenses' status as a therapeutic-incorporated device, they could be placed by a medical professional in a controlled setting, making this safe and convenient for both patient and parents. Only silicone hydrogels were examined as both of these applications would require continuous dosing, which would require continuous wear of the device. Since only silicone hydrogels are approved for continuous wear, this became a key limitation to the materials explored.

1.4.1.a. Chapter 2: Model Lens Loading

Chapter 2 examines model silicone contact lens systems for the delivery of atropine and roscovitine. While this is presented as contact lenses, it could easily be extended to other scleral material modules if that was preferred by the clinician. The objective was to determine how the material properties and drug release were impacted by the incorporation of different monomers (DMA, TRIS, TRIS-OH) and different drugs into the polymer material. These materials would reflect the compositions of commercial lenses, allowing for simpler transitions to commercial formulations, but would enable a more thorough study of the impact of individual parameters than could be afforded using existing contact lenses. Specifically, by self-fabricating, it would be possible to determine the impact of various material compositions and drug loading techniques, variables which could not be altered using pre-formed commercial lenses. This would allow deliberate

alterations to the hydrophobic and hydrophilic character of the material, facilitating the exploration of how these interfaces impact the drug loading and release. This was also an opportunity to determine if the drug impacted critical lens properties, such as water content or transparency, which would compromise its usefulness in a clinical application.

1.4.1.b. Chapter 3: Covalent Drug Incorporation

Building on the observations of Chapter 2, which concluded that sustained delivery was feasible from silicone hydrogels for these applications, it was desired to create a system that had additional mechanisms to control the release and would be more translatable to an industrially relevant synthesis process. Again, while presented as a contact lens system, this material could reside elsewhere on the anterior ocular surface. Specifically, silicone hydrogels undergo an extraction process, and while direct loading of the hydrogels had shown most effective in the Chapter 2 studies, this extraction would likely compromise the drug loading if it were to be applied commercially. Furthermore, the release shown in Chapter 2 primarily involved simple diffusion kinetics from the materials, however it was desired to have an additional opportunity to control the release kinetics, at least in part, to be sure that this system could meet a specific delivery target, which at the time was not known. It was hypothesized that the drug could be bound to a liable tether, which would be covalently bound to the lens material during synthesis. This would protect the drug during the extraction process, and the degradation of the tether would provide an additional point of control for the drug release kinetics. Such a system could utilize tethers of various lengths or compositions to create a carefully controlled

release profile, which could be tightly matched to the clinical dosing need. Additionally, this covalent system would enable the use of material compositions whose bulk properties were more desired, but whose interfacial interactions yielded poorer drug release kinetics in the previous studies.

1.4.2. Thesis Aim 2: Materials for Transscleral Delivery

While the first two chapters focused on developing a contact lens or contact lens-like material, the second aim of the work was to explore other materials whose properties would facilitate ocular drug delivery through a transscleral approach. Two materials were selected. The first was a self-assembling amphiphilic material, whose properties are determined in part by hydrophobic and hydrophilic interactions with its surroundings. The second was a PEG-PDMS material, whose metal-free "click" synthesis provided unique properties. Both of these materials could be used as an insert or rest in the cul-de-sac of the eye, again being placed by a medical professional to eliminate compliance issues, though alternative placements could also be explored.

1.4.2.a. Chapter 4: Self-Assembling Amphiphiles

Given the importance of hydrophobic interactions within these amphiphilic materials, they were ideal materials to determine how drugs of varying hydrophilicities would impact both the material characteristics and drug release, as they were likely to localize at different spots and interfaces within the material. This type of material is able to transition based on temperature and water content, and since it is believed that the

cubic phase is ideal for drug release, it was important to find a material that formed this phase at physiologically relevant conditions. Furthermore, using a material endogenous to body was preferable, as it reduced the likelihood of a toxic response. However, since hydrophobic interactions are so critical to the formation of these phases, it was imperative to understand how the drug loading impact the phase formation and transition characteristics, and this is explored in Chapter 4. This would ensure that the materials would form consistently and that there would be safe drug levels for the entire duration of drug release. Therefore, different drugs, loadings and material compositions were examined to better understand how these interactions impacted the overall drug release.

1.4.2.b. Chapter 5: Metal-Free PEG-PDMS

While PDMS has a long history of use in the body, its applications for drug release are limited due to its strong hydrophobic nature. While the incorporation of PEG can improve these properties, the synthesis often involves metal catalysts, such as platinum, which remain trapped in the material. While platinum has an excellent safety record, concern has been expressed over metals remaining in the material destined for human use; as well, residual platinum can cause the material to yellow over time. Additionally, many of the traditional modification strategies for silicones can be subjected to hydrophobic recovery, causing the beneficial properties imparted by the PEG to be reduced over time. This synthetic method developed in Chapter 5 allowed for a metal-free modification to integrate PEG into the bulk PDMS, yielding a material that could be useful for drug delivery applications.

1.4.2.c. Chapter 6: Additional Metal-Free PEG-PDMS

Given the beneficial properties noted in Chapter 5, further study of the materials and their properties were warranted in Chapter 6. Given the excellent wettability and reduced protein adsorption shown previously, it was prudent to explore the drug delivery capabilities of the materials. Modifications that could alter the hydrophobic and hydrophilic interface of the materials, such as adjusting the PEG substitution amounts, the crosslinking amounts and the PEG molecular weight, would provide insight into the drug's localization within the material, allowing the selection of a key material for tailorable drug release properties. Ultimately, understanding these interactions would allow an ideal material to be created that would yield the best delivery profile for its clinical application.

Throughout this thesis, we hope to demonstrate the importance of the hydrophilic/ hydrophobic interface as it pertains to drug delivery. Understanding how this impacts the drug release characteristics is critical to being able to create a delivery system that could be used to match a clinical drug release profile for either retinoblastoma or myopia.

1.5. References

Alvarez-Rivera F, Concheiro A, Alvarez-Lorenzo C. Epalrestat-loaded silicone hydrogels as contact lenses to address diabetic-eye complications. European Journal of Pharmaceutics and Biopharmaceutics. 2018;122:126-36.

Angelov B, Angelova A, Ollivon M, Bourgaux C, Campitelli A. Diamond-Type Lipid Cubic Phase with Large Water Channels. J Am. Chem. Soc. 2003;125:7188-9.

Bajgrowicz M, Chau-Minh P, Subbaraman LN, JonesL. Release of Ciprofloxacin and Moxifloxacin From Daily Disposable Contact Lenses From an In Vitro Eye Model. Investigative Ophthalmology & Visual Science. 2015;56(4):2234-42.

Brantley MA, Jr., Harbour JW. The molecular biology of retinoblastoma. Ocular immunology and inflammation. 2001;9(1):1-8.

Bremner R. A Potential Strategy to Block Tumour Initiation. OICR Presentation 05 August 2010.

Bremner R, Sage J. The origin of human retinoblastoma. Nature. 2014;514(7522):312-3.

Buttitta LA, Katzaroff AJ, Perez CL, de la Cruz A, Edgar BA. A double-assurance mechanism controls cell cycle exit upon terminal differentiation in Drosophila. Developmental cell. 2007;12(4):631-43.

Chen D, Livne-bar I, Vanderluit JL, Slack RS, Agochiya M, Bremner R. Cell-specific effects of RB or RB/p107 loss on retinal development implicate an intrinsically death-resistant cell-of-origin in retinoblastoma. Cancer cell. 2004;5(6):539-51.

Chen H, Brook MA, Sheardown H. Silicone elastomers for reduced protein adsorption. Biomaterials. 2004;25(12):2273-82.

Chen H, Yuan L, Song W, Wu Z, Li D. Biocompatible polymer materials: role of protein–surface interactions. Progress in Polymer Science. 2008;33:1059-87.

Chia A, Chua WH, Tan D. Effect of topical atropine on astigmatism. The British journal of ophthalmology. 2009;93(6):799-802.

Chia A, Chua WH, Cheung YB, Wong WL, Lingham A, Fong A, Tan D. Atropine for the treatment of childhood myopia: safety and efficacy of 0.5%, 0.1%, and 0.01% doses (Atropine for the Treatment of Myopia 2). Ophthalmology 2012;119:347-54.

Choy YB, Park JH, McCarey BE, Edelhauser HF, Prausnitz MR. Mucoadhesive microdiscs engineered for ophthalmic drug delivery: effect of particle geometry and

formulation on preocular residence time. Invest Ophthalmol Vis Sci. Nov 2008;49(11):4808-4815.

Colas, André, and Jim Curtis. "Silicones." *Biomaterials Science: An Introduction to Materials in Medicine*. Ed. Buddy D. Rattner, Allan S. Hoffman, Frederick J. Schoen, and Jack E. Lemons. 3rd ed. Elsevier, 2013. 82-91.

Comings DE. A general theory of carcinogenesis. Proceedings of the National Academy of Sciences of the United States of America. 1973;70(12):3324-8.

Conn CE, Drummond CJ. Nanostructured bicontinuous cubic lipid self-assembly materials as matrices for protein encapsulation. Soft Matter 2013;9:3449-3464.

Creech J, Chauhan A, Radke C. Dispersive mixing in the posterior tear film under a soft contact lens. Ind Eng Chem Res. 2001;40:3015-26.

Dave V, Sharma S, Yadav S, Paliwal S. Advancement and tribulations in ocular drug delivery. Int J Drug Deliv. 2012;4:1-8.

DiCiommo D, Gallie BL, Bremner R. Retinoblastoma: the disease, gene and protein provide critical leads to understand cancer. Seminars in cancer biology. 2000;10(4):255-69.

Dimaras H, Kimani K, Dimba EAO, Gronsdahl P, White A, Chan HSL, Gallie BL. Retinoblastoma. Lancet. 2012; 379:1436-46.

Dixon P, Fentzke RC, Bhattacharya A, Konar A, Hazra S, Chauhan A. In vitro drug release and in vivo safety of vitamin E and cysteamine loaded contact lenses. International Journal of Pharmaceutics. 2018;544(2):380-91.

Ganesan P, Wildsoet CF. Pharmaceutical intervention for myopia control. Expert Rev Ophthalmol. 2010;5(6):759-87.

Gaudana R, Ananthula HK, Parenky A, Mitra AK. Ocular Drug Delivery. AAPS Journal. 2010;12(3):348-60.

Geroski DH, Edelhauser HF. Transscleral drug delivery for posterior segment disease. Advanced Drug Delivery Reviews. 2001;52:37-48.

Ghate D, Edelhauser HF. Ocular drug delivery. Expert Opin Drug Deliv. Mar 2006;3(2):275-287.

Greaves JL, Wilson CG. Treatment of diseases of the eye with mucoadhesive delivery systems. Adv Drug Deliv Rev. 1993;11:349-383.

Guidi G, Korogiannaki M, Sheardown H. Modification of Timolol Release From Silicone Hydrogel Model Contact Lens Materials Using Hyaluronic Acid. Eye & Contact Lens-Science and Clinical Practice. 2014;40(5):269-76.

Gulsen D, Li C, Chauhan A. Dispersion of DMPC liposomes in contact lenses for ophthalmic drug delivery. Curr Eye Res. 2005;30:1071-80.

Gupta H, Aqil M. Contact lenses in ocular therapeutics. Drug Discovery Today 2012;17:522-527.

Hamalainen KM, Kananen K, Auriola S, et al. Characterization of paracellular and aqueous penetration routes in cornea, conjunctiva, and sclera. Invest. Ophthalmol. Vis. Sci. 1997;38:627-634.

Harbour JW. Molecular basis of low-penetrance retinoblastoma. Archives of ophthalmology. 2001;119(11):1699-704.

Huang Y, Gui S. Factors affecting the structure of lyotropic liquid crystals and the correlation between structure and drug diffusion. RSC Adv. 2018;8:6978-87.

Hughes PM, Olejnik O, Chang-Lin JE, Wilson CG. Topical and systemic drug delivery to the posterior segments. Advanced drug delivery reviews. 2005;57(14):2010-32.

Hui A, Boone A, Jones L. Uptake and release of ciprofloxacin-HCl from conventional and silicone hydrogel contact lens materials. Eye Contact Lens. 2008;34:266-71.

Jankowiak M, Maciejewski H, Gulinski J., Catalytic reactions of hydrosiloxanes with allyl chloride. J. Organomet. Chem. 2005**;***690*(20),4478-87.

Kaasgaard T, Drummond CJ. Ordered 2-D and 3-D nanostructured amphiphile self-assembly materials stable in excess solvent. Physical chemistry chemical physics. 2006;8(43):4957-75.

Kaur IP, Aggarwal D, Singh H, Kakkar S. Improved ocular absorption kinetics of timolol maleate loaded into a bioadhesive niosomal delivery system. Graefes Arch Clin Exp Ophthalmol. Oct 2010;248(10):1467-1472.

Kim J, Conway A, Chauhan A. Extended delivery of ophthalmic drugs by silicone hydrogel contact lenses. Biomaterials. 2008;29(14):2259-69.

Kim J, Peng C, Chauhan A. Extended release of dexamethasone from silicone-hydrogel contact lenses containing vitamin E. J Controlled Release. 2010;48:110-6.

Knudson AG, Jr. Mutation and cancer: statistical study of retinoblastoma. Proceedings of the National Academy of Sciences of the United States of America. 1971;68(4):820-3.

Korogiannaki M, Guidi G, Jones L, Sheardown H. Timolol maleate release from hyaluronic acid-containing model silicone hydrogel contact lens materials. Journal of Biomaterials Applications. 2015;30(3):361-376.

Lee SB, Geroski DH, Prausnitz MR, Edelhauser HF. Drug Delivery through the sclera: effects of thickness, hydration, and sustained release systems. Experimental Eye Research. 2004;78:599-607.

Lee VHL, Robinson JR. Review: Topical ocular drug delivery: Recent developments and future challenges. J Ocul Pharmacol. 1986;2:67-108.

Li C, Chauhan A. Modeling ophthalmic drug delivery by soaked contact lenses. Ind Eng Chem Res. 2006;45:3718-34.

McNamara NA, Polse KA, Brand RJ, Graham AD, Chan JS, McKenney CD. Tear mixing under a soft contact lens: effects of lens diameter. Am J Ophthalmol. 1999;127:659.

Mitra AK. Ophthalmic Drug Delivery Systems, Second Edition. Marcel Dekker Inc New York 2003.

Morgan PB, Efron N, Helland M, Itoi M, Jones D, Nichols JJ, et al. Global trends in prescribing contact lenses for extended wear. Contact lens & anterior eye. 2011;34(1):32-5.

Norton LW, Koschwanez HE, Wisniewski NA, Klitzman B, Reichert WM. Vascular endothelial growth factor and dexamethasone release from nonfouling sensor coatings affect the foreign body response. J Biomed Mater Res A. 2007;81(4):858-69.

Ostrow G, Kirkeby L. Update on myopia and myopic progression in children. International ophthalmology clinics. 2010;50(4):87-93.

Pacal M, Bremner R. Insights from animal models on the origins and progression of retinoblastoma. Current molecular medicine. 2006;6(7):759-81.

Peng CC, Ben-Shlomo A, Mackay EO, Plummer CE, Chauhan A. Drug delivery by contact lens in spontaneously glaucomatous dogs. Curr Eye Res. 2012;37:204-11.

Pham TT, Jaafar-Maalej C, Charcosset C, Fessi H. Liposome and niosome preparation using a membrane contactor for scale-up. Colloids and Surfaces B: Biointerfaces. 2012;94:15-21.

Phan CM, Bajgrowicz M, Gao H, Subbaraman LN, JonesLW. Release of Fluconazole from Contact Lenses Using a Novel In Vitro Eye Model. Optometry and Vision Science. 2016,93(4):387-394.

Rathore KS. In-situ gelling ophthalmic drug delivery system: An overview. Int J Pharm Pharm Sci. 2010;2:30-34.

Sagnella SM, Conn CE, Krodkiewska I, Drummond CJ. Soft ordered mesoporous materials from nonionic isoprenoid-type monoethanolamide amphiphiles self-assesmbled in water. Soft Matter 2009;5:4823-34.

Sagnella SM, Conn CE, Krodkiewska I, Moghaddam M, Seddon JM Drummond CJ. Ordered nanostructured amphiphile self-assembly materials from endogenous nonionic unsaturated monoethanolamide lipids in water. Langmuir 2010A;26:3084-94.

Sagnella SM, Conn CE, Krodkiewska I, Moghaddam M, Seddon JM Drummond CJ. Endogenous nonionic saturated monoethanolamide lipids: Solid State, Lyotropic Liquid Crystalline, and Solid Lipid Nanoparticle Dispersion Behavior. J. Phys. Chem. B 2010B;114:1729-37.

Sangwan M, McCurdy SR, Livne-Bar I, Ahmad M, Wrana JL, Chen D, Bremner R. Established and new mouse models reveal E2f1 and Cdk2 dependency of retinoblastoma, and expose effective strategies to block tumor initiation. Oncogene 2012;31:5019-28.

Santamaria D, Barriere C, Cerqueira A, Hunt S, Tardy C, Newton K, et al. Cdk1 is sufficient to drive the mammalian cell cycle. Nature. 2007;448(7155):811-5.

Sasaki H, Yamamura K, Nishida K, et al. Delivery of Drugs to the Eye by Topical Application. Ocular Drug Delivery Systems. 1996;15: 583-620.

Schultz C, Breaux J, Schentag J, Morck D. Drug delivery to the posterior segment of the eye through hydrogel contact lenses. Clinical & experimental optometry. 2011;94(2):212-8.

Saettone MF, Burgalassi S, Chetoni P. Ocular bioadhesive drug delivery systems. In: Mathiowitz E, Chickering DE, Lehr CM, eds. *Bioadhesive drug delivery systems. Fundametnals, novel approaches and development.* New York: Marcel Dekker; 1999:601-640.

Shah SS, Denham LV, Elison JR, Bhattacharjee PS, Clement C, Huq T, et al. Drug delivery to the posterior segment of the eye for pharmacologic therapy. Expert review of ophthalmology. 2010;5(1):75-93.

Shields CL, Fulco EM, Arias JD, Alarcon C, Pellegrini M, Rishi P, Bianciotto CG, Shields JA. Retinoblastoma frontiers with intravenous, intraarterial, periocular, and intravitreal chemotherapy. Eye. 2013;27:253-64.

Shih YF, Chen CH, Chou AC, Ho TC, Lin LL, Hung PT. Effects of different concentrations of atropine on controlling myopia in myopic children. Journal of ocular pharmacology and therapeutics. 1999;15(1):85-90.

Stadler WM, Vogelzang NJ, Amato R, Sosman J, Taber D, Liebowitz D, et al. Flavopiridol, a novel cyclin-dependent kinase inhibitor, in metastatic renal cancer: a University of Chicago Phase II Consortium study. Journal of clinical. 2000;18(2):371-5.

Trueblood JH, Rossomondo RM, Wilson LA, Carlton WH. Corneal contact times of ophthalmic vehicles. Evaluation by microscintigraphy. Arch Ophthalmol. Feb 1975;93(2):127-130.

Tyler AII, Barriga HMG, Parsons ES, McCarthy NLC, Ces O, Law RV, Seddon JM, Brooks NJ. Electrostatic swelling of bicontinous cubic lipid phases. Soft Matter 2015;11:3279-86.

Ward WK, Troupe JE. Assessment of chronically implanted subcutaneous glucose sensors in dogs: the effect of surrounding fluid masses. ASAIO J. 1999;45(6):555-61.

White CJ, Byrne ME. Molecularly imprinted therapeutic contact lenses. Expert Opin Drug Deliv. 2010;7:765-80.

Wu L, Timmers C, Maiti B, Saavedra HI, Sang L, Chong GT, et al. The E2F1-3 transcription factors are essential for cellular proliferation. Nature. 2001;414(6862):457-62.

Yu CL, Tucker MA, Abramson DH, Furukawa K, Seddon JM, Stovall M, et al. Cause-specific mortality in long-term survivors of retinoblastoma. Journal of the National Cancer Institute. 2009;101(8):581-91.

2. Atropine and Roscovitine Release from Model Silicone Hydrogels

Frances Lasowski, Heather Sheardown*

Department of Chemical Engineering, McMaster University, 1280 Main Street West, Hamilton ON L8S 4L7, Canada

* Corresponding author: sheardow@mcmaster.ca

Objectives:
Determining the impact of drug loading, specifically atropine and roscovitine, into model silicone contact lens materials to determine their impact on the lens properties and subsequent release kinetics to determine feasibility for potential childhood ocular treatments.

Main Scientific Contributions:
- Preparation of atropine and roscovitine loaded hydrogels at various material compositions.
- Preparation of drug loaded hydrogels at various loading levels and by various loading techniques.
- Property measurements of the materials, including core properties associated with contact lenses, noting the impact of drug incorporation.
- Investigating drug release from the various materials, noting the differences in kinetics particularly as they relate to the various material properties.

Publication Information:
Published in *Optometry and Vision Science* (Vol. 93 No. 4 April 2016).

Author Contribution:
Frances was responsible for the experimental work (synthesis and characterization of the contact lenses, property measurements, drug release experiments) and paper write-up. The work was done in consultation with and under the supervision of Dr. Heather Sheardown. Dr. Heather Sheardown revised the draft to the final version.

2.1. Abstract

Purpose: The delivery of drugs to the front of the eye has a low level of compliance and results in significant losses of drug. In pediatric patients, chronic eye diseases such as myopia and retinoblastoma can potentially be treated pharmacologically, but the risk associated with the delivery of high drug concentrations coupled with the need for regular dosing, limits their effectiveness. The current study examined the model silicone hydrogel materials for the delivery of atropine, for the treatment of myopia and CYC202 for the potential treatment of retinoblastoma.

Methods: Model silicone hydrogel materials comprised of TRIS and DMAA were prepared with the drug incorporated during synthesis. Various materials properties, with and without incorporated drug were investigated including water uptake, water contact angle and light transmission. Drug release was evaluated under sink conditions into phosphate buffered saline.

Results: The results demonstrate that low levels of both of the drugs can be incorporated into model silicone hydrogel materials without adversely affecting critical materials properties such as water uptake, light transmission and surface hydrophilicity. Extended release of both drugs was possible, with releases of at least two weeks being feasible. While a burst effect was noted, this was thought to be due to surface bound drug and therefore storage in an appropriate packaging solution could be used to overcome this if desired.

Conclusions: Silicone hydrogel materials have the potential to deliver drugs to pediatric patients, overcoming the need for regular drop instillation and allowing for the

maintenance of drug concentration in the tear film over the period of wear. This represents an attractive and viable option for treating a host of ophthalmic disorders in children including myopia and retinoblastoma.

2.2. Introduction

The treatment of ocular aliments is commonly achieved through topical eye drops, although many drugs delivered have less than a 5 minute residence time, and thus only 1-5% of the drug penetrates ocular tissue.[1] The remainder of this drug is cleared from the eye and enters the systemic circulation, which can cause various side effects depending on the nature of the therapeutic. Eye drops also suffer from poor patient compliance, which is problematic in populations such as young children and for long-term treatments such as myopia and glaucoma.[2] Therefore, controlled delivery systems that could improve the bioavailability of the therapeutics have been investigated.

Contact lenses have been investigated previously to deliver therapeutics, as they act as a slow, equilibrating reservoir and the prolonged corneal residence time improves bioavailability.[2, 3] The increased prevalence of silicone hydrogel extended wear lenses in the market[4] has created the option to use contact lenses for continuous drug delivery. While earlier studies focused on conventional daily wear lens materials, the utility of silicone based materials for drug release has been evaluated in many cases recently, showing significant promise.[2, 5-23] With silicone based materials, it is desired to create a drug-eluting contact lens that could be worn for extended periods of time where the release kinetics result in therapeutic concentrations for the wear period recommended by

the lens manufacturer, without compromising the optical properties of the contact lens itself. Treatment of diseases in children with such materials would be particularly advantageous, overcoming the need for frequent drop instillation while taking advantage of the fact that younger patients are more likely to be willing adopters of lens technologies. The current study focuses on the use of lenses for the potential treatment of two specific childhood ocular conditions.

Retinoblastoma, an intraocular malignancy affecting about 1 in 20,000 children,[24, 25] appears as a yellow-white mass in the retina, often surrounded by dilated blood vessels. Mutations on the Rb gene, resulting in a compromised Rb protein, and additional mutations in other regulatory proteins are believed to contribute to the disease.[24] CdK inhibitors, such as CYC202 (R-roscovitine), have shown to be potentially effective in preventing retinoblastoma, and treatment with these drugs could block tumor initiation in genetically susceptible populations.[26] Treatment with lenses is appealing in this application, as penetration of the globe is prohibited due to fears of tumor seeding through the puncture site while minimizing systemic side effects.

Atropine has been studied since the 1970s as a pharmacologic means to arrest myopia, a much more common condition than retinoblastoma. It is believed that atropine has a biochemical effect on the retina or sclera that causes remodeling of the sclera associated with eye growth,[27] thus allowing it to exude an effect on the overgrowth associated with myopia. While this therapy shows some success, concentrations must be tightly controlled to reduce side effects[28] and additional complications, such as growth upon treatment completion,[29] limits its effectiveness. Both drugs show heat lability,

making them amenable to delivery via a drug delivery system. Furthermore, since CYC202 and atropine, whose similarly sized structures are shown in Figure 2.1, are required for use in young, developing children, it is desirable to create a delivery vehicle to reduce side effects by localizing drug delivery while ensuring patient compliance and minimizing invasiveness.

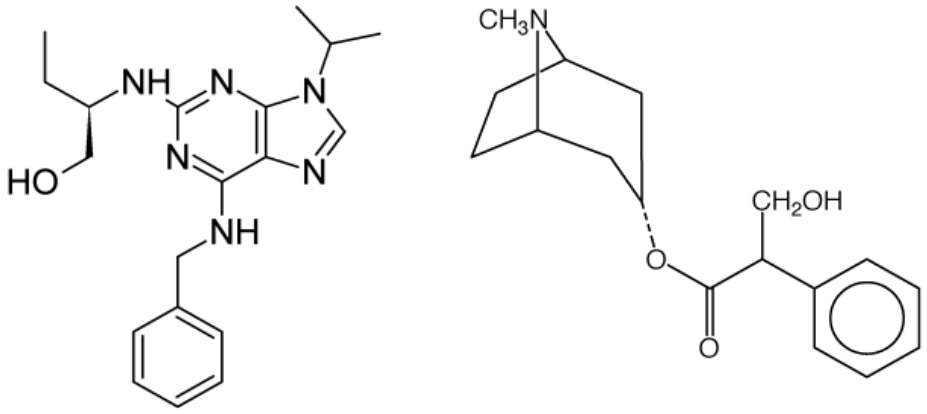

Figure 2.1. Structure of molecules. CYC202 on left, atropine on right.

Therefore, the aim of this study was to evaluate silicone hydrogel materials as a potential drug delivery method for the delivery of CYC202 and atropine. Our laboratory has previously developed commercially-similar model silicone lenses to facilitate the study of both direct drug loading and entrapment by soaking in drug solutions. In the current work, the release parameters of these drugs under various loading conditions were examined while ensuring the essential lens properties of the contact lens are maintained.

2.3. Materials and Methods

2.3.1. Materials

N,N-dimethylacrylamide (DMA), ethylene glycol dimethacrylate (EGDMA) and atropine were purchased from Sigma-Aldrich Chemicals (Oakville, ON). CYC202 was purchased from Selleck (Houston, TX). 3-Methacryloxypropyltris(trimethylsiloxy)silane (TRIS) and 3-(3-methacryloxy-2-hydroxypropoxy) propylbis(trimethylsiloxy)methylsilane (modified TRIS or TRIS-OH) were purchased from Gelest Inc. (Morrisville, PA). Irgacure 184 was generously supplied by BASF Corp. Plexiglas G-UVT for casting molds was supplied by Altuglas (Bristol, PA). All other reagents were purchased from Sigma-Aldrich unless otherwise stated.

2.3.2. Hydrogel Synthesis

Model hydrogel lenses used DMA and a silicone monomer, either TRIS or modified TRIS, in various ratios shown in Table 1 as previously described.[30] All were initiated with Irgacure 184 (0.1 wt%) and crosslinked using EGDMA (3.3 wt%). Prior to use, all monomers were passed through inhibitor remover packed columns to ensure the removal of monomethyl ether hydroquinone (MMEQ). The materials were prepared with or without CYC202 (0.5 wt%) and atropine (0.5 wt% or 2 wt%) during synthesis. No degradation of the drugs due to UV exposure or heat treatment was found when examined using NMR and UV-spectrometry. Using Material 4 as an example, 0.5 wt% of atropine was dissolved in an 80:20 molar ratio of DMA:TRIS solution containing 3 mol% EGDMA and allowed to mix for at least 5 minutes. Irgacure 184 (1 wt%) was dissolved

into the formulation then immediately syringed into a UV-transparent acrylic plate mold and polymerized in a 400W UV chamber (Cure Zone 2 Con-trol-cure, Chicago, IL) for 15 minutes. The mold included a 1 mm Teflon spacer. Individual discs were bored to 7.94 mm, except for Materials 19-21 which required a short hydration period in a phosphate buffered saline (PBS) solution before being cut.

2.3.3. Material Characterization

2.3.3.a. Water Equilibrium Content

The equilibrium water content (EWC) was determined using a mass balance method. The masses of the dry discs (M_D) were obtained after drying in a 40°C for at least 24 hours. These were compared to the hydrated masses (M_H), as shown in Equation 1. The hydrated mass was obtained after soaking the discs in a PBS solution for 48 hours. Residual droplets were removed prior to the masses being examined.

$$EWC\% = \frac{M_H - M_D}{M_H} \cdot 100\% \qquad (1)$$

2.3.3.b. Surface Wettability

Surface wettability was assessed using the advancing contact angle using a Kruss DSA Contact Angle Apparatus. Materials were swollen for at least 48 hours and placed flat on a slide. A single drop of MilliQ water was placed on the surface, allowing the contact angle to be measured under magnification.

2.3.3.c. Transmittance

Using light transmittance, as measured by UV-VIS spectrophotometry, the transparency of the hydrogels was assessed. Using a 96-well plate, 5.55 mm discs were hydrated in 100 µL of Milli-Q water for 24 hours and the transmittance was measured from 400 nm to 700 nm.

2.3.4. Drug Loading, Release and Analysis

Atropine was directly loaded into the hydrogel materials as shown in Table 1. CYC202 was either directly loaded into the hydrogels or was loaded by soaking using control materials in a 2 mg/mL CYC202 solution, prepared in 50:50 water:methanol. This solvent composition was chosen to overcome the limited solubility of CYC202 in water. Briefly, 7.94 mm control disks were transferred to 1 mL of the uptake solution for 7 days. These were then dried at 40°C for at least 24 hours before being used for any release experiments. Drug release experiments were completed in 1 mL of PBS (pH 7.4) at 37°C; to ensure sink conditions, the discs were transferred to fresh PBS at regular intervals, initially at 1, 3, 6, 9, 12, 24, 48, 72, 96 and 120 hours, then at least 24 hours apart at later time points. The drug elution was measured by UV-spectrophotometry at 292 nm for CYC202 and by HPLC at 254 nm for atropine. Percent drug release was then calculated as the average amount of drug released at that time point divided by the sum of the drug release at all time points for each material. Results were analyzed statistically using t-test with a significance level of 95% or where multiple factors were examined simultaneously, ANOVA with post hoc testing using Tukey analysis was used.

2.4. Results and Discussion

2.4.1. Material Characterization

2.4.1.a. Water Equilibrium Content

Since water content is often correlated to the on-eye comfort of contact lenses, the EWC of the model lenses were measured and shown in Table 2. All four material formulations were significantly different from each other ($p<0.05$). Many of the materials achieved the 20-40% EWC range shown by most commercial contact lenses, and these were most closely examined for their drug release profiles.[31] Swelling levels lower than 20% would be expected to lead to significant corneal discomfort and therefore not reasonable for the proposed application. Both the incorporation of the modified TRIS and greater DMA content resulted in higher water contents. This was expected, as these materials are more hydrophilic and thus are more likely to retain water in the hydrogel. Not surprisingly, DMA content appears to have a greater impact on the EWC than the modified TRIS material; this is likely due to its stronger hydrophilic character. The 50/50 DMA/TRIS materials exhibited very little swelling, as demonstrated by the low EWC. While this material was quite stiff and not suitable as a contact lens, it was included to better understand the subsequent release kinetics for these materials and the effect of increased hydrophobic character on release of a hydrophobic drug such as CYC202. The EWC of the materials were not affected by the presence of the drugs. This is likely due to the small amounts of drugs added relative to the bulk composition of the lenses. Based on these results, the 80/20 materials with both the regular and modified TRIS materials and

the 70/30 materials with the modified TRIS were the most promising compositions for modeling the properties of contact lenses.

2.4.1.b. Transparency of Hydrogel

Since high optical transparency is an essential property of a contact lens, it was necessary to determine how the various material compositions and drug loadings affected the light transmittance. As shown in Table 2, all of the materials showed high transmittance at 600 nm, though the control materials with the greater DMA content, and thus the higher EWC, did show a slight improvement. Given the hydrophobic nature of the TRIS materials, it is expected that small, light scattering, silicone-rich domains form in the hydrogels. It is likely that these are smaller in the material that has less silicone. However, it is clear that in both a high silicone instance (50%) and a low silicone instance (20%), the domains are sufficiently small to give over 90% transmittance. Furthermore, the materials tested were approximately 1 mm in thickness. Since commercial contact lenses are much thinner than this, it is expected that these values would improve with a thinner sample, though this was limited by the molds used. Similar to the EWC, the incorporation of the drugs does not significantly affect the transmittance, particularly critical to the use of silicone hydrogel materials for drug release. Since the amount of drug is small and it is fully dissolved in the monomer solution prior to curing, it is not expected that the drug itself will alter the domain formation. Therefore, it is not expected that the drug incorporation by direct loading would have affected the transparency.

2.4.2. Surface Wettability

In order to ensure comfort while blinking and maintain a stable tear film, a contact lens must be highly wettable. Table 3 compares the wettability of various materials, as measured by the advancing contact angle. While silicones are known to have high contact angles, the incorporation of the DMA is able to decrease these substantially. The incorporation of atropine by direct loading, swelling or imprinting does not affect the surface wettability. This is expected, as it did not have any impact on the bulk properties of the gel when entrapped during synthesis. This demonstrates that if any atropine is adsorbed to the material during the soaking, it does not have an appreciable influence on the surface wettability.

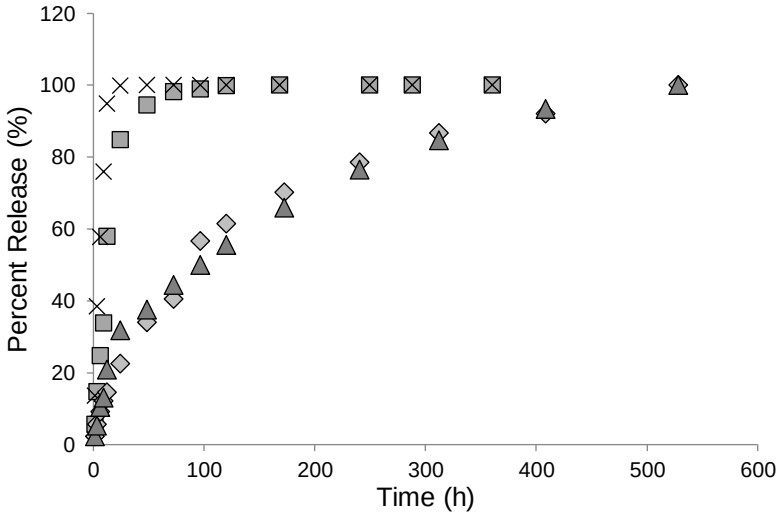

Figure 2.2. Atropine release from various materials: Square- Material 4, X- Material 5, Diamond- Material 12, Triangle- Material 13.

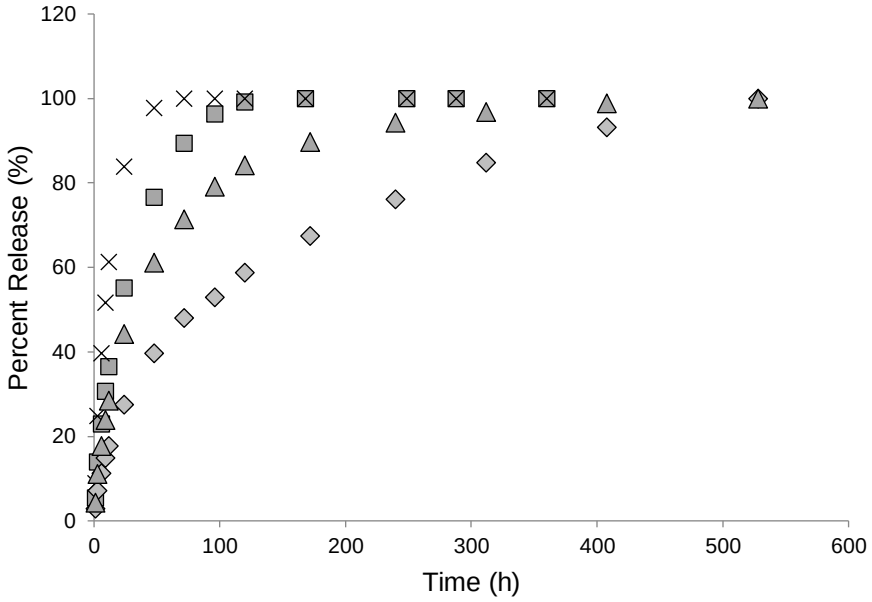

Figure 2.3. Atropine release from various materials: Square- Material 6, X- Material 7, Diamond- Material 14, Triangle- Material 15.

2.4.3. Drug Release Direct Loading

The drug release profiles from materials that incorporated the therapeutics during synthesis are shown in Figures 2.2-2.4, including the release of 0.5% CYC202, 2% atropine and 0.5% atropine respectively from both the 70/30 and 80/20 DMA/TRIS or DMA/TRIS-OH materials. While drug release studies were completed using the 50/50 material composition, given the low swelling of the material (less than 20%), these were determined to be less appropriate for a contact lens application and thus the profiles are not shown.

With atropine, the materials with the greater DMA (80 mol%) released the atropine more quickly, regardless of the loading amounts. However, all materials with this high DMA composition show a large burst release, with most of the drug being released in the first 2-4 days depending on the amount initially loaded. However, since

this is dependent on the loading, it is possible that this could be extended out slightly further with an even greater loading.

Furthermore, the material loading also has an effect on the cumulative amount of drug released, as expected. The greater the amount of drug loaded, the greater the amount of drug release. As shown in Table 4, most, if not all, of the drug is released from these materials with a reasonable water content. Due to the difficulty of measuring small amounts of drug, it is expected that the materials with higher than 100% of drug are a product of slightly higher drug loading during initial incorporation. However, with the lower DMA content (50 mol%), it is clear that much of the drug remains in the material. This is expected, as atropine is likely trapped in the silicone domains of the materials formed during synthesis. While these domains are small, they likely have limited swelling, and the drug is therefore required to diffuse through this domain, into the water channels in the other domains, and then out of the material. This is highly correlated to the swelling, as the materials that showed the least swelling also exhibited the greatest amount of residual drug in the matrix. For the materials with greater swelling, since atropine displays only moderately hydrophobic behaviour and has some solubility in water, compounded with its lack of functional groups that interact with the silicone phase, it is likely that most of the drug will partition into the more hydrophilic phases in the presence of swelling.

Therefore, while increasing the loading amount would result in a more extended release profile, there would also be a greater amount of drug released, which could be problematic for atropine. Specifically, there are many side effects associated with

atropine, such as light sensitivity from pupil dilation[28], and these would likely be worse from higher release amounts of atropine. It has also been shown that only a small amount of atropine is required to be effective for treatment in many instances, so lower release amounts are likely desirable.[32]

The incorporation of modified TRIS increased the release rate in the higher loading amount, most pronounced in the materials with the greater TRIS content, but showed no significant effect at lower loading. It is likely that at higher DMA compositions, this hydrophilic phase dictates the release profile, so the slightly more hydrophilic TRIS does not have a large impact. However, at the lower DMA levels, the TRIS component has a greater influence on the release parameters, and thus the release rate is greater with the modified TRIS. Since there is more drug present in this phase at the higher loading, it is likely it is able to exert a more appreciable change on the release rate.

In order to effectively treat ocular conditions, a controlled, sustained release of therapeutics is required from the contact lens material. Extended-wear lenses, such as silicone hydrogels, can be worn for up to 30 days continuously, although this depends on the manufacturer's recommendation. It has been suggested that to improve patient compliance, regular intervals are required, such as changing the lenses every week or every two weeks. Considering the materials with the most appropriate EWC, sustained drug release is possible for one week at the lower loading and over two weeks at the higher loading for atropine, which is likely appropriate for use in children. However, materials 12 and 14 (70/30 with the modified TRIS) provided the best release profile with

the appropriate material swelling, as the release is the most gradual and consistent over the duration of the release, although there was a still a burst release with both of these materials. This would mean that the amount of drug released in the first couple of days of wear would be greater than that at the end of the wear time, which is not desirable. It may be possible to modulate this during the packaging of the material, as it would likely experience some drug release during that time as it equilibrates with the packing solution.

Figure 2.4 shows the release for CYC202 from the various materials. Similar to atropine, the release is controlled by the rate of diffusion of the drug. It appears that the material composition has less of an influence on the profile of the drug release here than with atropine, as the modified materials consistently released faster, but the profiles were quite similar between for a given TRIS monomer. This is likely due to the lower solubility of CYC202 in water and that many aromatic rings and few hydrophilic moieties are not likely to repel the silicone phase. Specifically, the modified TRIS materials have a higher water content, which likely exposes more drug to water channels. Given the limited solubility of the drug in water, it is likely that these internal water channels become quickly saturated, so the drug release is limited by the time to diffuse through these paths. Greater material water content facilitates greater drug diffusion. This is clear from the long release profiles seen with CYC202, and the amount of drug which remains in the matrix, as shown in Table 4. Similar to atropine, this appears to depend on the swelling of the material, though there is clearly a drug dependency, as more CYC202 is retained in the matrix than atropine for a given material composition.

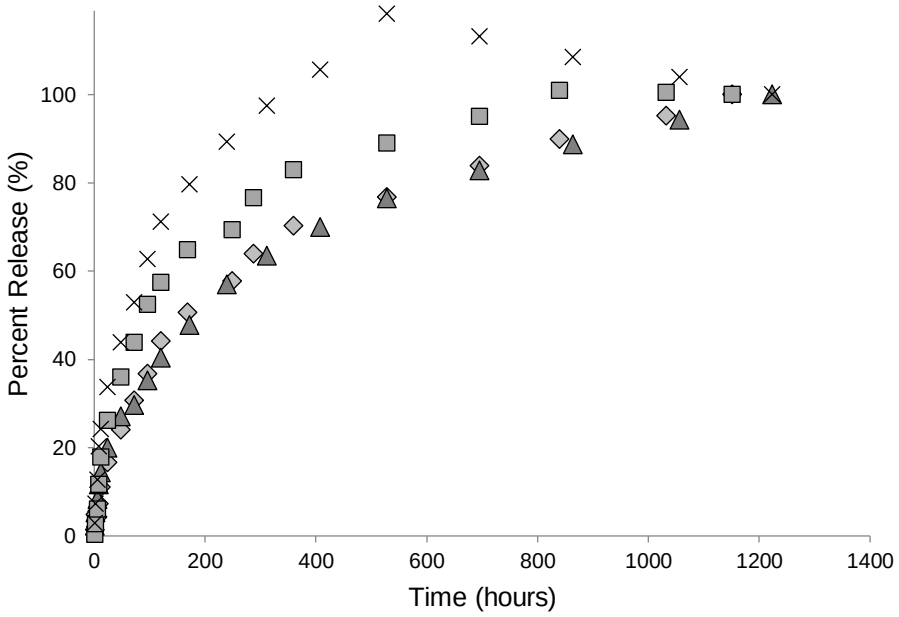

Figure 2.4. CYC202 release from various materials: Diamond- Material 8, Square- Material 9, Triangle- Material 16, X- Material 17.

Similar to atropine, only a small amount of CYC202 is expected to be required to exhibit its therapeutic effect.[26] It is expected that the 30-55 μg released from these 40 mg materials overall will be sufficient for this application, though *in* vivo models are required to confirm this. Therefore, a lower loading with a slow release profile is ideal. Unlike atropine, however, the treatment regime with CYC202 is expected to be short for retinoblastoma. Therefore, having a burst release, as seen by all of the materials examined, may be beneficial. Depending on the treatment time required, the most appropriate material composition could be selected. This is particularly important, as these materials showed release in excess of 30 days, which would be longer than any lens is recommended for wear. However, for both of these systems, it is important to note that these materials are thicker than commercial lenses. Therefore, thinner discs are expected

to increase the release rate, as it is believed this is controlled by diffusion. However, other factors such as the release medium, mixing and most importantly the release volume, may also slow these release parameters relative to the experimental conditions. Therefore, this would require further testing in an *in vivo* system.

2.4.4. Drug Release - Soaked Loading

Control materials 1-3 were explored to determine the extent to which the drug release could be tailored based on the material composition, particularly when the materials are soaked in a drug solution to load. While materials that incorporated the therapeutics during synthesis were able to load a greater amount of drug than those loaded by soaking, there may be manufacturing difficulties associated with a direct loading technique, particularly as these lens would likely require an extraction step to remove unreacted monomers. These materials were loaded in a methanol/water blend to increase the swelling of the material during loading and allow a greater loading concentration, as the solubility of CYC202 in water is quite limited. While it was not possible to precisely measure the uptake of the materials, it is expected that more drug remains entrapped in the material when loading with a methanol blend than just water. This is likely due to the increased swelling of the silicone domains in methanol, where the drug to freely enters and becomes trapped after drying. Since these domains experience much less swelling in water alone, this drug is not able to access water channels to dissolve and be subsequently released.

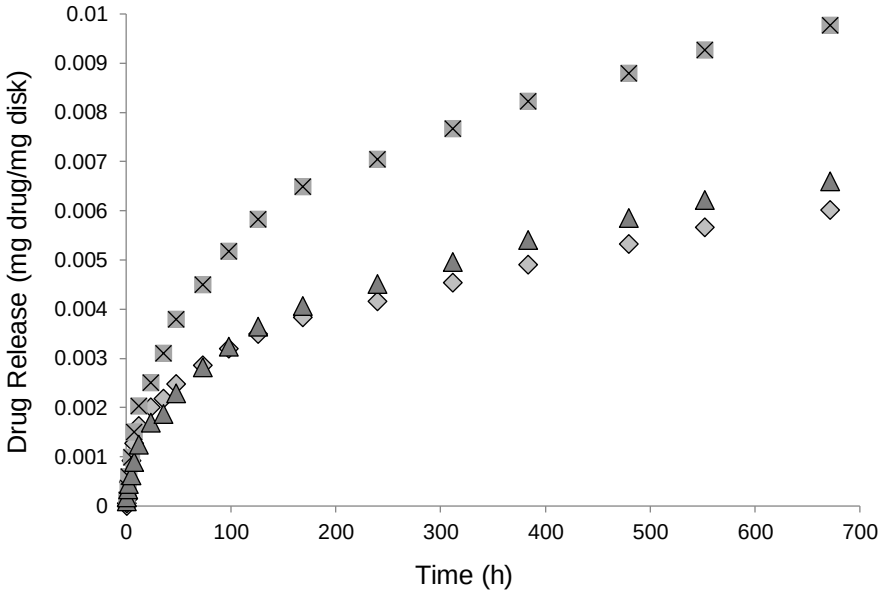

Figure 2.5. CYC202 release from various materials soak loaded in 2 mg/mL 50:50 H_2O:Methanol solution: Diamond- Material 1, Square- Material 2, Triangle- Material 3.

Figure 2.5 shows that, using this loading technique, the release of CYC202 is possible for over two weeks. There is a similar trend with the soak-loaded release profiles. The incorporation of only 10 mol% modified TRIS does not appear to affect the uptake and subsequent release profile, while the incorporation of 20 mol% has a great impact. When the kinetics of the soaked release profile are examined over a month, they are very similar. However, their cumulative releases do show different total amounts of drug release. This could be due to differences in the uptake properties of the material during the soaking or the difference in the swelling of the material. While it is unclear what concentrations would be required in the posterior of the eye to treat the diseased condition, this profile is likely tailorable based on the loading concentrations of the drugs.

Of note, while the thickness of the materials is greater than that of typical contact lens materials, the overall fraction of drug released is not expected to be different than would be expected for thinner lens materials with similar loading. The surface area of edge is substantially less than the surface area of the faces of the device meaning that edge effects can be neglected in both cases. However the total amount of drug released is expected to be lower since the total amount of drug loaded is greater than would be the case with thinner materials.

Table 2.1- Hydrogel compositions evaluated.

Material Composition	DMA (mol%)	TRIS (mol%)	TRIS-OH (mol%)	Atropine (wt%)	CYC202 (wt%)
1 (80/20 Control)	80	20			
2 (80/20-OH Control)	80		20		
3 (80/10/10-OH Control)	80	10	10		
4 (80/20 Low Atropine)	80	20		0.5	
5 (80/20-OH Low Atropine)	80		20	0.5	
6 (80/20 High Atropine)	80	20		2	
7 (80/20-OH High Atropine)	80		20	2	
8 (80/20 CYC202)	80	20			0.5
9 (80/20-OH CYC202)	80		20		0.5
10 (70/30 Control)	70	30			
11 (70/30-OH Control)	70		30		
12 (70/30 Low Atropine)	70	30		0.5	
13 (70/30-OH Low Atropine)	70		30	0.5	
14 (70/30 High Atropine)	70	30		2	
15 (70/30-OH High Atropine)	70		30	2	
16 (70/30 CYC202)	70	30		0.5	
17 (70/30-OH CYC202)	70		30	0.5	
18 (50/50 Control)	50	50			
19 (50/50 Low Atropine)	50	50		0.5	
20 (50/50 High Atropine)	50	50		2	
21 (50/50 CYC202)	50	50			0.5

Table 2.2- Equilibrium water content values and transmittance data at 600 nm for various material compositions (n=5).

Material	Composition (mol%)	Average EWC	Transmittance
1	80/20 DMA/TRIS	27.2 ± 1.4 %	97.0 ± 0.4 %
2	80/20 DMA/TRIS-OH	32.5 ± 1.1 %	
4	80/20 DMA/TRIS Low Atropine	27.9 ± 1.5%	96.8 ± 3.4 %
6	80/20 DMA/TRIS High Atropine	29.2 ± 1.1%	98.0 ± 0.9 %
8	80/20 DMA/TRIS CYC202	26.55 ± 0.5%	89.2 ± 7.2 %
10	70/30 DMA/TRIS	15.8 ± 1.5 %	
11	70/30 DMA/TRIS-OH	22.1 ± 0.9 %	
18	50/50 DMA/TRIS	3.51 ± 1.1 %	92.9 ± 1.5 %
19	50/50 DMA/TRIS Low Atropine	4.3 ± 1.1%	92.4 ± 2.0 %
20	50/50 DMA/TRIS High Atropine	4.5 ± 1.9%	97.3 ± 1.4 %
21	50/50 DMA/TRIS CYC202	2.8 ± 0.6%	91.7 ± 5.6 %

Table 2.3- Advancing contact angles on Material 1 discs (synthesized without atropine) and Material 6 discs (synthesized with atropine), after soaking with 2 mg/mL atropine solution or PBS solution.

Synthesis	Soaking	Average Value (°)
Material 1	*Without Atropine (n=3)*	64.7 ± 3.0
	With Atropine (n=4)	69.2 ±7.9
Material 6	*Without Atropine (n=3)*	59.8 ± 8.9
	With Atropine (n=4)	70.6 ± 116

Table 2.4- Total amount of drug release from various materials based on anticipated loading (n=4).

Material	Amount Released
4	122%
5	95%
6	135%
7	102%
8	28%
9	24%
12	107%
13	117%
14	100%
15	121%

16	24%
17	16%
19	33%
20	33%
21	17%

2.5. Conclusion

In order to overcome compliance issues and minimize the need for frequent instillation of high concentrations of drug, model silicone hydrogel materials were examined for their potential to deliver atropine and CYC202. From these studies, it is clear that the drug releases can be altered based on both the monomer content and ratio of hydrophobic to hydrophilic components, meaning that the composition of the lens material will likely have to be tailored to some extent in order to obtain the desired release kinetics. However, the release was shown to also vary based on structure and nature of the therapeutic itself, as well as its loading concentration. Sufficient drug loading is possible from the initial manufacture of the lenses and can be varied to deliver an ideal cumulative release. It is also possible to load the drugs after manufacture by soaking and achieve sustained release profiles. These materials present a potential method to deliver both CYC202 and atropine that would be appropriate for use with children.

2.6. Acknowledgements

The authors would like to acknowledge the financial support of the 20/20 NSERC Ophthalmic Materials Research Network.

2.7. References

1. Kim J, Conway A, Chauhan A. Extended delivery of ophthalmic drugs by silicone hydrogel contact lenses. Biomaterials 2008;29:2259-69.

2. Hsu KH, Gause S, Chauhan A. Review of ophthalmic drug delivery by contact lenses. J Drug Deliv Sci Tech 2014;24:123-35.

3. Schultz C, Breaux J, Schentag J, Morck D. Drug delivery to the posterior segment of the eye through hydrogel contact lenses. Clin Exp Optom 2011;94:212-8.

4. Morgan PB, Efron N, Helland M, Itoi M, Jones D, Nichols JJ, van der Worp E, Woods CA. Global trends in prescribing contact lenses for extended wear. Cont Lens Anterior Eye 2011;34:32-5.

5. Achouri D, Alhanout K, Piccerelle P, Andrieu V. Recent advances in ocular drug delivery. Drug Devel Ind Pharm 2013;39:1599-617.

6. Baranowski P, Karolewicz B, Gajda M, Pluta J. Ophthalmic drug dosage forms: Characterisation and research methods. Scientific World Journal 2014.

7. Bengani L, Chauhan A. Are contact lenses the solution for effective ophthalmic drug delivery? Future Med Chem 2012;4:2141-3.

8. Bengani LC, Hsu KH, Gause S, Chauhan A. Contact lenses as a platform for ocular drug delivery. Exp Opin Drug Del 2013;10:1483-96.

9. du Toit LC, Pillay V, Choonara YE, Govender T, Carmichael T. Ocular drug delivery - a look towards nanobioadhesives. Exp Opin Drug Del 2011;8:71-94.

10. Guidi G, Hughes TC, Whinton M, Brook MA, Sheardown H. The effect of silicone hydrogel contact lens composition on dexamethasone release. J Biomater Appl 2014;29:222-33.

11. Guidi G, Korogiannaki M, Sheardown H. Modification of timolol release from silicone hydrogel model contact lens materials using hyaluronic acid. Eye Contact Lens-Sci Clin Practice 2014;40:269-76.

12. Hsu KH, Fentzke RC, Chauhan A. Feasibility of corneal drug delivery of cysteamine using vitamin E modified silicone hydrogel contact lenses. Eur J Pharm Biopharm 2013;85:531-40.

13. Hui A, Willcox M, Jones L. In vitro and in vivo evaluation of novel ciprofloxacin-releasing silicone hydrogel contact lenses. Invest OphthalmolVis Sci 2014;55:4896-904.

14. Jung HJ, Abou-Jaoude M, Carbia BE, Plummer C, Chauhan A. Glaucoma therapy by extended release of timolol from nanoparticle loaded silicone-hydrogel contact lenses. J Controlled Rel 2013;165:82-9.

15. Knight OJ, Lawrence SD. Sustained drug delivery in glaucoma. Curr Opin Ophthalmol 2014;25:112-7.

16. Liu SY, Jones L, Gu FX. Nanomaterials for ocular drug delivery. Macromol Biosci 2012;12:608-20.

17. Mahomed A, Tighe BJ. The design of contact lens based ocular drug delivery systems for single-day use: Part (I) Structural factors, surrogate ophthalmic dyes and passive diffusion studies. J Biomater Applications 2014;29:341-53.

18. Phan CM, Subbaraman L, Jones L. Contact lenses for antifungal ocular drug delivery: a review. Exp Opin Drug Deliv 2014;11:537-46.

19. Phan CM, Subbaraman L, Liu SY, Gu F, Jones L. In vitro uptake and release of natamycin Dex-b-PLA nanoparticles from model contact lens materials. J Biomater Sci Polym Edn 2014;25:18-31.

20. Sankaridurg P, de la Jara PL, Holden B. The future of silicone Hydrogels. Eye Contact Lens - Sci Clin Practice 2013;39:125-9.

21. Tieppo A, Boggs AC, Pourjavad P, Byrne ME. Analysis of release kinetics of ocular therapeutics from drug releasing contact lenses: Best methods and practices to advance the field. Contact Lens Ant Eye 2014;37:305-13.

22. White CJ, McBride MK, Pate KM, Tieppo A, Byrne ME. Extended release of high molecular weight hydroxypropyl methylcellulose from molecularly imprinted, extended wear silicone hydrogel contact lenses. Biomaterials 2011;32:5698-705.

23. White CJ, Tieppo A, Byrne ME. Controlled drug release from contact lenses: a comprehensive review from 1965-present. J Drug Deliv Sci Tech 2011;21:369-84.

24. Brantley MA, Jr., Harbour JW. The molecular biology of retinoblastoma. Ocul Immunol Inflamm 2001;9:1-8.

25. Pacal M, Bremner R. Insights from animal models on the origins and progression of retinoblastoma. Curr Mol Med 2006;6:759-81.

26. Sangwan M, McCurdy SR, Livne-Bar I, Ahmad M, Wrana JL, Chen D, Bremner R. Established and new mouse models reveal E2f1 and Cdk2 dependency of retinoblastoma, and expose effective strategies to block tumor initiation. Oncogene 2012;31:5019-28.

27. Chia A, Chua WH, Tan D. Effect of topical atropine on astigmatism. Br J Ophthalmol 2009;93:799-802.

28. Shih YF, Chen CH, Chou AC, Ho TC, Lin LL, Hung PT. Effects of different concentrations of atropine on controlling myopia in myopic children. J Ocul Pharmacol Ther 1999;15:85-90.

29. Ostrow G, Kirkeby L. Update on myopia and myopic progression in children. Int Ophthalmol Clin 2010;50:87-93.

30. Weeks A, Morrison D, Alauzun JG, Brook MA, Jones L, Sheardown H. Photocrosslinkable hyaluronic acid as an internal wetting agent in model conventional and silicone hydrogel contact lenses. J Biomed Mater Res A 2012;100A:1972-82.

31. Efron N, Morgan PB, Cameron LD, Brennan NA, Goodwin M. Oxygen permeability and water content of silicone hydrogel contact lens materials. Optom Vision Sci 2007;84:328-33.

32. Chia A, Chua WH, Cheung YB, Wong WL, Lingham A, Fong A, Tan D. Atropine for the treatment of childhood myopia: safety and efficacy of 0.5%, 0.1%, and 0.01% doses (Atropine for the Treatment of Myopia 2). Ophthalmology 2012;119:347-54.

3. **Tethered Roscovitine Release from Model Contact Lenses**

Frances Lasowski[1], Vida Rahmani[1], Talena Rambarran[1], Moiz Mikail[2], Heather Sheardown[1*]

[1]Department of Chemical Engineering, McMaster University, 1280 Main Street West, Hamilton ON L8S 4L7, Canada

[2]Department of Chemistry and Chemical Biology, McMaster University, 1280 Main Street West, Hamilton ON L8S 4M1, Canada

* Corresponding author: sheardow@mcmaster.ca

Objectives:
This work sought to create a covalent drug linkage into the model silicone hydrogel material to facilitate longer term release using a method that would be more commercially relevant by allowing for an extraction process, while understanding the impact of different tether spacers on both the lens properties and the subsequent drug release.

Main Scientific Contributions:
- Preparation of conjugated roscovitine to a PEGMA-lactide based tether.
- Preparation of the tether-loaded hydrogels at various lactide spacer amounts.
- Property measurements of the materials, including core properties associated with contact lenses, noting the impact of drug-tether incorporation.
- Investigating drug release from the various tethered materials, noting the differences in kinetics particularly as they relate to the tether length.

Author Contribution:
Frances was responsible for the idea of tethering the drug into the model lens, the experimental plan and design for all experiments, the interpretation of the results and the paper write-up. Dr. Vida Rahmani was responsible for conducting the experiments as per the plan. Moiz Mikhail was responsible for the initial synthesis of the lactide conjugate. Dr. Talena Rambarran aided in the protocol to create the lactide conjugate, supervising the work of Moiz, and also helped with the interpretation of all NMR work. The work was done in consultation with and under the supervision of Dr. Heather Sheardown. Dr. Heather Sheardown revised the draft to the final version.

3.1. Abstract

Drug delivery to the eye remains a challenge due to low compliance and drug loss. This is particularly true in pediatric populations, such as those who are at risk of hereditary retinoblastoma. With a new preventative treatment proposed, utilizing the cyclin-dependent kinase inhibitor roscovitine (CYC202), a sustained delivery system from a contact lens has been evaluated in the current work. Using a labile lactide spacer, comprised of poly(ethylene glycol) methacrylate, varying lactide units and succinic anhydride, the drug was covalently incorporated into model silicone lenses (consisting of 80 mol% N,N-dimethylacrylamide and 20 mol% of a modified silicone). This enabled a greater amount of the drug to remain in the material following a soxhlet extraction with isopropyl alcohol. The incorporation of the tether and drug did not substantially alter the bulk properties of the materials, with their water content remaining between 32-36% and their transmittance remaining at over 90% at 600nm. Drug release from these materials exceeded 2 weeks, with the longer lactide tethers showing greater release as expected. This demonstrates that these covalently modified materials have the potential to be used to deliver roscovitine and potentially other drugs in a sustained manner.

3.2. Introduction

Retinoblastoma is an intraocular malignancy affecting about 1 in 20,000 children [Brantley 2001, Pascal 2006] with approximately one third of affected children developing tumors bilaterally. Due to mutations on the *RB1* gene, a compromised Rb protein is produced, impeding tumor-suppression. [Brantley 2001] The cone precursor cells are unusually sensitive to the loss of *RB1*, resulting in their cancerous transformation. [Bremner 2014] Cyclin-dependent kinase (CdK) inhibitors, such as CYC202 (R-roscovitine), have shown the potential to be effective in preventing retinoblastoma, and treatment with these drugs could block tumor initiation in genetically susceptible populations. [Sangwan 2012] This chemopreventative treatment would be for use in young, developing children and thus would require a local, minimally invasive drug delivery method to reduce side effects and ensure patient compliance.

While the treatment of ocular aliments is commonly achieved through topical eye drops, these drugs are quickly flushed from the eye, and thus only 1-5% of the drug penetrates ocular tissue. [Kim 2008] Since the remainder of these drugs enters the systemic circulation, this would result in significant side effects with CYC202. Additionally, eye drops also suffer from poor patient compliance due to the difficulty of instillation, particularly in pediatric populations. [Hsu 2014] Intravitreal injections are often used for ocular therapies in the posterior segment of the eye. However, in addition to being highly invasive, these injections are problematic for retinoblastoma, as they can result in tumor seeding, and are thus used cautiously after the failure of other treatment

options. [Munier 2013] Therefore, contact lenses were explored as an alternative drug delivery device.

Contact lenses have been investigated previously to deliver therapeutics, as they act as a slow, equilibrating reservoir and the prolonged corneal residence time improves bioavailability. [Hsu 2014, Schultz 2011] The increased prevalence of silicone extended wear lenses in the market [Morgan 2011] has created the option to use contact lenses for continuous drug delivery, with their utility being evaluated in many cases recently, showing significant promise. [Hsu 2014, Lasowski 2016, Bengani 2013, Hui 2014, Sankaridurg 2013] While it has been shown previously by our group that CYC202 can be incorporated into model silicone hydrogel materials by direct entrapment during synthesis and absorption after synthesis [Lasowski 2016], both of these suffer from practical limitations that reduce their potential as a clinical treatment. Since commercial silicone hydrogels are often extracted to remove unreacted monomers and initiators, much of the drug loaded during direct entrapment synthesis will be lost, leading to waste of drug and poor retention of the therapeutic agent in the final contact lens. Conversely, soaking the final lens in a solution of drug after production often results in a short-lived release profile, typically characterized by an initial burst release.

To overcome these issues, the present work aims to covalently incorporate CYC202 into a model silicone hydrogel lens using a labile bond. This method of incorporation would allow a release profile that can be more easily tailored to meet the specific disease needs and utilize a more industrially relevant synthetic method, all without changing the bulk properties of the lens. Specifically, a poly(ethylene glycol)

methacrylate (PEGMA) polymer with a degradable lactide linkage, previously described by Nuttelman et al., [2006, Benoit 2006], was covalently bonded with CYC202 and incorporated into model silicone lens materials, previously described by the Sheardown group. [Lasowski 2016, Guidi 2014, Weeks 2012] The varied lactide spacer units would presumably allow the tailorable release of the drug from the hydrogel matrix.

3.3. Materials and Methods

3.3.1. Materials

N,N-dimethylacrylamide (DMA) and ethylene glycol dimethacrylate (EGDMA) were purchased from Sigma-Aldrich Chemicals (Oakville, ON). CYC202 (Roscovitine) was purchased from Selleck (Houston, TX). 3-(3-methacryloxy-2-hydroxypropoxy) propylbis(trimethylsiloxy)methylsilane (modified TRIS or TRIS-OH) was purchased from Gelest Inc. (Morrisville, PA). Irgacure 184 was generously supplied by BASF Corp. Plexiglas G-UVT for casting molds was supplied by Altuglas (Bristol, PA). All other reagents were purchased from Sigma-Aldrich unless otherwise stated.

3.3.2. Synthesis of Drug Monomer (PEGMA-Lac-Suc-CYC202)

The synthesis for the degradable tether was based on work described by Nuttelman et al., [2006, Benoit 2006], although some modifications to the procedure were made to improve conversion and to simplify purification. Poly(ethylene glycol) methacrylate (PEGMA) (M_n~350 g/mol, 6.24 mmol) and dilactide were added in stoichiometric ratios 1:1 and 1:5 to prepare PEGMA-Lac2x and PEGMA-Lac10x

respectively. The contents were heated to 110°C to melt all of the dilactide, after which a catalytic amount of stannous octoate (0.03 mmol) was added. The contents of the flask were sealed and purged with nitrogen for 10 mins. The reaction mixture was stirred for 24hrs at 110°C. This resulting product (PEGMA-Lac) was then cooled to 70°C and succinic anhydride (18.72 mmol), 4-dimethylaminopyridine (DMAP) (0.32 mmol) and 35 mL chloroform were added to the reaction mixture. The contents were refluxed at 70°C for 72hrs and subsequently washed twice with 50 mL of HCl (0.1 M) and twice with 50 mL of saturated NaCl solution. The organic layer was dried over magnesium sulfate and filtered through Whatman #40 filter paper. The product (PEGMA-Lac-Suc) was dried under vacuum and ^{1}H NMR (NMR, Bruker, 600 MHz) was performed to confirm successful synthesis. PEGMA-Lac-Suc (0.2 mmol), diisopropyl carbodiimide (DIC) (0.2 mmol) and DMAP (0.1 mmol) were then dissolved in 15 mL of chloroform. CYC202 (0.2 mmol) was added and the solution was stirred at room temperature for 72 hrs in the dark. The reaction mixture was washed twice with 25 mL of HCl (0.01 M) and twice with 25 mL of saturated NaCl solution, with the organic layer dried over sodium sulfate and filtered through Whatman #40 filter paper. PEGMA-Lac-Suc-Ros was dried under vacuum and ^{1}H NMR was performed to confirm the product. The product was then dissolved in dichloromethane (DCM) and loaded onto a silica gel column for further purification. DCM was used to remove the reactants and side product and acetone was used to remove the product from the column. The fractions containing product were combined together and dried under vacuum. The product was characterized using ^{1}H NMR, to verify that the desired product was obtained and its purity. As controls,

PEGMA-Lac2x was prepared without the addition of CYC202 along with PEG-Lac2x-Ros which used a monomethoxy poly(ethylene glycol) in place of the poly(ethylene glycol) methacrylate in the appropriate stoichiometric amount.

3.3.3. Hydrogel Synthesis

Model hydrogel lenses were comprised of DMA and a silicone monomer, modified TRIS, in an 80:20 mol ratio as previously described. [Lasowski 2016] All were initiated with Irgacure 184 (~1 wt%) and crosslinked using EGDMA (3 wt%). Prior to use, monomethyl ether hydroquinone (MEHQ) was removed from the monomers by passing the reagents over inhibitor remover. The materials, outlined in Table 3.1, were prepared by mixing free drug or a drug-conjugated methacrylate with the hydrogel monomer solution. No degradation of the drug due to UV exposure or heat treatment was found when examined using ^{1}H NMR and UV-spectroscopy. Using Material 6 as an example, 43.9 mg of the PEGMA-Lac2x-Ros monomer, which contained 16.8 mg of CYC202, was dissolved in an 80:20 molar ratio of DMA:TRIS-OH solution containing 3 wt% EGDMA and allowed to mix for at least 10 minutes. For all of the materials, the amounts of DMA, TRIS-OH, and EGDMA were adjusted in order to achieve ~1 wt% of CYC202 incorporation in the final mixing solution. Irgacure 184 (0.8 wt%) was dissolved into the formulation then immediately placed into a UV-transparent acrylic plate mold and polymerized in a 400W UV chamber (Cure Zone 2 Con-trol-cure, Chicago, IL) for 15 minutes. The mold included a 0.5 mm Teflon spacer. The hydrogels were removed from the mold and individual discs were bored to 7.94 mm. While the aim

was to incorporate ~1 wt% CYC202, the actual amount of CYC202 incorporated was used for all drug loading and release calculations.

3.3.4. Material Characterization

3.3.4.a. Equilibrium Water Content

The equilibrium water content (EWC) was determined using a mass balance method. The masses of the dry discs (M_D) were obtained after drying in a 37°C for at least 48 hours. These were compared to the hydrated masses (M_H), as shown in Equation 1. The hydrated mass was obtained after soaking the discs in MilliQ water for 48 hours. Residual droplets were removed prior to the masses being examined.

$$EWC\% = \frac{M_H - M_D}{M_H} \cdot 100\% \qquad (1)$$

3.3.4.b. Transmittance

Using light transmittance, as measured by UV-VIS spectrophotometry (Spectramax Plus 384, Molecular Devices, Corp, Sunnyvale, CA, USA), the transparency of the hydrogels was assessed. Using a 48-well plate, 7.94 mm discs were hydrated in 250 µL of Milli-Q water for 48 hours and the transmittance was measured from 400 nm to 700 nm.

3.3.4.c. Organic Extractables

The organic extractable material was determined using a mass balance method. The masses of the initial dry discs (M_I) were obtained immediately after synthesis. These

were compared to the final masses (M_F), as shown in Equation 2. The disc materials were extracted together with isopropyl alcohol for 2 hours using a soxhlet at 110°C and dried for at least 72 hours at room temperature and a 37°C for 48 hours. To estimate the drug retention in the materials post extraction, the difference was calculated between the total amount of drug initially loaded in all of the discs used for extraction, determined by mass, and the amount of drug removed during extraction, assessed by UV at 293 nm. To calculate the initial drug loading for release experiments, this amount was divided by the total amount of drug initially loaded and expressed as a percentage. It is important to note that as these are done in a single large batch, these values are an estimate only, as it is not possible to quantify the error.

$$Extractables\% = \frac{M_I - M_F}{M_I} \cdot 100\% \quad (2)$$

3.3.4.d. Drug Release and Analysis

Control and drug-loaded discs were placed in 1 mL of PBS (pH 7.4) at 37°C; to ensure sink conditions, the discs were transferred to fresh PBS at regular intervals, initially at 1.5, 3.5, 6, 24 hours and then at least of intervals of at least 24 hours. The drug release was measured by UV-spectrophotometry (Spectramax Plus 384, Molecular Devices, Corp, Sunnyvale, CA, USA) at 293 nm. Tests were completed to ensure the free CYC202 and tethered CYC202 showed the same UV absorbance readings prior to testing, ensuring that all released CYC202 was accurately captured. The amount of CYC202 released was normalized to the dry mass of the disc. Percent drug release was calculated

as the average amount of drug released at that time point divided by the total amount of drug loaded into the material, as determined after the extraction.

3.3.4.e. Drug Activity

PEGMA-Lac10x-Ros was dissolved in a 50:50 mixture of D_2O and MeOD-d_4 (pH=5.0) and monitored by ^{1}H NMR, demonstrating the tether is stable under mildly acidic conditions. 50 μL deuterated PBS was added to the polymer, bringing the pH to 7.4 solution for physiologically-relevant degradation conditions. The degradation was monitored by ^{1}H NMR at 1 hour, 16 hours, 30 hours, 97 hours, 146 hours, 205 hours and 267 hours, at which point NaOH base was added to accelerate the degradation. The spectra were calibrated to the MeOD-d4 solvent residual peak at 3.31 ppm. The peak at 5.67-5.75 ppm, corresponding to one of the methacrylate CH_2 peaks, was integrated to an internal standard of 1. The lactide CH peak (5.03-5.29 ppm) was used to determine the extent of degradation over time.

3.4. Results

3.4.1. Synthesis of the Drug Monomer

The synthetic scheme for the synthesis of the tethered drug monomer is given in Figure 3.1. In Step 1, the number of lactic acid units added to the PEGMA chain was controlled by varying the molar ratio of PEGMA:dilactide, as previously described [Nuttelman 2006, Benoit 2006], with three different variants synthesized: Lac0x, Lac2x and Lac10x. The actual number of lactic acid repeats added was analyzed using ^{1}H NMR

($CDCl_3$ for Lac0x and Lac2x and acetone-d_6 for Lac10x) using the peaks produced by the methyl and methylene protons at ~1.5 and ~5.5/6.1 ppm, respectively, although this step was skipped for the Lac0x variant. This resulted in Lac2x having approximately 2 units on average and Lac10x having approximately 9 units on average. These three variants demonstrated the impact of the lactic acid repeat unit on the drug release. Specifically, Material 5 (Lac0x, with no lactide linker) was not present in the previous study, but was added here, as it was anticipated that this shorter linkage would lead to the longest release. As a control, Material 4 (PEG-Lac2x-Ros) was synthesized with PEG substituted for PEGMA in Step 1, with the intention of it serving as a control to determine the effect of a non-covalently bonded linker within the system, which was also not previously present.

In Step 2, the succinic anhydride ring was opened to add a terminal carboxyl moiety on the PEGMA-Lac-Suc monomer, [Nuttelman 2006, Benoit 2006] which would subsequently be used to covalently link the drug, CYC202, though altered reaction conditions improved conversion. The successful addition of the succinic acid was verified with ^{1}H NMR with the succinylated product peak appearing around ~ 2.6 ppm. Near quantitative conversion of the product was verified for all three of the tethered products.

As shown in Step 3, using diisopropyl carbodiimide (DIC) as the coupling agent, the carboxylic group on the tether monomer was coupled with the primary hydroxyl functional group on the CYC202 molecule. As a control, PEGMA-Lac2x was synthesized omitting this third step (covalently incorporating CYC202) and was used to determine the effect of the PEGMA and lactide on the material. ^{1}H NMR was used once again to verify

formation of product, using the CYC202 methyl peak appearing at around ~0.9 ppm. Further purification was required using a silica column to remove all of the urea impurities, which resulted in yields between 20 and 30%.

3.4.2. Material Characterization

3.4.2.a. Equilibrium Water Content

Since water content is often correlated to the on-eye comfort of contact lenses, the EWC of the model lenses were measured and shown in Table 3.2. All of the materials achieved 32-36% EWC, which is well within the 20-40% EWC range shown by most commercial contact lenses. [Efron 2007] As previously reported, both the incorporation of the modified TRIS and greater DMA content result in higher water contents, as these materials are more hydrophilic and thus are more likely to retain water in the hydrogel, and were therefore specifically chosen for this application. [Lasowski 2016] Similarly, as previously noted, the EWC of the materials were not substantially affected by the presence of the free drugs [Lasowski 2016] nor by the presence of the tethered drug monomer developed herein. This is likely due to the small amounts of drugs added relative to the bulk composition of the lenses.

3.4.2.b. Transparency of Hydrogel

Since high optical transparency is an essential property of a contact lens, it was necessary to determine how the various material compositions and drug loadings affected the light transmittance. At least 80% visible light transmittance is typical for contact

lenses, however transmittance is ideally greater than 90%. [Korogiannaki 2015] The materials were tested over the visible range wavelengths (400-700 nm), showing values exceeding 85% transmittance for all experimental materials, with Table 3.2 the transmittance at 600 nm specifically. The only exception was Material 3, a control material, which showed values around 75% at some of the lower wavelengths. The maintenance of the optical transparency was expected, as it was previously reported that model lenses retain their transparency despite drug loading. [Lasowski 2016] Again, since the amount of drug is small and it is fully dissolved in the monomer solution prior to curing, it is not expected that the drug itself will alter the hydrophobic domain formation occurring within the material due to the hydrophobic nature of the TRIS materials. Similarly, the incorporation of the PEGMA and the lactide units are also not sufficient to disrupt the domain formation, likely again to their small loading levels. Therefore, the potential application of these materials for contact lenses remains viable. Furthermore, the materials tested were approximately 0.5 mm in thickness. Since commercial contact lenses are much thinner than this, it is expected that these values would improve with a thinner sample, though this was limited by the molds used.

3.4.2.c. Organic Extractables

The organic extractables are shown in Table 3.3 for all materials. The control lens materials contained ~ 5% organic extractables, while materials containing CYC202 were slightly higher, having between 8-11% extractables; the tether control material (Material 3) was in between, at 6.4% extractables. While there is a slight upward trend in the

extractables for the materials which contained CYC202, many of these were not statistically significant. This is again expected, as the tether loading levels were a small percentage of the total material. The differences in the mass of the discs between the different materials likely contributed more to the difference in extractables, as some discs had quite small masses; this is a product of the mold used and was difficult to keep consistent. While the extractables were expressed as a percentage to try to account for this, it is likely that there is more error associated with the smaller sized discs, which were typically the drug-containing discs due to the molds used.

The estimate for drug loading is also provided in Table 3.3. Since all of the discs were extracted together in the soxhlet, it is not possible to estimate the error on these values. As expected, the free drug resulted in a lower amount of drug retained, approximately 33%. By comparison, the tethered drug retention ranged from 33-50%. Whiles these values are lower than expected, it is suspected that this variability was in part due to the presence of non-tethered CYC202 and tethered dimers in the drug monomer mixtures, as suggested from the NMR profiles after the column. In some instances, this appears to be up to 25% of the drug product, and it is likely these smaller or non-covalently attached components would more readily leave the material. It is anticipated that these values could be increased with a more refined elution protocol on the column. All drug release profiles have been modified based on the estimated loadings after extraction.

3.4.3. Drug Release

The drug release profiles from the hydrogel materials after extraction are shown in Figure 3.2. These values account for the specific amount of drug loaded into each material and the retention of the drug after extraction. Only the release values up to 400 hours are reported, as this has been estimated that the treatment duration for this condition would be approximately 14 days after birth. However, the release is expected to continue for a longer duration if needed.

All of these release profiles are characterized by a burst release, particularly with the lactide linkers, with a substantial amount of the drug being released in the first 24 hours. However, the relative amount of drug released during the burst varies according to the number of lactide units, with the greater number of lactides showing a smaller percentage of drug release associated with the burst portion. This suggests that the amount of drug in the burst phase could be controlled by drug loading and the length of the lactide tether. This burst could also be influenced by the composition of the hydrogel, as previous studies have shown that higher DMA amounts result in a larger burst release [Lasowski 2016]. All materials show a slower release rate after 100 hours, although a linear release rate is maintained. This similarity in profiles is not surprising as the water content of the materials is similar, and it is known that this influences the drug release. To effectively use CYC202 as a chemopreventative measure for retinoblastoma, a sustained, long lasting release profile of the therapeutic is required, so this profile is amenable to such an application.

When considering the two lactide spacers, the drug conjugate was released slower when covalently bonded into the material with the PEGMA than compared to its PEG counterpart. This was expected, as the non-covalently bonded drug conjugate could diffuse from the hydrogel intact, resulting in its increased exposure to hydrolytic degradation and thus releasing more CYC202. This suggests that this is an additional tailorable factor, as mixtures of conjugates could influence the overall release profile.

As expected, the conjugate with the greatest number of lactide units (Lac10) releases the fastest, which is consistently with previously reported results [Nuttelman 2006, Benoit 2006]. Conversely, when the lactide linker is removed (Lac0), the release is quite slow, and the material with two lactide units releases in between these values. As expected, the greater number of ester linkages increases the probability that CYC202 or its conjugate will be released in a given time, as the number of hydrolytically labile sites is greater. Since the water contents of these materials were all similar, it is expected that Lac10 would have the fastest release profile under these loading conditions, as the water content influences the diffusion rates and exposure for hydrolytic degradation; specifically, in highly swollen gels, pseudo first-order degradation kinetics of the lactide space have been previously reported [Nuttelman 2006, Benoit 2006]. However, it should be noted that there is likely a limit to the number of lactide linkages or drug conjugate loading levels, after which point they would impact the hydration of the hydrogel and could result in a slower release profile. Again, by including multiple tether lengths, specific release targets could be achieved.

Furthermore, as the number of lactide units increase, the likelihood of producing drug conjugates, where the CYC202 is still covalently bonded to lactide units, also increases. While the cellular activity of conjugated CYC202 has not been explored, it is anticipated that unconjugated drug will have the greatest in vivo activity; therefore, all the drug must eventually return to its free state, regardless of how it is released from the hydrogel. While it is expected that this would eventually occur, previous literature reports that the drug is successfully hydrolyzed within 12 hours in aqueous solution to free drug. [Nuttelman 2006] Furthermore, work by Siparsky et al. [1998] suggests that autocatalytic hydrolysis of poly(lactic acid) chains by the terminal lactic acid unit can speed up degradation of these units, resulting in the released drug being biologically active faster. This would render the breakage of the first ester bond, which would remove any part of the tether from the gel, the rate limiting step, and is representative of what we have measured in this study; however, this could be validated with in vitro cellular studies.

While only a small amount of CYC202 is expected to be required to exhibit its therapeutic effect, [Sangwan 2012] *in vivo* models are required to confirm the exact amount of drug. Therefore, these tailorable profiles with slow releases profile are likely ideal. The treatment regime with CYC202 is expected to be short for retinoblastoma. Therefore, having a burst release, as seen by all of the materials examined, may be beneficial, particularly as there are ways to tailor it based on material composition and varied amounts of covalently and non-covalently incorporated drug. Therefore, depending on the treatment time required, the most appropriate drug loading combination could be selected. It is important to note that these materials are thicker than commercial lenses,

and thinner discs are expected to have an increased release rate, as it is believed this is controlled by diffusion. However, other factors such as the release medium, mixing and most importantly the release volume, may also slow these release parameters relative to the experimental conditions. Therefore, this would require further testing in an *in vivo* system.

3.4.4. Drug Activity

This study was completed to determine how quickly the lactide units are breaking and confirm that over time, all of the lactide units would break to fully release the drug. At pH 5, the peaks corresponding to the lactide CH were stable, and thus this was used to store the material before the study began. PBS was added to the sample adjusting the pH to 7.4. This was chosen for the bulk of the study, as it is within the pH range of human tears [Abelson 1981] and could be deuterated for the purpose of NMR. As seen in Figure 3.3, the degradation of the lactide units begins almost immediately, though this rate slows around 100 hours, at which point approximately 30% of the lactide bonds have been degraded. However, there remains steady degradation throughout the study, with 40% degradation apparent after the 11 days. This corresponds well to the drug release curves, as the releases from the lactide linkers begin to also slow around the 100 hour mark. To show that all of the bonds would eventually be degraded, base (NaOD) was added to accelerate the degradation, adjusting the pH to 13. Within 24 hours, the NMR confirmed that all of the ester lactide CH bonds and succinic ester bond were eliminated, demonstrating complete degradation to free lactic acid and succinic acid.

3.5. Conclusions

In order to minimize the need for frequent or invasive instillations of high concentrations of drug, model silicone hydrogel materials were examined for their potential to deliver CYC202. The drug was covalently incorporated into the lenses with a labile bond to ensure manufacturability in commercial settings without substantially changing the bulk properties of the lenses. From this study, it is clear that the drug release can be altered based on the drug conjugate components and drug loading, meaning that the lens materials can be tailored to some extent in order to obtain the desired release kinetics. Specifically, longer lactide spacers provide a faster release than shorter spacers. Sufficient drug loading is possible from the initial manufacture of the lenses and can be varied to deliver an ideal cumulative release. These materials present a potential industrially-relevant method to deliver CYC202 as a chemo-preventative agent for retinoblastoma that would be appropriate for use with children.

3.6. Acknowledgements

The authors would like to acknowledge the financial support of the C20/20 Ontario Research Fund.

3.7. References

Abelson MB, Udell IJ, Weston JH. Normal human tear pH by direct measurement. Archives of Ophthalmology 1981;99:301.

Bengani L, Chauhan A. Are contact lenses the solution for effective ophthalmic drug delivery? Future Medicinal Chemistry 2012;4:2141-3.

Benoit DSW, Nuttelman CR, Collins SD, Anseth KS. Synthesis and characterization of a fluvastatin-releasing hydrogel delivery system to modulate hMSC differentiation and function for bone regeneration. Biomaterials 2006;27,6102–6110.

Brantley MA, Jr., Harbour JW. The molecular biology of retinoblastoma. Ocul Immunol Inflamm 2001;9:1-8.

Bremner R, Sage J. Cancer: The origin of human retinoblastoma. Nature 2014;514,312–313.

Efron N, Morgan PB, Cameron LD, Brennan NA, Goodwin M. Oxygen permeability and water content of silicone hydrogel contact lens materials. Optometry and Vision Science 2007;84:328-33.

Guidi G, Korogiannaki M, Sheardown H. Modification of Timolol Release From Silicone Hydrogel Model Contact Lens Materials Using Hyaluronic Acid. Eye & Contact Lens-Science and Clinical Practice 2014;40:269-76.

Hsu KH, Gause S, Chauhan A. Review of ophthalmic drug delivery by contact lenses. Journal of Drug Delivery Science and Technology 2014;24:123-35.

Hui A, Willcox M, Jones L. In Vitro and In Vivo Evaluation of Novel Ciprofloxacin-Releasing Silicone Hydrogel Contact Lenses. Investigative Ophthalmology & Visual Science 2014;55:4896-904.

Kim J, Conway A, Chauhan A. Extended delivery of ophthalmic drugs by silicone hydrogel contact lenses. Biomaterials 2008;29:2259-69.

Korogiannaki M, Guidi, G, Jones, L, Sheardown H. Timolol maleate release from hyaluronic acid-containing model silicone hydrogel contact lens materials. J. Biomater. Appl. 2015;30,361–76.

Lasowski F, and Sheardown H. Atropine and Roscovitine Release from Model Silicone Hydrogels. Optometry and Vision Science 2016;93,404–411.

Morgan PB, Efron N, Helland M, Itoi M, Jones D, Nichols JJ, van der Worp E, Woods CA. Global trends in prescribing contact lenses for extended wear. Cont Lens Anterior Eye 2011;34:32-5.

Munier FL, Gaillard MC, Balmer A, Beck-Popovic M. Intravitreal chemotherapy for vitreous seeding in retinoblastoma: Recent advances and perspectives. Saudi J. Ophthalmol. 2013;27,147–150.

Nuttelman CR, Tripodi MC, Anseth KS. Dexamethasone-functionalized gels induce osteogenic differentiation of encapsulated hMSCs. J. Biomed. Mater. Res. Part A 2006;76A,183–195.

Pacal M, Bremner R. Insights from animal models on the origins and progression of retinoblastoma. Curr Mol Med 2006;6:759-81.

Sangwan M, McCurdy SR, Livne-Bar I, Ahmad M, Wrana JL, Chen D, Bremner R. Established and new mouse models reveal E2f1 and Cdk2 dependency of retinoblastoma, and expose effective strategies to block tumor initiation. Oncogene 2012;31:5019-28.

Sankaridurg P, de la Jara PL, Holden B. The Future of Silicone Hydrogels. Eye & Contact Lens-Science and Clinical Practice 2013;39:125-9.

Schultz C, Breaux J, Schentag J, Morck D. Drug delivery to the posterior segment of the eye through hydrogel contact lenses. Clin Exp Optom 2011;94:212-8.

Siparsky GL, Voorhees KJ, Miao F. Hydrolysis of Polylactic Acid (PLA) and Polycaprolactone (PCL) in Aqueous Acetonitrile Solutions: Autocatalysis. J. Polym. Environ. 1998;6,31–41.

Weeks A, Morrison D, Alauzun JG, Brook MA, Jones L, Sheardown H. Photocrosslinkable hyaluronic acid as an internal wetting agent in model conventional and silicone hydrogel contact lenses. Journal of Biomedical Materials Research Part A 2012;100A:1972-82.

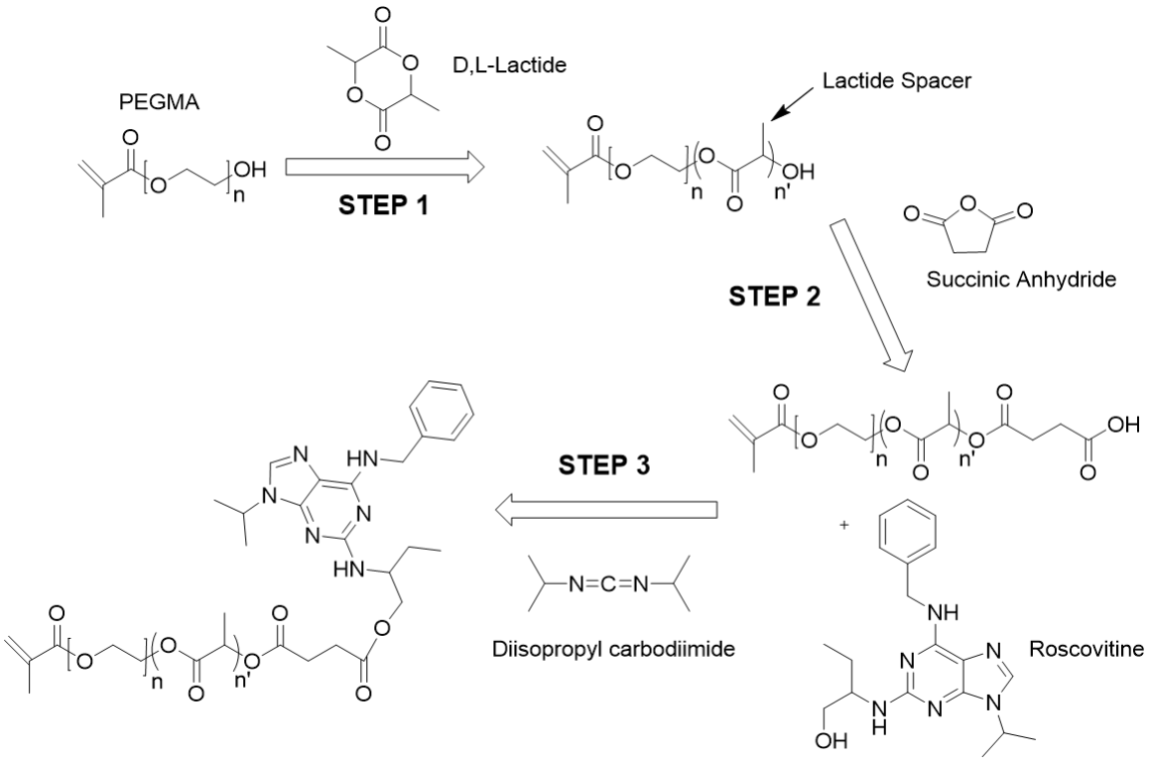

Figure 3.1 Synthetic scheme for drug conjugate (PEGMA-Lac-Suc-CYC202).

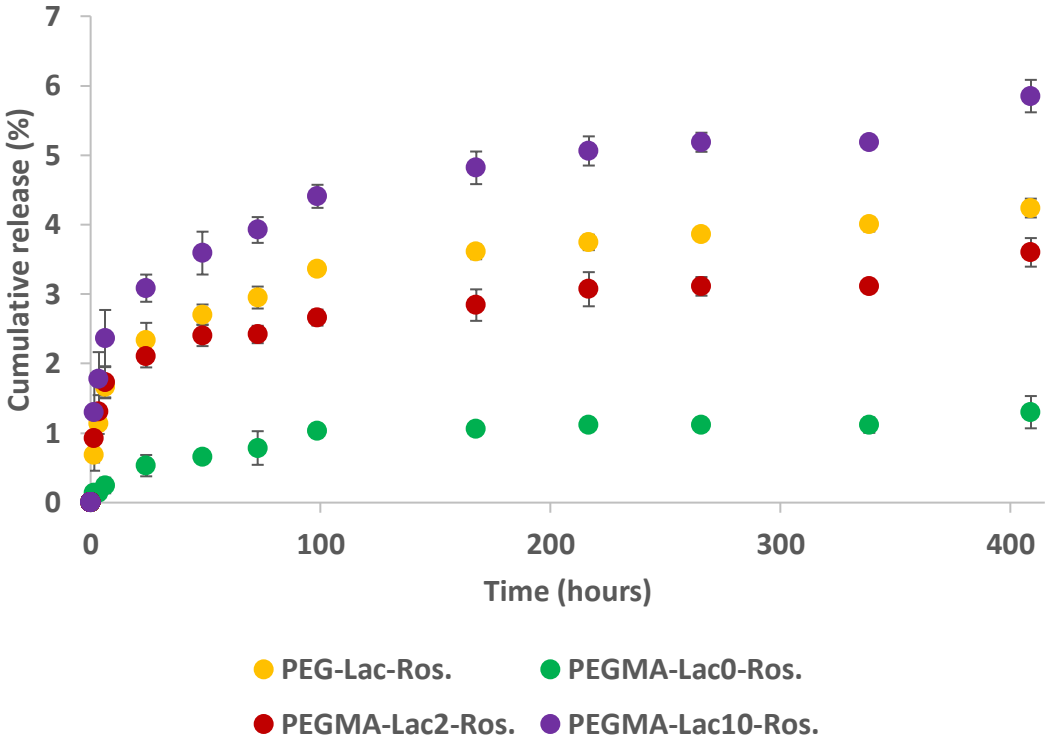

Figure 3.2 CYC202 release from various materials after extraction.

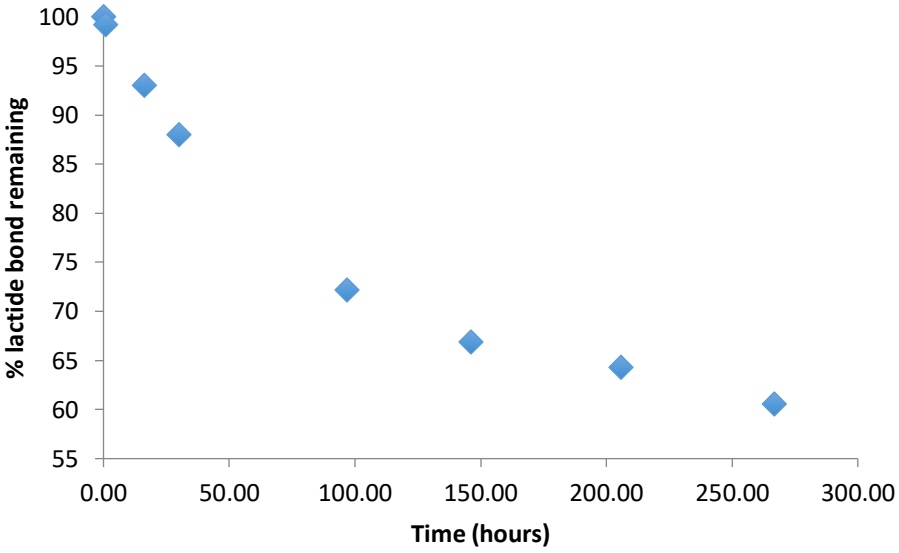

Figure 3.3 Lactide bond degradation in PBS (pH 7.4) as determined by ^{1}H NMR.

Table 3.1 Hydrogel compositions, noting both the hydrogel composition and the drug tether amounts.

	Material Name	DMA (mol%)	TRIS-OH (mol%)	EGDMA (wt%)	Irgacure 184 (wt%)	Relevant Tether (wt%)	CYC202 (wt%)
1	Control	77.5	19.4	3.0	0.8	-	0
2	Free Drug	77.2	19.3	2.9	0.7	-	0.97
3	PEGMA-Lac2x	77.1	19.3	2.9	0.8	1.60	0
4	PEG-Lac2x-Ros	77.1	19.3	2.9	0.8	2.56	0.98
5	PEGMA-Lac0x-Ros	77.1	19.3	2.9	0.9	2.17	0.98
6	PEGMA-Lac2x-Ros	77.1	19.3	2.9	0.8	2.55	0.98
7	PEGMA-Lac10x-Ros	77.0	19.2	2.8	1.0	4.05	0.96

Table 3.2 Equilibrium water content (n=4) and optical transmittance values (n=3) for the hydrogel materials after extraction. Optical transmittance values were obtained at 600 nm.

Material	Average EWC (%)	Transmittance (%)
1	32.1 ± 0.6	98.4 ± 0.4
2	35.2 ± 0.8	98.5 ± 1.2
3	35.4 ± 1.0	98.7 ± 0.4
4	33.6 ± 0.7	98.6 ± 0.1
5	32.2 ± 0.3	97.1 ± 1.7
6	34.8 ± 0.4	98.5 ± 0.3
7	35.9 ± 1.0	98.8 ± 0.5

Table 3.3 Organic extractables for the hydrogel materials after soxhlet extraction. The error is expressed as a percentage based on the standard deviations of the assumed pairings. The drug bound is an estimate of how much CYC202 remained in the material after the soxhlet extraction process.

Material	Extractables (%)	Drug Bound
1	5.1 ± 1.5	N/A
2	10.7 ± 1.7	33%
3	6.4 ± 1.2	N/A
4	10.8 ± 0.8	43%
5	10.6 ± 5.1	50%
6	8.7 ± 1.8	33%
7	8.0 ± 1.7	46%

4. Self-Assembling Amphiphilic Materials for Use in Sustained Ocular Drug Delivery

Frances Lasowski[1], Vida Rahmani[1], Sharon Sagnella[2], Heather Sheardown[1*]

[1]Department of Chemical Engineering, McMaster University, 1280 Main Street West, Hamilton ON L8S 4L7, Canada

[2]CSIRO Molecular and Health Technologies, PO Box 184, North Ryde, NSW 1670, Australia

Corresponding author: sheardow@mcmaster.ca

Objectives:
This work sought to create a self-assembling material from two known pure materials that formed a cubic phase at appropriate physiological conditions, which would enable its use for drug delivery in ocular applications. Once appropriate materials were created, the aim was to understand the kinetics of drug delivery from these material in sink conditions.

Main Scientific Contributions:
- Preparation of materials at various LEA and OEA compositions.
- Characterization of these various material compositions.
- Preparation of drug loaded materials at various loading levels.
- Characterization of the drug loaded materials.
- Investigating drug release from the various materials, noting the differences in kinetics particularly as they relate to the various material compositions and drug loading levels.

Author Contribution:
Frances was responsible for all experimental ideation and planning, as well as conducting most of the experimental work (all work related to synthesis, DSC, water penetration, DLS, SAXS and most of the drug release experiments) and paper write-up. Dr. Vida Rahmani conducted one drug release according to the experimental plan. The work was done in consultation with and under the supervision of Dr. Sharon Sagnella while at CSIRO in Australia (all work related to synthesis, DSC, water penetration, DLS and SAXS) and Dr. Heather Sheardown while at McMaster (drug release and material degradation). Dr. Heather Sheardown revised the draft to the final version.

4.1. Abstract

Amphiphilic molecules which self-assemble in excess water and are stable against dilution have been explored as potential sustained-release drug delivery materials. In this study, combinations of the endogenous molecules oleoylethanolamide (OEA) and linoleoylethanolamide (LEA) were explored for the potential delivery of roscovitine, R547 and atropine in a transscleral application. It was found that materials consisting of 80-90% LEA exhibited the best properties at physiologically relevant conditions. When loaded with various drugs, sustained delivery over at least a month was possible into sink conditions for all drugs. The release profiles could be tailored based on the type of drug, its loading levels, and the material composition. Specifically, loadings around 5% for atropine and roscovitine both displayed release profiles that appeared to be influenced by both diffusion and the degradation of the bulk material. These materials therefore have the potential to be used for the treatment of retinoblastoma and myopia in children.

4.2. Introduction

Ocular drug delivery remains a challenge and would benefit from sustained-release formulations that would enable therapeutic drug concentrations for multiple days with a single dose. [Gaudana 2010] Such a formulation would reduce the frequency of administration, increasing patient compliance, [Hsu 2014] and reduce unwanted side effects associated with current overdosing protocols. Lyotropic liquid crystals, which are amphiphilic molecules that self-assemble in excess water and are stable against dilution, could be used as a formulation to enable this sustained-release. While the phase behaviour

and self-assembly of these molecules has historically been examined to understand their role in biomembranes, more recently their role in controlled drug delivery has been explored. [Sagnella 2009, Conn 2013]

In particular, this could help overcome current drug delivery limitations in the eye, where current non-invasive treatments, such as eye drops, result in extremely low drug penetration to the ocular tissue and potential systemic side effects. [Kim 2008] Instead, these self-assembled amphiphiles could be used in a transscleral approach, overcoming the need for frequent eye drop instillation. This would be particularly beneficial for diseases in paediatric populations, such as myopia and retinoblastoma, which can be treated pharmaceutically with atropine [Chia 2009] and roscovitine [Sangwan 2012] respectively but which require ongoing management and can be challenging to deliver. [Shih 1999]

The hydrophilic and hydrophobic domains of amphiphiles allow them to self-assemble into aggregates, generally in an attempt to minimize the interaction of the hydrophobic components with the water solvent. [Kaasgaard 2006] These materials are capable of forming five phases, which can be “normal” or “reverse”, depending on their packing parameter, as shown in Figure 4.1. However, the molecules of interest in the current work have an effective reverse wedge shape. [Sagnella 2010A] These phases are important for drug delivery, as the release kinetics would be strongly impacted by the phase formed at a given temperature and water content.

The first phase is a fluid lamellar phase, consisting of a one-dimensional stack of flat amphiphilic bilayers. The next is an inverse bicontinuous cubic phase that forms at

relatively low curvatures and consists of a single continuous bilayer that subdivides space into two interpenetrating, but not connected, water networks. These are further characterized as Pn3m, Im3m and Ia3d depending on their crystallographic space group, based on the Schwartz diamond, primitive and Schoen gyroid minimal surfaces respectively. [Kaasgaard 2006, Tyler 2015] This phase is of the most interest for drug delivery applications. [Sagnella 2010A, Sagnella 2010B] These can then transition to a hexagonal phase, which appears as cylinders. Finally, disordered packing leads to a L_2 inverse micellar phase. These transitions are shown in Figure 4.2, with the reverse bicontinuous cubic phases shown in Figure 4.3.

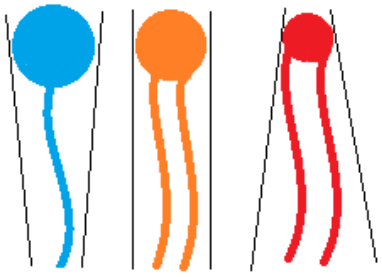

Figure 4.1 Amphiphiles of different shapes, forming a "normal" phase on the left (blue), lamellar phase in the centre (orange) and "reverse" phase on the right (red) [Adapted from Kaasgaard 2006].

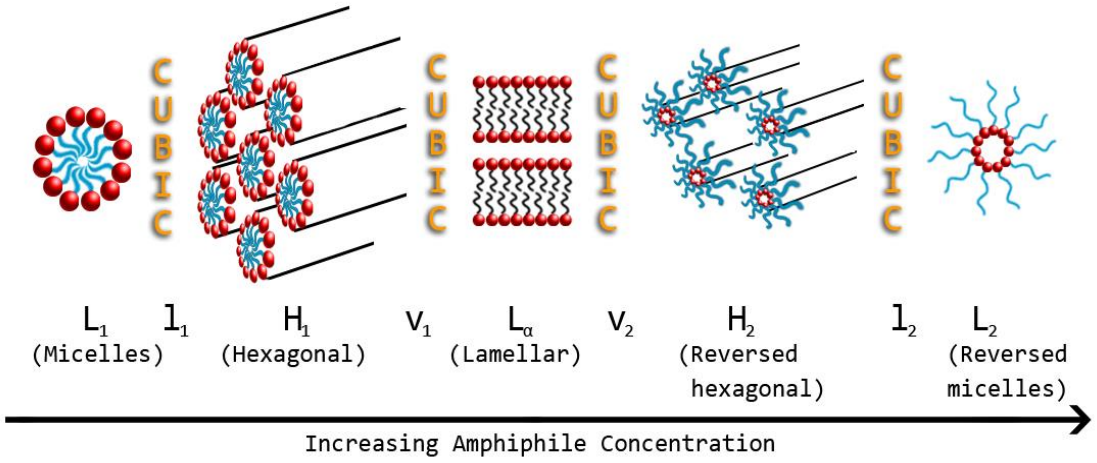

Figure 4.2 The "ideal" sequence of phases of amphiphile concentration and temperature. Subscripts 1 and 2 refer to "normal" and "reverse" phases respectively [Adapted from Kaasgaard 2016].

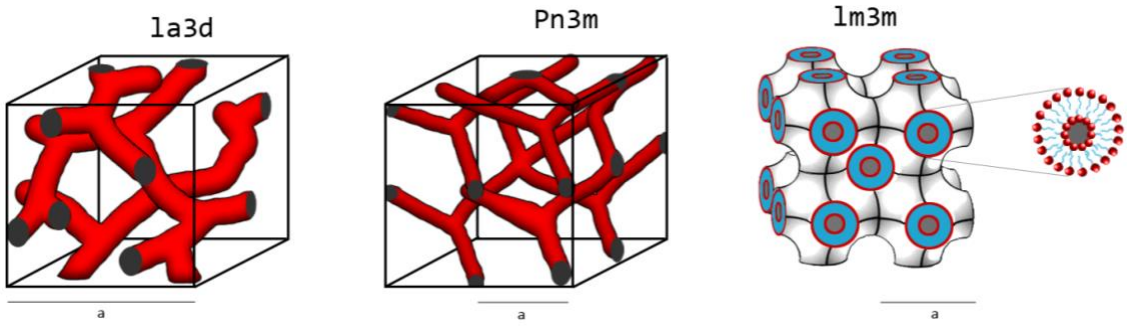

Figure 4.3 The three observed reverse bicontinuous cubic phases [Adapted from Kaasgaard 2016].

Oleoylethanolamide and linoleoylethanolamide, whose structures are shown in Figure 4.4, are endogenous unsaturated *n*-acylethanolamides that are thought to have the

potential to provide a matrix for sustained drug release. [Sagnella 2010A] However, both of these molecules form cubic phases at temperatures that are not ideal for ocular delivery.

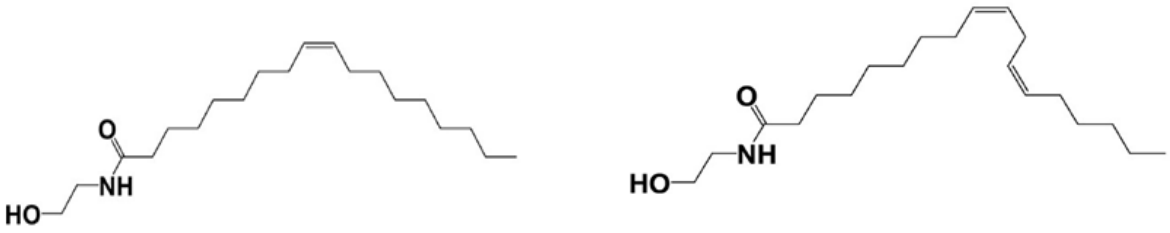

Figure 4.4 Structure of amphiliphiles- oleoylethanolamide (OEA) on left, linoleoylethanolamide (LEA) on right.

It was hypothesized that new materials, synthesized as mixtures of these pure amphiphiles, would yield properties more amenable to drug delivery for the anterior and posterior segments of the eye, specifically having transitions at appropriate temperatures while providing long term controlled drug release. It is believed that while the incorporation of therapeutics into these new materials will change their properties, these combinations will be amenable to sustained drug release.

4.3. Materials and Methods

4.3.1. Materials

All reagents were purchased from Sigma-Aldrich. Atropine was purchased from Sigma-Aldrich Chemicals and roscovitine was purchased from Selleck (Houston, TX). A Milli-Q Plus Ultrapure water system was used to obtain high purity water.

4.3.2. Monoethanolamide Amphiphile Synthesis

The monoethanolamides were prepared as described previously. [Sagnella 2010A, Ramakrishnan 1997] Briefly, the fatty acids were dissolved in dichloromethane (DCM) and reacted with 2 mol equivalents of oxalyl chloride for 2 hours. Excess oxalyl chloride was evaporated and the resulting fatty acid chloride was added dropwise to 2 mol equivalent ethanolamide in DCM for 2 hours. The resulting product was filtered using Whatman 542 filter paper and rinsed sequentially with 4% citric acid, 4% bicarbonate solution and Milli-Q water. The purity of each monoethanolamide, oleoylethanolamide (OEA) and linoleoylethanolamide (LEA), was determined by NMR, HPLC and LC/MS. For the mixture products, these pure materials were combined in set ratios after being dissolved in tert-butanol (TBA), and identified subsequently according to the amount of LEA in the mixture. The TBA was subsequently removed to yield the final mixtures.

4.3.3. *Dispersions*

Dispersions were created using a modification of the methods by Fong et al., [2005] whereby various mixtures were mixed at high shear with an Ultraturrax homogenizer for 5 minutes and stabilized using poloxamer-407 (1% w/w) dissolved in Milli-Q water. The particle sizes were then measured using a Malvern Zetasizer Nano ZS (Malavern Instruments, Sutherland, Australia) at room temperature. Samples that did not create a stable, liquid mixture at room temperature were not examined.

4.3.4. Differential Scanning Calorimetry

To characterize the materials, differential scanning calorimetry (DSC) was performed using a Mettler DSC822 system with a Mettler TSO 801RO sample robot (Mettler Toledo, Melbourne, Australia) to determine the energies and peak temperatures of the endotherms. Samples were run at a scan rate of 2.5°C/min and data were collected using the STARe software package. Some samples were run at 0.1°C/min to resolve overlapping peaks. Calibrations were based on an indium peak.

4.3.5. Water Penetration into Amphiphiles

Water penetration into the amphiphiles was assessed using an Olympus GX51 inverted optical microscope (Olympus Allustralia Pty. Ltd., Melbourne, Australia) via polarizing optical microscopy in the presence and absence of cross polarizing lenses. A small amount of crystalline monoethanolamine amphiphile was placed onto a microscope slide and heated to melting. A cover slip was placed over the melted amphiphile and it was cooled to room temperature prior to the addition of water, which subsequently infiltrated the amphiphile by means of capillary action. Then, these samples were heated at a maximum rate of 1°C/min by a Linkam PE94 hot stage (Linkam Scientific Instruments Ltd., Surry, England) and allowed to equilibrate before the analysis was completed.

4.3.6. Small Angle X-ray Scattering

Small angle x-ray scattering (SAXS) was used to determine phase assignment and lattice parameters for all materials at various temperatures. For the dispersion results, the Australian synchrotron (point collimation) was used. Here, samples of known water content were prepared and allowed to equilibrate for at least 12 hours in capillary tubes. Tests were conducted with consultation and supervision from experts at the Australian National University (ANU), CSIRO and Synchrotron staff according to typical policies. Exposure times included 1 second, 2 seconds and 5 seconds, with temperatures increasing in 5 degree increments with an opportunity for equilibration. The vials were sealed to ensure evaporation could not affect the phases. All other materials were tested at ANU using a custom SAXS machine (line collimation). Here, paste cells were used, allowing for samples that were substantially more viscous. Temperatures examined were 25, 35 and 45°C, with 30 minute equilibration time allotted between tests. All results were analyzed using SAXSquant, with phase assignment and lattice parameters determined based on characteristic X-ray diffraction peaks with reciprocal spacings. [Sagnella 2010A, Angelov 2003]

4.3.7. Drug Release & Amphiphile Degradation Studies

Atropine, roscovitine and R547 were dissolved in DCM and added to the amphiphile mixtures in the indicated amounts (5 or 10% w/w) then aliquoted into vials. The DCM was then evaporated off and 37°C Milli-Q water added to the samples, resulting in a total volume of either 5 mL or 10mL. These volumes were confirmed to be sufficient to maintain sink conditions for the relative samples. Samples were placed in a

shaking 37°C incubator. The water was substantially replaced at regular intervals (for example, 9 mL replaced with fresh water in a 10 mL sample); this prevented any disturbance to the samples themselves. Individual drug release results were analyzed by UV-spectrometry or HPLC at 254 nm for atropine, 293 nm for roscovitine and 320 nm for R547.

Degradation studies were performed at pre-set time intervals. The samples were weighed and placed in vials, with the mass of the vial noted. 10mL of water was added to each of these samples. At the pre-determined intervals, the water was removed from the samples and the samples were allowed to dry for 3 days at 37°C. The differential weights were noted.

4.4. Results and Discussion

4.4.1. Water Penetration

Water penetration scans of the amphiphile systems were examined for LEA amounts ranging from 0% to 100% in 5%-10% intervals. This involved the direct observation of the birefringence to obtain a rapid assessment of the lyotropic behaviour of the mixtures. Under cross polarizers, dark bands indicate cubic and micellar phases and textured birefringent bands indicate anisotropic phases, such as lamellar and hexagonal. [Rosevear 1954] Without cross polarizers, it is possible to determine the number of isotropic phases based on refractive index discontinuities. Taken together, the sequence of phases formed at the interface allows for circumstantial phase identification based on the viscosity and texture. [Sagnella 2010A]

For all materials examined, self-assembled, polarized phases developed as water content and temperature increased. Importantly, as the amount of LEA in the material increased, the temperature at which the polarized phases formed decreased. This was expected, as the greater unsaturation results in an increased volume, which in turn promotes a more wedge-shaped molecule that has an increased desire for curvature; this then yields a phase further along the continuum shown in Figure 4.2. This was consistent with the lower cubic phase transition temperatures of LEA compared to OEA in previous work. [Sagnella 2010A] These data are also supported by the SAXS analysis.

Figures 5 and 6 show two example mixtures at different temperatures: 30% LEA sample at 37°C and 60% LEA at 45°C with and without cross polarizers. In Figure 4.5, an anisotropic phase (lamellar), which appears as a textured band, is visible at low water content and isotropic phases are visible at higher water content. SAXS data, shown later, was required to identify the specific isotropic phase.

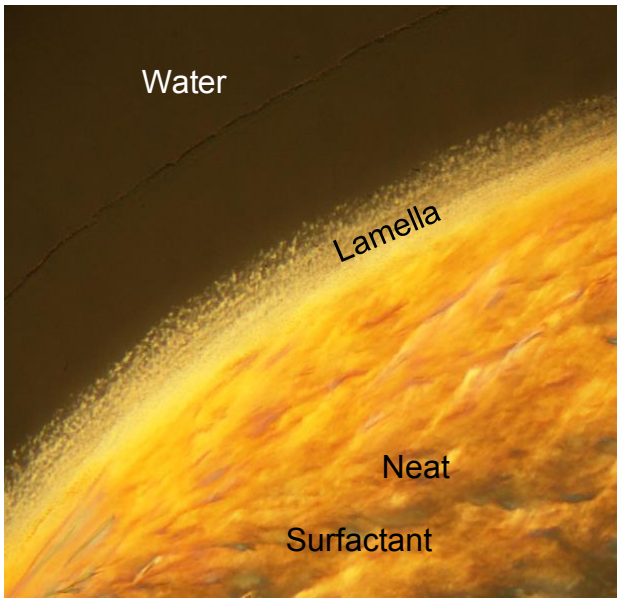

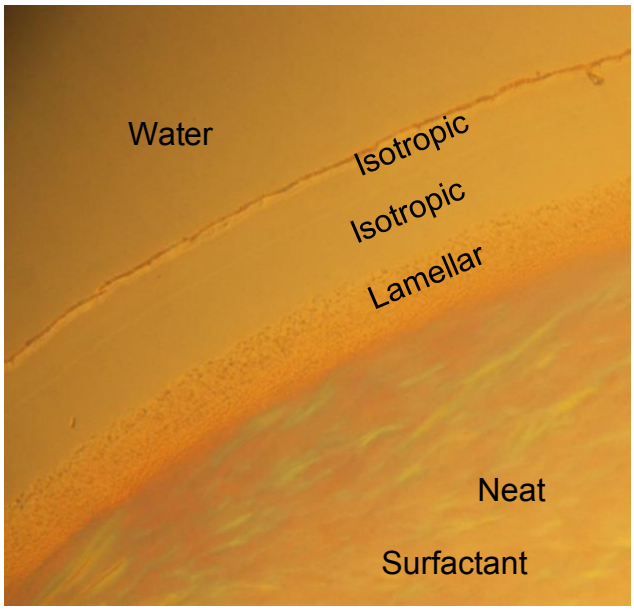

Figure 4.5 30% LEA at 37°C with cross polarizers (left) and without cross polarizers (right).

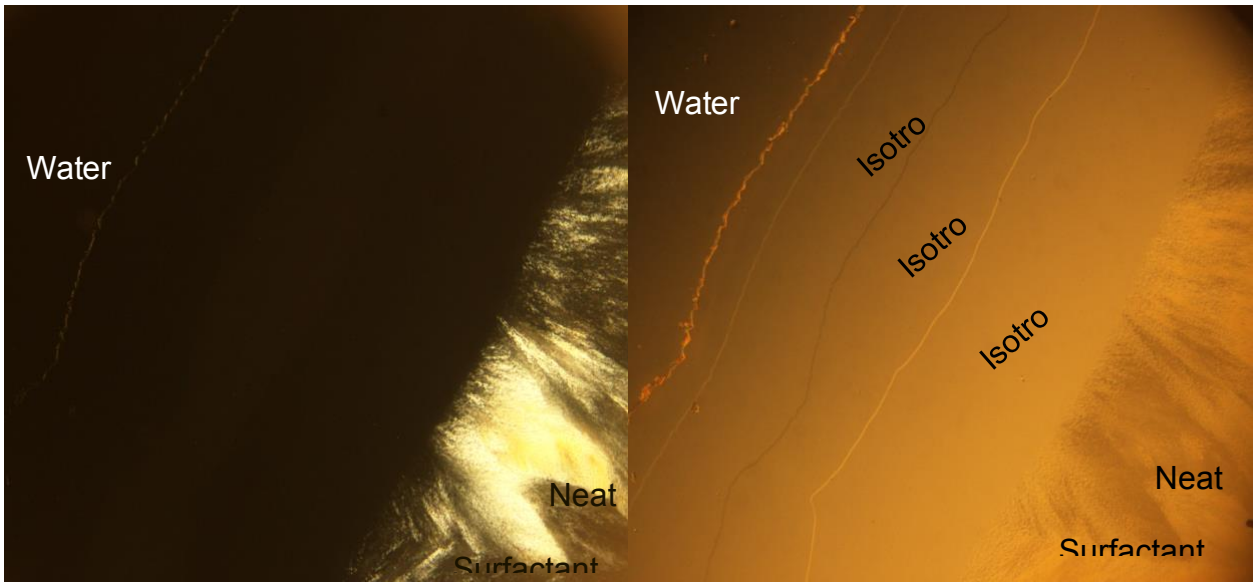

Figure 4.6 60% LEA at 45°C with cross polarizers (left) and without cross polarizers (right).

Similarly, Figure 4.6 shows a 60% LEA sample at 45°C with and without cross polarizers. Here, only isotropic phases at the water/amphiphile interface are visible. This trend indicates that the phase behaviour can be manipulated based on the composition, temperature and water content, which could be used to tailor drug delivery for specific applications.

4.4.2. Differential Scanning Calorimetry (DSC)

Differential scanning calorimetry results were obtained for all mixtures of LEA; the results for select mixtures are shown in Figure 4.7. Each mixture experienced transition temperatures between that of the pure OEA and LEA transitions, as indicated

by the peak maxima of the endotherms. The measurements for the pure compounds were consistent with previous work, with the melting temperature of pure OEA occurring around 60°C and pure LEA occurring around 40°C. [Sagnella 2010A] These transition temperatures were also consistent with the crystal-isotropic transition temperature observed during the water penetration scans. As the amount of LEA in the materials increased, the transition temperature decreased until it reached that of pure LEA. This was expected, as the additional *cis* unsaturation disrupts the close packing of the crystal structure, which in turn lowers the melting point. This relationship between the degree of unsaturation in amphiphiles and the transition temperatures has been seen previously, including with other C18 amphiphiles that differed in the polar head group. [Sagnella 2010A, Wells 2006]

There are small endothermic pre-transitions visible in all samples characteristic of long saturated chain fatty acids. [Ramakrishnan 1997] As in previous work, [Sagnella 2010A] the OEA samples display two pre-transitions, while the LEA samples display only one. The mixtures appear to display a combination, with lower LEA content showing two and higher LEA content displaying one. The pre-transitions likely represent polymorphic transitions. This is suspected because pure oleic acid, from which OEA is derived, has a well-documented transition from the γ- to α- form. [Sagnella 2010A] The difference between these two forms is the conformation of the hydrocarbon chain between the double bond and terminal methyl group. In the γ-form they are all in the trans structure, however they become disordered and liquid-like in the α-form. [Sagnella

2010A, Inoue 2004A, Inoue 2004B] Therefore, it is likely that these transitions represent a similar phenomenon.

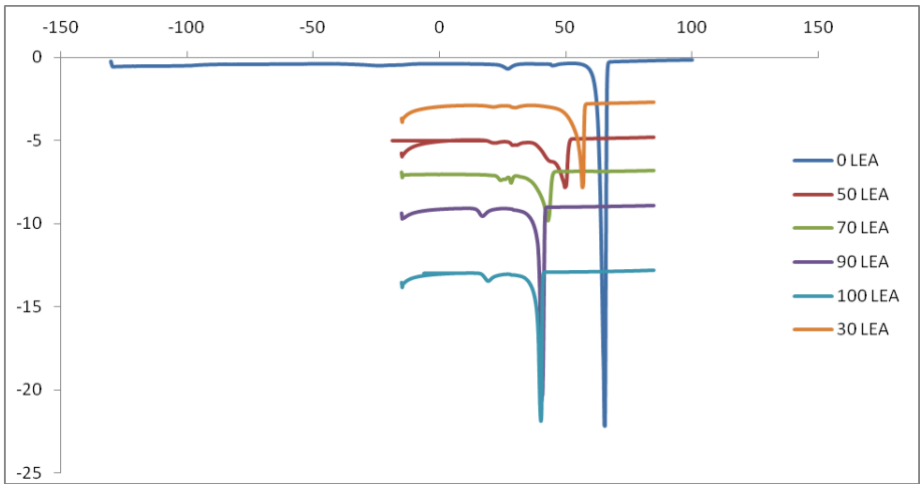

Figure 4.7 Differential scanning calorimetry of pure OEA, pure LEA and various mixtures of the two components. Scan rate 2.5°C/min.

4.4.3. SAXS

Small-Angle X-ray Scattering (SAXS) analysis was performed to assign the cubic phase present at various temperatures for materials of varying LEA content. This was used to compliment other analysis techniques. Experiments using paste cells were performed with 10% water and excess water (40%) at temperatures ranging from 25°C to 45°C. Relevant samples demonstrating the overall trends in temperature and lattice parameter are shown in Table 4.1.

These results confirmed that, in excess water, cubic phases, namely Pn3m, were formed at temperatures below 35°C for materials containing higher amounts of LEA. This is ideal, as a cubic phase would be preferred for drug delivery, and this would likely be

around 35-37°C in the eye and elsewhere in the body. By 45°C, the highest amounts of LEA had melted to an L_2 state, suggesting that in a warmer environment, the phase structure breaks down. This would not work well for drug delivery, as it would likely result in the dumping of the drug; however, this should not be the case at physiological conditions with the correct mixtures. Furthermore, there is a phase change observed in the same mixtures depending on the water content, suggesting that this also plays a role in the drug delivery possibilities. This suggests that a mixture could be chosen that has a flowing phase at 10% water but a cubic phase at excess water. Therefore, the material could be injected to the required site, which ideally is in an aqueous environment, and undergo a phase transition to cubic phase for the controlled delivery of the drug. It is expected, however, that once on the eye or in the body, the conditions would be the equivalent of excess water, and thus all drug release experiments were conducted based on this scenario.

These results also showed that the presence of therapeutic agents alters the material's phase transitions in a similar fashion to an increase in temperature. This is expected, as the drug likely interferes with the packing arrangement of the molecules, and causes them to take on a higher curvature, which in turns leads to the development of different phases.

Table 4.1 Example SAXS phases and lattice parameters, as determined by analysis with paste cells at ANU. The +/- shows the error on the parameter measurement, where the % Error suggests the likelihood that the phase determination is incorrect.

Material	Tempera-ture (°C)	Cubic Phase	Lattice Parameter	+/-	% Error
30 LEA, Excess Water	25	Lamellar	4.764	0.016	0.330
	35	Pn3m	8.584	0.121	1.406

	45	Pn3m	8.094	0.055	0.682
70 LEA, 5% R547,10% Water	25	Ia3d	9.131	0.033	0.357
		Pn3m	6.738	0.012	0.172
	35	L_2	3.640	-	-
	45	L_2	3.655	-	-
70 LEA, 5% R547, Excess Water	25	Pn3m	9.101	0.025	0.272
	35	Pn3m	8.231	0.011	0.132
	45	Pn3m	7.796	0.012	0.149
90 LEA, Excess Water	25	Pn3m	10.214	0.076	0.743
	35	Pn3m	7.755	0.021	0.276
	45	L_2	4.431	-	-
90 LEA, 10% cyc202, Excess Water	25	Pn3m	7.836	0.114	1.455
	35	Pn3m	7.351	0.027	0.367
	45	L_2	3.716	-	-

Results obtained for dispersions using capillary tubes at the Australian Synchrotron are shown in the Table 4.2. In some of these instances, only one or two diffraction peaks were observed, and thus a definite phase assignment is not possible. Therefore the most likely phase assignment based on the SAXS measurements, visual observations via polarizing microscopy and a comparison with previously reported systems are shown. The resultant phases were different from the paste samples also in excess water, likely due to the presence of a stabilizer. The phases and transition temperatures seen in both types of SAXS analysis are consistent with the observed melt from the water penetration experiments and the phase transition temperatures observed with the DSC.

Table 4.2 Example SAXS phases and lattice parameters, as determined by analysis with capillary tubes at the synchrotron. The +/- shows the error on the parameter measurement, where the % Error suggests the likelihood that the phase determination is incorrect.

Material	Temperature (°C)	Cubic Phase	Lattice Parameter	+/-	% Error
30% LEA	25	Lamellar	48.044	0.040	0.083
	30	Lamellar	48.261	0.056	0.116
		Im3m	147.479	1.020	0.692
	35	Im3m	124.693	0.044	0.035
	40	Im3m	116.325	0.145	0.124
	50	L_2	-	-	-
90% LEA	25	Im3m	123.524	3.501	2.835
	30	Im3m	117.866	2.416	2.049
	35	Im3m	111.199	2.832	2.547
	40	Im3m	106.658	2.688	2.521
	50	L_2	-	-	-

4.4.4. Dispersions

The amphiphile systems generally form a cubic phase in excess water, with this acting much like a paste. While this has many applications, it could also be desirable to have systems, perhaps containing therapeutics, as an emulsion of small particles. However, since these particles are not stable, poloxmer-407 was added to the dispersion. As with any dispersion, the polydispersity of the particles is an important characteristic. Therefore, materials with varying LEA content in excess water, namely those from 60% LEA to 100% LEA, were examined. This range was selected as these materials were fluid at room temperature in excess water.

Differential light scattering (DLS) results for these materials, depicted in Figure 4.8, showed the particle size to consistently be around 160-170 nm with a polydispersity (PDI) generally less than 0.22. These values were considered appropriate for the application.

As indicated in Table 2, SAXS analysis revealed the phase of the dispersions to be Im3m. This was surprising as it is different than the results from the bulk material in excess water. It is suspected that the difference in the cubic phase is due to the presence of the poloxmer-407, which was used as a stabilizer for the dispersions. While it was not feasible to conduct the DLS or SAXS testing without a stabilizer present, it would be possible to reevaluate the phase with varying amounts of stabilizer. Therefore, there is the potential for more tailored delivery from this alternative phase formation and particle distribution if these dispersions were to be used in the future.

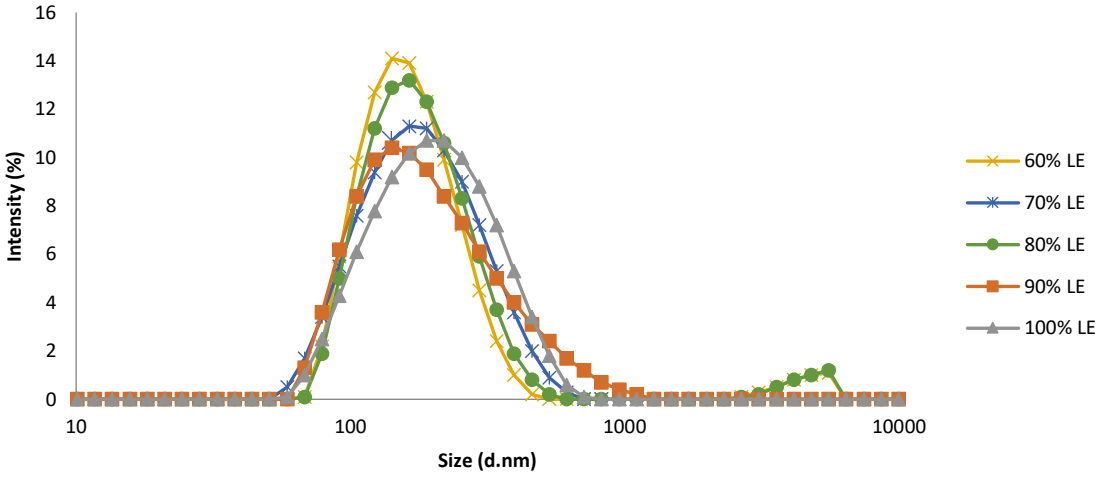

Figure 4.8 Differential Light Scattering results for 60-100% LEA containing materials.

4.4.5. Drug Release

Various drugs were loaded into different material compositions to determine the drug release profiles in sink conditions. Roscovitine release, loaded at 5% in 80% LEA, was conducted into 5 mL of water and is shown in Figure 4.9.

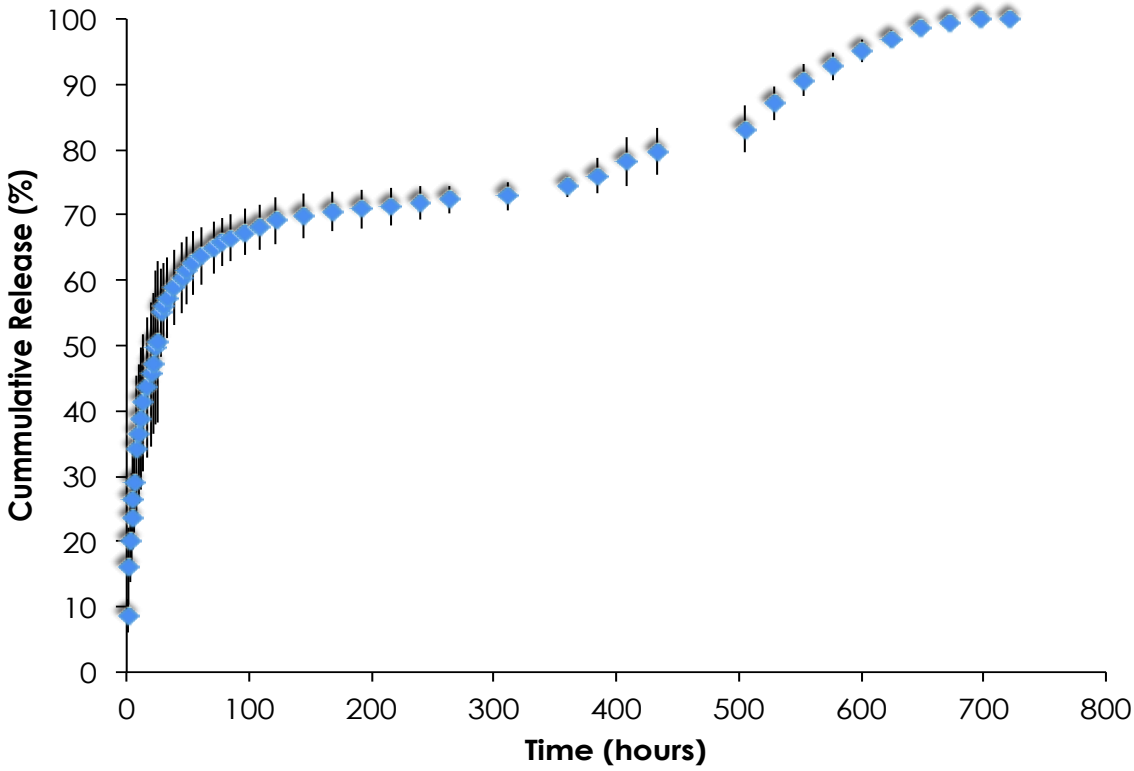

Figure 4.9 Roscovitine release from 80% LEA loaded at 5% released into 5mL.

From these results, it is clear that the materials are capable of sustained drug release over a number of days, at which point they begin to degrade and alter the release profile. The error associated with these results is mostly likely attributable to the differences in shape and weight of the materials in their respective containers, as the profiles for each individual composition appears similar and consistent.

It is clear there is an initial burst release from the amphiphile system, which is followed by a secondary release particularly as the materials begins to experience some degradation. It was clear from this, however, that very little degradation occurs at the initial time points. This was confirmed through the degradation study (Figure 4.14).

This 5% roscovitine loaded study was repeated into 10 mL of water and 90% LEA was also studied. The two stage release is again visible in both of these samples, with the initial burst beginning to plateau around 200 hours and the release resuming around 400 hours, at which point some degradation is known to take place. While there is a slightly greater burst seen in the 80% LEA samples, this is likely due to the slightly larger water channels, as Table 4.1 demonstrated that the water channel size deceased with increasing LEA content. This confirmed that indeed, with the lower roscovitine loading levels, regardless of the volume of release (though both were at sink conditions), there is a lag associated with the onset of degradation. Specifically, this degradation may enlarge the water channels of the materials, which would facilitate more drug leaving the materials.

The drug loading was also increased to 10% in the 90% LEA materials. While this material has a smaller burst and shows a slight lag early on, it is mostly lacking the dual release seen in the 5% loading. This is likely due to the dehydrating effect that the presence of the drug has on the water channels within the materials, as shown in Table 4.1 and consistent with literature [Mohammady 2009]. Therefore, when there is the highest about of drug loaded initially, the water channels are smaller, thus providing a slower release. However, as the amount of drug decreases in the material, the channels enlarge allowing a greater percentage of the drug to escape. Given the greater amount of drug, it may be less susceptible to the degradation of the materials once the larger water channels are available.

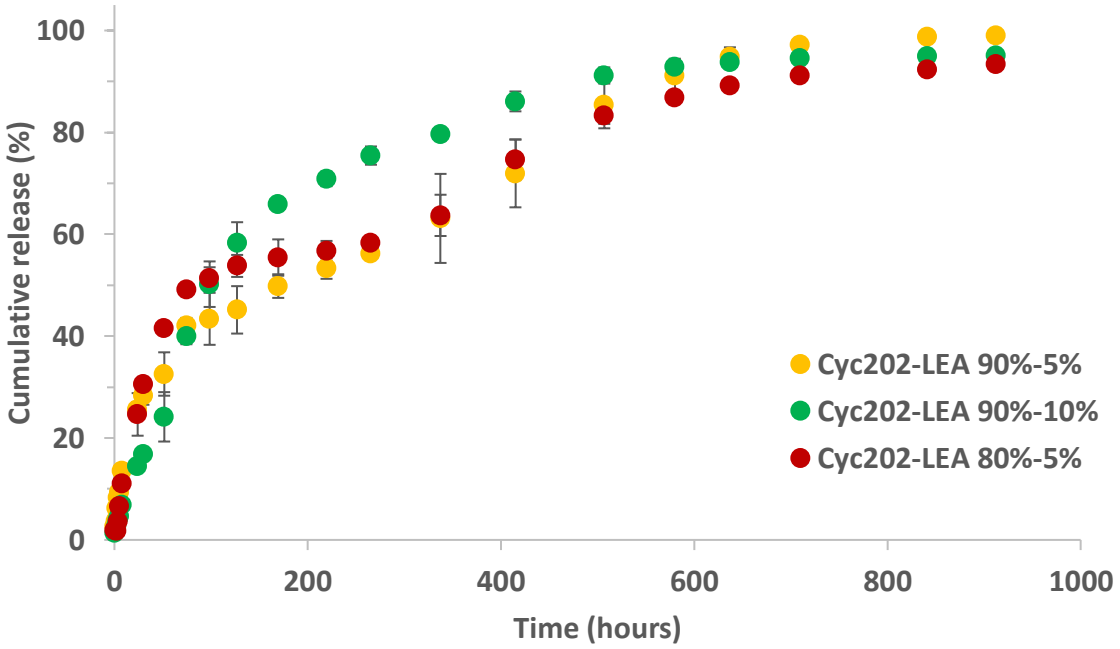

Figure 4.10 Roscovitine release from 80% LEA loaded at 5% (red) and 90% LEA loaded at 5% (yellow) and 10% (green), released into 10 mL of water.

This is further exemplified in Figure 4.11, which shows the amount of drug released at the early time points. Here, the first 35 hours show similar release amounts, but the 10% loaded materials then rapidly increase their release to double that of the 5% loaded material, as expected. This trend remains in place until the release is over, resulting in 0.848 mg released from the 5% loaded materials and 1.46 mg released from the 10% loaded materials.

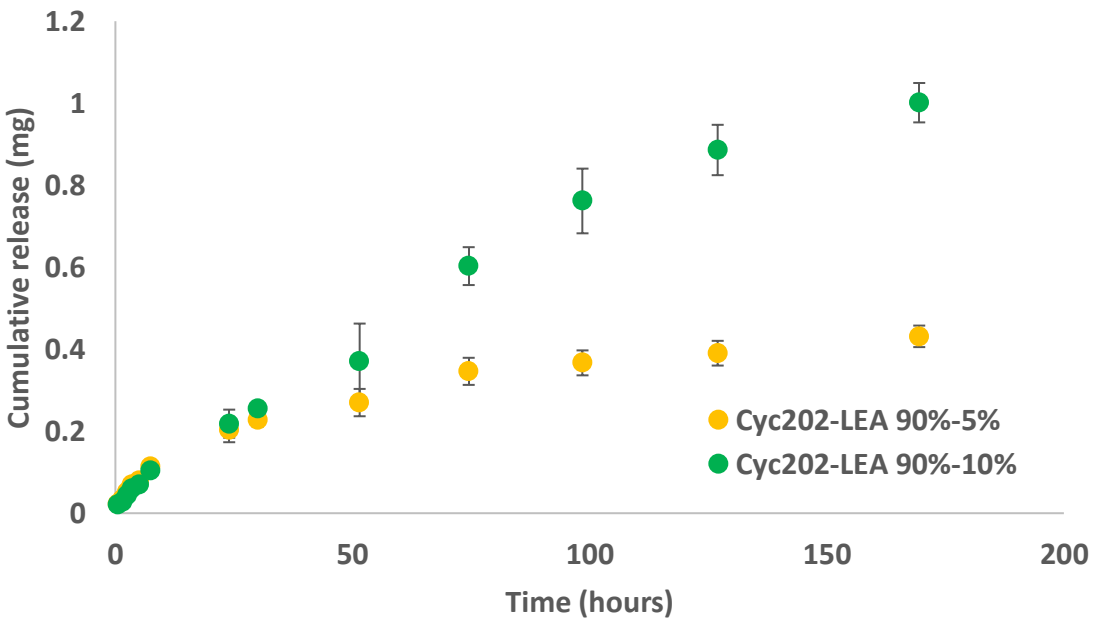

Figure 4.11 Roscovitine release from 90% LEA loaded at 5% (yellow) and 10% (green), released into 10 mL of water up to 200 hours.

Figure 14.12 shows a similar profile to the 5% roscovitine-loaded materials for the 5% atropine-loaded materials, released into 5 mL of water. Again, it is clear that the materials are capable of sustained drug release over numerous days, at which point they begin to degrade altering the release profile. Also, similar to the 10% roscovitine-loaded materials, atropine may strongly influence the water channel size, as the more hydrophilic nature of the drug would cause it concentrate around the polar head of the material and thus closer to the water channels. [Huang 2018] Again, since the presence of drug is known to dehydrate the water channels [Mohammady 2009], the presence closer to them would be expected to do this to a greater extent, even though the drug is loaded at a lower concentration than when this was shown for roscovitine. However, once the drug begins

to be released, the water channels would enlarge and the drug release would continue, indicating why, similar to the 10% roscovitine-loaded materials, the plateau is quite small. This would be complemented by the degradation of the materials, which appears to also be slightly faster, as the release resumes here around 200 hours, as opposed to at 350 hours seen in the roscovitine release for the same 80% LEA system. These differences could be due to the way that the presence of the drug (in this case, a more soluble drug) influences the lattice parameters of the material. Once the drug begins to be released, it is likely the resulting material will have larger water channels characteristic of the 80% LEA material, and thus may degrade more readily; the increased solubility of the drug would facilitate a faster release into these water channels and out of the material.

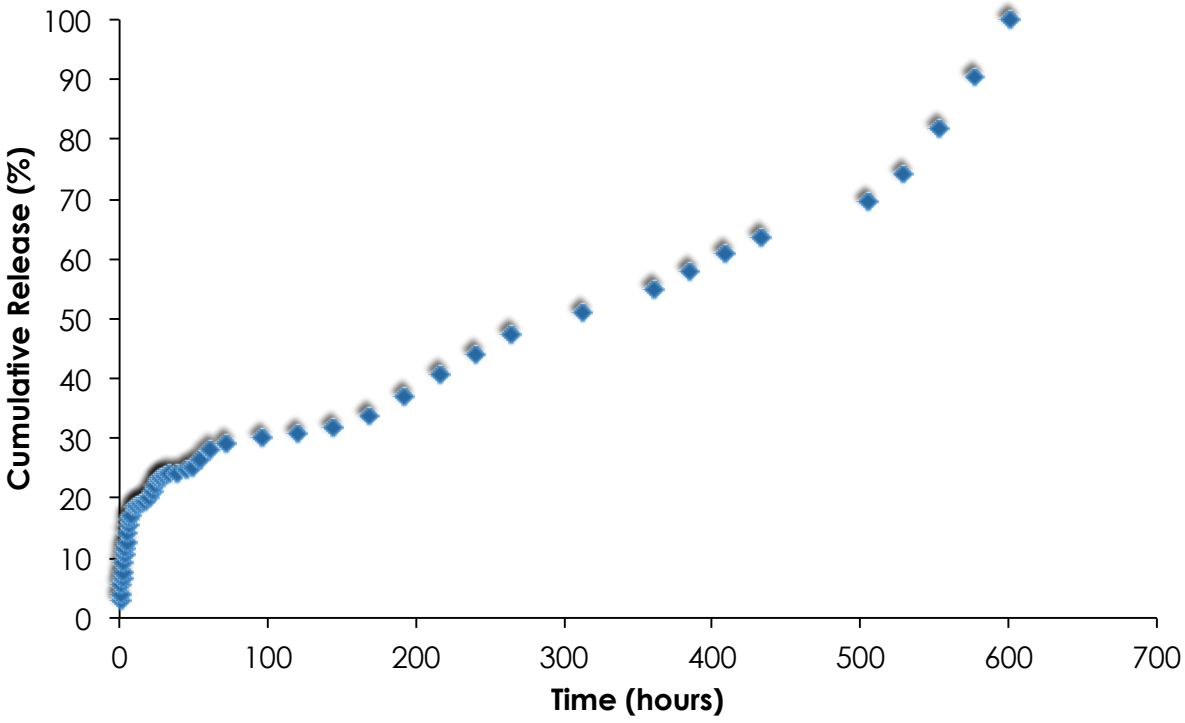

Figure 4.12 Atropine release from 80% LEA loaded at 5% released into 5 mL.

The final drug examined was R547, as shown in Figure 4.13. While also loaded at 5% into 90% LEA, this drug only shows an initial burst release followed by a slow, steady release driven by diffusion. There does not appear to be any plateau or changes from the degradation of the materials as seen in the other release profiles. This is likely due to the increased relative hydrophobicity of this drug, as its loading is likely concentrated in the tail region of the bicontinuous phase, [Huang 2018] suggesting that it may have less of an influence on the lattice parameter than other, more hydrophilic drugs. Furthermore, its release is likely much more mediated by its own slow diffusion from the lipid tails into the water channels within the material. Therefore, even as the material begins to degrade and the length of the path to the bulk water is decreased, this drug is still substantially limited by the diffusion into the water channels.

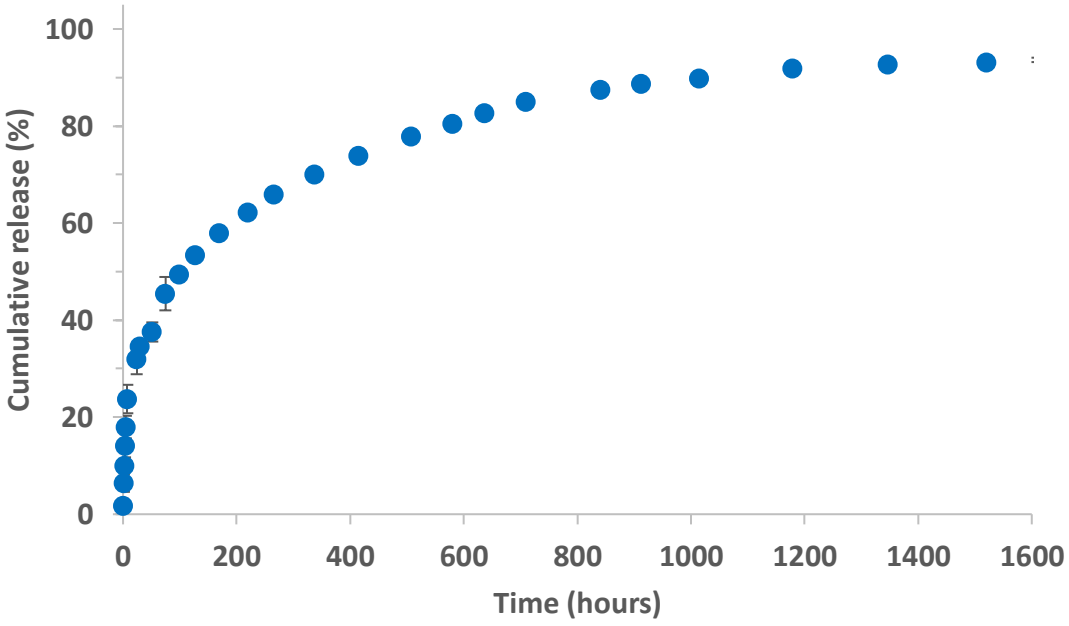

Figure 4.13 R547 release from 90% LEA loaded at 5%, released into 10 mL

4.4.6. Material Degradation

The degradation of the material was monitored by weighing at specific time intervals as shown in Figure 4.14. At most time points, there is not a significant difference between the 80% LEA and 90% LEA materials. For both materials, there is a decrease in mass around 21-28 days, after which the amounts plateau. This is not surprising, as this degradation process is an equilibrium process, and it is likely that the liquid was saturated by 28 days. Unlike the drug release samples, these degradation samples were not subjected to any liquid turnover or mechanical disruption, and thus likely maintained more integrity than the drug release samples. However, since the material does not necessarily remain in one large piece, it would not be possible to confidently conduct this study with any sort of fluid replacement, as one could not be certain some pieces of material were not inadvertently removed. Therefore, the purpose of this study was to show that, while the materials are stable against dilution, there is some loss occurring due to equilibrium with the bulk fluid. It is likely in both a sampling environment and in vivo environment, this degradation would be accelerated, as there would never be an equilibrium reached due to constant fluid turnover. However, this degradation would still be expected to be slow, as it takes weeks to reach equilibrium in these conditions.

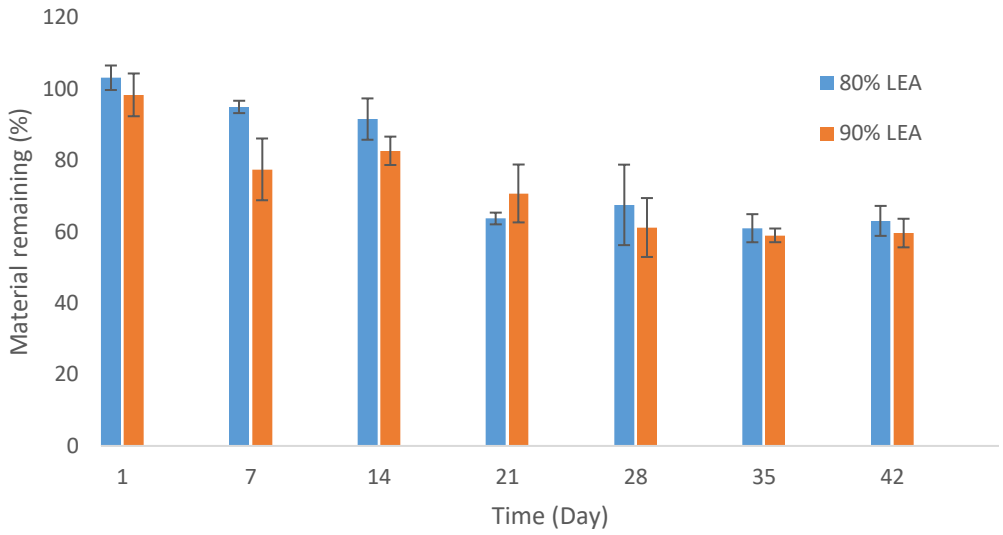

Figure 4.14 Amount of material remaining at various time points for 80% LEA (blue) and 90% LEA (red), as determined by mass.

Overall, these results demonstrate that the system is highly dependent on the characteristics of the drug and the material loading, with much of the system being tailorable based on drug loading and the material composition.

4.5. Conclusion

Current work with the amphiphile system has shown it is possible to create new, uniform materials as combinations of oleoylethanolamide and linoleoylethanolamide that display useful properties. These combinations yield materials with cubic phase transition properties appropriate between the pure substances, making them suitable for ocular drug delivery. The temperature of these transitions can also vary according to the amount and type of therapeutic present and are highly dependent on water content. This has the

potential to yield a material that could be used for the treatment of various conditions including retinoblastoma and myopia. These amphiphiles can further be modified by creating dispersions, which could potentially yield an injectable capability. Drug release with high LEA content systems have shown release capabilities in excess of one month in sink conditions.

4.6. Acknowledgements

The authors would like to thank Minoo Moghaddam and Liliana de Campo for their assistance with the SAXS testing and interpretation. Thank you to Ben Muirhead for creating the first three figures and Kirk Green for help with the LCMS work. This work was supported by the NSERC 20/20 Ophthalmic Materials Research Network. Frances Lasowski was supported by the NSERC Michael Smith Foreign Study Supplement.

4.7. References

Angelov B, Angelova A, Ollivon M, Bourgaux C, Campitelli A. Diamond-Type Lipid Cubic Phase with Large Water Channels. J Am. Chem. Soc. 2003;125:7188-9.

Chia A, Chua WH, Tan D. Effect of topical atropine on astigmatism. Br J Ophthalmol 2009;93:799-802.

Conn CE, Drummond CJ. Nanostructured bicontinuous cubic lipid self-assembly materials as matrices for protein encapsulation. Soft Matter 2013;9:3449-3464.

Fong C, Krodkiewska I, Wells D, Boyd BJ, Booth J, Bhargava S, McDowall A and Hartley PG. Submicron Dispersions of Hexosomes Based on Novel Glycerate Surfactants. Australian Journal of Chemistry 2005;58:683.

Gaudana R, Ananthula HK, Parenky A, Mitra AK. Ocular Drug Delivery. AAPS Journal 2010;12:348-360.

Huang Y, Gui S. Factors affecting the structure of lyotropic liquid crystals and the

correlation between structure and drug diffusion. RSC Adv. 2018;8:6978-87.

Hsu KH, Gause S, Chauhan A. Review of ophthalmic drug delivery by contact lenses. Journal of Drug Delivery Science and Technology 2014;24:123-35.

Inoue T, Hisatsugu Y, Ishikawa R, Suzuki M. Solid-liquid phase behavior of binary fatty acid mixtures. 1. Oleic acid/stearic acid and oleic acid/behenic acid mixtures. Chem. Phys. Lipids 2004A;127:143-52.

Inoue T, Hisatsugu Y, Ishikawa R, Suzuki M. Solid-liquid phase behavior of binary fatty acid mixtures. 2. Mixtures of oleic acid with lauric acid, myristic acid, and palmitic acid. Chem. Phys. Lipids 2004B;127:161-73.

Kaasgaard T and Drummond CJ. Ordered 2-D and 3-D nanostructured amphiphile self-assembly materials stable in excess *solvent.* Phys Chem Chem Phys 2006;8:4957-75.

Kim J, Conway A, Chauhan A. Extended delivery of ophthalmic drugs by silicone hydrogel contact lenses. Biomaterials 2008;29:2259-69.

Mohammady SZ, Pouzot M, Mezzenga R. Oleolyethanolamide-Based Lyotropic Liquid Crystals as Vehicles for Delivery of Amino Acids in Aqueous Environment. Biophysical Journal 2009;96:1537-46.

Ramakrishnan M SV, Komath SS, Swamy MJ. Differential scanning calorimetric studies on the thermotropic phase transitions of dry and hydrated forms of N-acylethanolamines of even chainlengths. Biochimica et biophysica acta Biomembranes 1997;1329:302.

Rosevear F. The Microscopy of hte Liquid Crystalline Neat and Middle Phases of Soaps and Synthetic Detergents. The Journal of the American Oil Chemists' Society 1954;31:628-639.

Sagnella SM, Conn CE, Krodkiewska I, Drummond CJ. Soft ordered mesoporous materials from nonionic isoprenoid-type monoethanolamide amphiphiles self-assesmbled in water. Soft Matter 2009;5:4823-34.

Sagnella SM, Conn CE, Krodkiewska I, Moghaddam M, Seddon JM Drummond CJ. Ordered nanostructured amphiphile self-assembly materials from endogenous nonionic unsaturated monoethanolamide lipids in water. Langmuir 2010A;26:3084-94.

Sagnella SM, Conn CE, Krodkiewska I, Moghaddam M, Seddon JM Drummond CJ. Endogenous nonionic saturated monoethanolamide lipids: Solid State, Lyotropic Liquid Crystalline, and Solid Lipid Nanoparticle Dispersion Behavior. J. Phys. Chem. B 2010B;114:1729-37.

Sangwan M, McCurdy SR, Livne-Bar I, Ahmad M, Wrana JL, Chen D, Bremner R. Established and new mouse models reveal E2f1 and Cdk2 dependency of retinoblastoma, and expose effective strategies to block tumor initiation. Oncogene 2012;31:5019-28.

Shih YF, Chen CH, Chou AC, Ho TC, Lin LL, Hung PT. Effects of different concentrations of atropine on controlling myopia in myopic children. J Ocul Pharmacol Ther 1999;15:85-90.

Tyler AII, Barriga HMG, Parsons ES, McCarthy NLC, Ces O, Law RV, Seddon JM, Brooks NJ. Electrostatic swelling of bicontinous cubic lipid phases. Soft Matter 2015;11:3279-86.

Wells D, Fong C, Drummond CJ. Nonionic urea surfactants: formation of inverse hexagonal lyotropic liquid crystalline phases by introducing hydrocarbon chain unsaturation. J Phys Chem B 2006;110:12660-5.

5. Amphiphilic Thermoset Elastomers from Metal-Free, Click Crosslinking of PEG-Grafted Silicone Surfactants

Talena Rambarran[1], Ferdinand Gonzaga[1], Michael A. Brook[1*], Frances Lasowski[2], Heather Sheardown[2]

[1]Department of Chemistry and Chemical Biology, McMaster University, 1280 Main Street West, Hamilton ON L8S 4M1, Canada
[2]Department of Chemical Engineering, McMaster University, 1280 Main Street West, Hamilton ON L8S 4L7, Canada

* Corresponding author: mabrook@mcmaster.ca

Objectives:
This work sought to develop a methodology to modify silicones with a hydrophilic component like PEG that did not require the use of catalysts in the final stages, thus eliminating the need for purification and reducing the toxicity seen with metal catalysts that are not adequately removed from materials. The PEG was incorporated to increase the hydrophilic character and improve the material properties such as increased water content and decreased fouling, which would enable their use as a biomaterial.

Main Scientific Contributions:
- Development of method to make a silicone-PEG elastomers without the use of a catalyst using the metal-free azide-alkyne click reaction
- The properties of a wide suit of materials were examined and the properties can be tuned based on the amount and molecular weight of PEG and Silicone used
- The potential suitability in biological systems was briefly investigated (protein adsorption)

Publication Information:
Published in *Journal of Polymer Science, Part A: Polymer Chemistry* (Vol. 53 2015 p1082-1093).

Author Contribution:
Dr. Talena Rambarran and Dr. Ferdinand Gonzaga were responsible for the material design and most experimental work (synthesis and characterization of the elastomers, Shore hardness, rheology, water uptake and contact angles) and the relevant sections in the paper write-up. Frances planned and conducted the protein adhesion experiments, as well as writing up the corresponding portion of the paper. The work was done primarily in consultation with and under the supervision of Dr. Michael Brook, who revised the draft to the final version. Dr. Heather Sheardown oversaw the radiolabeling and cellular experiments.

5.1. Abstract

The hydrophobicity of silicone elastomers can compromise their utility in some biomaterials applications. Few effective processes exist to introduce hydrophilic groups onto a polysiloxane backbone and subsequently crosslink the material into elastomers. This problem can be overcome through the utilization of metal-free click reactions between azidoalkylsilicones and alkynyl-modified silicones and/or PEGs to both functionalize and crosslink silicone elastomers. Alkynyl-functional PEG was clicked onto a fraction of the available azido groups of a functional polysiloxane, yielding azido reactive PDMS-g-PEG rake surfactants. The reactive polymers were then used to crosslink alkynyl-terminated PDMS of different molecular weights. Using simple starting materials, this generic yet versatile method permits the preparation and characterization of a library of amphiphilic thermoset elastomers that vary in their composition, crosslink density, elasticity, hydrogel formation, and wettability. An appropriate balance of PEG length and crosslink density leads to a permanently highly wettable silicone elastomer that demonstrated very low levels of protein adsorption.

5.2. Introduction

Polysiloxanes (PDMS) are a class of materials that find use in an extensive range of applications, including microfluidic devices[1] and biomaterials,[2] due to their broad range of desirable properties including high gas permeability, high flexibility, optical transparency, very low toxicity, high thermal stability, and moldability.[3] However, the high hydrophobicity of silicones can limit their use in biomaterials applications. For example,

significant lipid and protein adsorption[3,4,5] onto hydrophobic surfaces can be problematic in the eye;[6] in the most serious cases, extensive biofouling can lead to ocular diseases.

Numerous strategies to modify the surface of silicones to yield improved wettability have been reported. In some cases, strong chemical treatments can cause oxidative surface damage that can lead to reduced biocompatibility.[7,8,9,10] Alternative strategies utilize surface passivation by a variety of hydrophilic polymers, notably poly(ethylene glycol)(PEG).[11] Irrespective of the process used to render silicones hydrophilic, the surfaces generally suffer from hydrophobic recovery (an initially hydrophilic surface becomes hydrophobic over time). Amphiphilic copolymer networks, in which both the surface and the interior of the siloxane network possess enhanced hydrophilicity, represent a new class of promising materials for a range of applications,[12,13] including in biomaterials applications: [14,15,16,17] the silicone hydrogels used in contact lenses fall into this category.

The incorporation of dangling PEG chains into a silicone network to improve water wettability has been reported; however, the procedures for their preparation generally require dry reagents and inert conditions, [18] and/or leave potentially harmful metal catalysts trapped within the material.[19,20] For example, the copper-catalyzed azide-alkyne 1,3-dipolar cycloaddition, known as 'click' chemistry (CuAAC),[21,22,23,24] has been utilized in a wide variety of applications, including the functionalization of polymeric materials[25] and the synthesis of amphiphilic hydrogels.[26] This highly efficient process that leads to a variety of interesting materials is catalyzed by Cu(I) salts, the toxicity of which can be a drawback for biological applications. Despite the excellent safety record of the silicone elastomers

used as biomaterials, concerns have been raised when metallic catalyst residues (tin-, copper- or platinum-based) remain in the materials.

Alternative metal-free 'click' strategies have been employed for biological or polymer functionalization, notably the creative use of ring strained alkynes.[27,28] Recently, it has been shown that the Huisgen[29] 1,3-dipolar cycloaddition of azides to alkynes ('click' chemistry) can be used to thermally functionalize and crosslink silicones, without the use of a catalyst, at low temperatures and without generating any by-products.[30] This strategy was used to create thermoset elastomers (referred to as elastomers hereafter) containing excess reactive groups (azido- or alkynyl-) that could subsequently graft hydrophilic macromolecules and polymers (such as alkynyl-PEG) to create a more hydrophilic elastomer surface.[31] It was also demonstrated that alkynyl-PEG could be grafted onto an azido-functional PDMS backbone using the metal-free strategy at less than stoichiometric ratios, preserving reactive groups for controlled sequential functionalization.[32]

Herein, we report an extension of the metal-free methodology for the preparation of amphiphilic silicone-PEG networks that involves first creating PDMS-g-PEG surfactants containing reactive azido groups that can subsequently be used to crosslink alkyne-terminated PDMS. We reasoned that grafting PEG chains throughout the entire elastomer network would increase the inherent wettability and, if appropriately formulated, could circumvent the possibility of hydrophobic recovery over time, as the material, a silicone hydrogel when water swollen, would ideally be homogenous throughout its entire body. The simple, versatile and efficient methodology allows control over a range of experimental parameters, including the molecular weight of PEG, the graft density, the

PDMS molecular weight and, subsequently, the crosslink density and ability to form a hydrogel.

5.3. Experimental

5.3.1. Materials

(Chloropropyl)methylsiloxane-dimethylsiloxane copolymer (14-16 mol % (chloropropyl)methylsiloxanes, MW 7,500-10,000 $g \cdot mol^{-1}$, trimethylsiloxy-terminated), octamethylcyclotetrasiloxane (D_4), and 1,3-bis(hydroxybutyl)tetramethyldisiloxane were obtained from Gelest. Propiolic acid (95%), monomethoxy poly(ethylene oxide) (av. mol. wt: 2000), monomethoxy poly(ethylene oxide) (av. mol. wt: 750), monomethoxy poly(ethylene oxide) (av. mol. wt: 350), poly(ethylene oxide) (av. mol. wt: 400), propiolic acid (95%), sodium azide (99.5%), (dimethylamino)pyridine (DMAP, 99%) and tetra-*n*-butylammonium azide were obtained from Sigma-Aldrich. All materials were used as received.

5.3.2. Methods

IR analyses were performed on a Bio-Rad infrared spectrometer (FTS-40). ^{1}H and ^{13}C NMR spectra were recorded at room temperature on a Bruker AV600 spectrometer (at 600 and 150 MHz, respectively) or Bruker AC-200 spectrometer (at 200 MHz for ^{1}H), using deuterated solvents ($CDCl_3$).

Contact angles were measured on a Kruss DSA 100 using 18.1 mΩ·cm water (Easypure® II, RF ultrapure water system). Samples were submerged in deionized water for 2 weeks prior to being measured and all measurements were performed in triplicate.

The % water uptake of the samples was measured after soaking in deionized water for 1 day and 14 days, respectively. Samples were placed in separate vials in 5 mL of deionized water for either 1 or 14 d and their masses were measured (wet mass – m_w). Each sample was then dried in vacuo for 24 h and the mass was measured (dry mass – m_d). The % water uptake is defined as $(m_w-m_d)/m_d*100$. The reported values are the average of triplicate experiments.

Rheological measurements were undertaken using an ARES 4X733707T-CE using 7 mm parallel plates. Dynamic strain sweep experiments at frequency 1 Hz were performed for all samples to determine the linear dynamic range of the strain. Dynamic frequency sweep (stain controlled) experiments were performed for all samples in triplicate, using a strain in the linear dynamic range (1, 5 or 10).

Atomic force microscopy (AFM, Veeco Dimension Icon) was measured using Scan Asyst mode (the resonance frequency = 0.4 N/m and scanning frequency 2 Hz) with a silicon tip. The roughness factor (R_Q) was determined for an area of 5 x 5 μm^2.

The quantity of water soluble extractables was determined by placing pre-weighed samples (m_i) that had been dried (in vacuo for 24 h at 60 °C, 56 mmHg) into deionized water for 24 h. The elastomers were removed from the water/extracts and dried in vacuo (24 h at 60 °C, 56 mmHg) and the final mass was determined (m_f). The % aqueous extractables were calculated as: % extractable = $(m_i - m_f)/m_i *100$. All samples were measured in triplicate.

The quantity of organic soluble extractables was determined by placing pre-weighed samples (m_i) that had been dried (in vacuo for 24 h at 60 °C, 56 mmHg) into a

sealed vial with dichloromethane for 24 h. The elastomers were removed from the DCM/extracts and dried in vacuo (24 h at 60 °C, 56 mmHg) and the final mass was determined (m_f). The % organic extractables were calculated as: % extractable = (m_i – m_f)/m_i *100. All samples were measured in triplicate.

5.3.3. General Synthesis

A representative example of the synthesis is detailed below. Detailed experimental procedures for all of the polymers and materials, including an elastomer created with α,ω-propiolated PEG (Figure 5.1), are provided in the Supporting Information along with characterization; this includes images of the materials, storage modulus plots from rheological characterization, infrared spectra, quantity of aqueous and organic extractables, water uptake and an experimental section for the protein adhesion study.

5.3.3.a. Azidoalkylsilicones

Poly(azidopropylmethyl)-co-(dimethylsiloxane) **1** was prepared as previously described[31] starting from commercially available (chloropropyl)methylsiloxane-dimethylsiloxane copolymer. ^{1}H NMR spectroscopy was used to determine the average molecular weight of a repeating unit: for every azido propyl chain (with a characteristic triplet at 3.23 ppm corresponding to the methylene unit in α of the azido group), 34.86 protons were integrated for the methylsiloxane moieties, corresponding to an average molecular weight of 537g·mol^{-1} per repeating unit (i.e., $(Me(N_3(CH_2)_3)SiO)_1(Me_2SiO)_5$).

5.3.3.b. α,ω-Silicone propiolates

Propiolate-terminated disiloxane was synthesized from 1,3-bis(hydroxybutyl)tetramethyldisiloxane and propiolic acid according to the previously

published procedure of Rambarran et al.[31] Higher molecular weight propiolate-terminated PDMS was grown from the disiloxane (end groups) via acid-catalyzed equilibration using D_4 to yield propiolate-terminated polysiloxane **2** (MW of 3,600 g·mol^{-1}), **3** (MW 7,800 g·mol^{-1}) and **4** (MW of 16,200 g·mol^{-1}); MW was determined by ^{1}H NMR.[31]

5.3.3.c. PEG-monopropiolates

PEG mono-propiolate **5** (MW of 406 g·mol^{-1}, determined by ^{1}H NMR), **6** (MW of 813 g·mol^{-1}, determined by ^{1}H NMR), and **7** (MW of 2060 g·mol^{-1}, determined by ^{1}H NMR) were prepared from monomethoxy poly(ethylene oxide) according to a previously described procedure.[33]

***Synthesis of low molecular weight* 5 *PEG (406 g·mol^{-1}) -modified, functional silicones* 8, 9 *and* 10**

The syntheses of silicone amphiphiles **8**, **9** and **10** were carried out by reacting polymer **1** with propiolate-terminated PEG **5** in non-stoichiometric ratios such that 25, 50 or 75% (respectively for **8**, **9** and **10**) of the available azido groups were 'clicked', i.e., reacted with, PEG-monopropiolates. A representative procedure is illustrated below for the synthesis of **8**: polymers **1** (0.73 g, 1.36 mmol) and **5** (0.14 g, 0.34 mmol, 0.25 eq.) were placed into a vial followed by the addition of 1.5 mL of $CHCl_3$. The vial was sealed and the mixture was heated at 60 °C with stirring for 18 h, at which time the reaction was found to be complete by ^{1}H NMR (0.87 g, quant.). The solvent was removed from the reaction by blowing a stream of nitrogen over the mixture.

1 (1.09 g, 2.03 mmol) and **5** (0.42 g, 1.03 mmol), homogenized with 4 mL of $CHCl_3$, were reacted to produce **9** (1.51 g, quant.).

1 (1.62 g, 3.02 mmol) and **5** (0.92 g, 2.25 mmol), homogenized with 5 mL of $CHCl_3$, were reacted to produce **10** (quant.; reaction required additional 24 h).

8*:* ^{1}H NMR ($CDCl_3$, 600 MHz, δ): 0.05 to 0.09 (s, 31.9H, SiC*H*$_3$, *11*), 0.47-0.51 (m, 0.5H, SiC*H*$_2$CH$_2$CH$_2$triazole, *1*), 0.53-0.59 (m, 1.5H, C*H*$_2$CH$_2$CH$_2$N$_3$, *1'*), 1.61-1.67 (m, 1.5H, SiCH$_2$C*H*$_2$CH$_2$N$_3$, *13*), 1.91-1.99 (m, 0.5H, SiCH$_2$C*H*$_2$CH$_2$triazole, *2*), 3.22 (t, *J*=6.0 Hz, 1.5H, C*H*$_2$N$_3$, *14*), 3.37 (s, 0.75H, -OCH$_3$, *9*), 3.55 (t, *J*=6.0 Hz, 1H, C*H*$_2$OCH$_3$, *8*), 3.64-3.65 (m, ~5H, -OC*H*$_2$C*H*$_2$O-, *10*), 3.68 (m, 0.5H, C*H*$_2$CH$_2$OCH$_3$, *7*), 3.79-3.84 (m, 0.5H, -COOCH$_2$C*H*$_2$, *6*), 4.35,4.66 (m, 0.5H total, SiCH$_2$CH$_2$C*H*$_2$triazole, *3A*, *3B*), 4.45, 4.48 (0.5H total, -COOC*H*$_2$ -, *5A*, *5B*), 8.07- 8.15 (multiple singlets, 0.25H, *H*CCCOO,*4A*, *4B*).

9: *(Major isomer 1,4 (A ~ 80%), Minor isomer 1,5 (B ~20%):* ^{1}H NMR ($CDCl_3$, 600 MHz, δ): 0.05 to 0.09 (s, 31.9H, SiC*H*$_3$, *11*), 0.47-0.51 (m, 1H, SiC*H*$_2$CH$_2$CH$_2$triazole, *1*), 0.53-0.59 (m, 1H, C*H*$_2$CH$_2$CH$_2$N$_3$, *1'*), 1.61-1.67 (m, 1H, SiCH$_2$C*H*$_2$CH$_2$N$_3$, *13*), 1.91-1.99 (m, 1H, SiCH$_2$C*H*$_2$CH$_2$triazole, *2*), 3.22 (t, *J*=6.0 Hz, 1H, C*H*$_2$N$_3$, *14*), 3.37 (s, 1.5H, -OCH$_3$, *9*), 3.55 (t, *J*=6.0 Hz, 1H, C*H*$_2$OCH$_3$, *8*), 3.64-3.65 (m, ~10H, -OC*H*$_2$C*H*$_2$O-, *10*), 3.68 (m, 1H, C*H*$_2$CH$_2$OCH$_3$, *7*), 3.79-3.84 (m, 1H, -COOCH$_2$C*H*$_2$, *6*), 4.35,4.66 (m, 1H total, SiCH$_2$CH$_2$C*H*$_2$triazole, *3A*, *3B*), 4.45, 4.48 (1H total, -COOC*H*$_2$ -, *5A*, *5B*), 8.07- 8.15 (multiple singlets, 0.5H, *H*CCCOO,*4A*, *4B*).

10: *(Major isomer 1,4 (A ~ 80%), Minor isomer 1,5 (B ~20%):* ^{1}H NMR ($CDCl_3$, 600 MHz, δ): 0.05 to 0.09 (s, 31.9H, SiC*H*$_3$, *11*), 0.47-0.51 (m, 1.5H, SiC*H*$_2$CH$_2$CH$_2$triazole, *1*), 0.53-0.59 (m, 0.5H, C*H*$_2$CH$_2$CH$_2$N$_3$, *1'*), 1.61-1.67 (m, 0.5H, SiCH$_2$C*H*$_2$CH$_2$N$_3$, *13*), 1.91-1.99 (m, 1.5H, SiCH$_2$C*H*$_2$CH$_2$triazole, *2*), 3.22 (t, *J*=6.0 Hz, 0.5H, C*H*$_2$N$_3$, *14*), 3.37 (s, 2.25H, -OCH$_3$, *9*), 3.55 (t, *J*=6.0 Hz, 1.5H, C*H*$_2$OCH$_3$, *8*), 3.64-3.65 (m, ~15H, -OC*H*$_2$C*H*$_2$O-, *10*), 3.68 (m, 1.5H, C*H*$_2$CH$_2$OCH$_3$, *7*), 3.79-3.84 (m, 1.5H, -COOCH$_2$C*H*$_2$, *6*), 4.35,4.66 (m, 1.5H total, SiCH$_2$CH$_2$C*H*$_2$triazole, *3A*, *3B*), 4.45, 4.48 (1.5H total, -COOC*H*$_2$ -, *5A*, *5B*), 8.07- 8.15 (multiple singlets, 0.75H, *H*CCCOO,*4A*, *4B*).

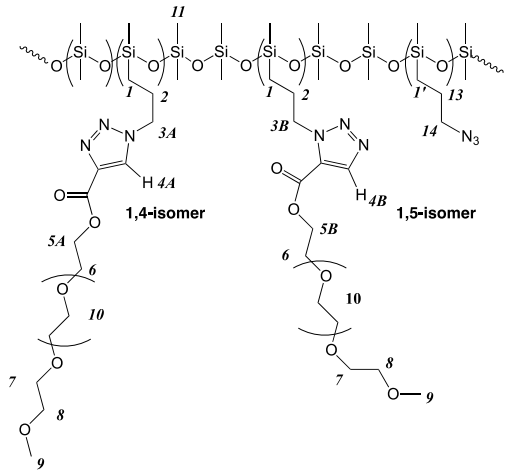

***Medium molecular weight 6 PEG (PEG-800 g·mol^{-1})-modified functional silicones* 11**, **12** ***and* 13** ***and high molecular weight* 7** ***PEG-modified (PEG 2060 g·mol^{-1}) functional silicone* 14**.

See Supporting Information for details.

Synthesis of Elastomers* 15**, **16**, **17: PEG 5 (400 g·mol^{-1})-functional networks crosslinked with PDMS 3 (7,800 g·mol^{-1})***

A representative procedure for the synthesis of PEG-functional PDMS networks **15-17** is illustrated by the synthesis of **15**. **8** (0.87 g, 0.34 mmol of alkynyl PEG, 1.02 mmol of azido groups) and **3** (3.98 g, 1.02 mmol of alkyne) were mixed with 5 mL toluene and stirred vigorously to homogenize the mixture. The mixture was poured into a 5 cm Pyrex Petri dish, covered and placed in a 55 °C oven for 18 h, at which time the rubber had cured.

The temperature was increased to 90 °C for an additional hour to ensure that the rubber was adequately crosslinked, and then removed from the heat and allowed to cool. An analogous process was repeated reacting **9** and **10** with **3** to create elastomers **16** and **17**, respectively (amounts of the reagents used can be found in Table 5.1). The materials were characterized by Shore OO hardness, IR, and rheology; **15** and **16** were additionally characterized by water contact angle (Table 5.2) and swellability in water, (Figure 5.3 B).

Synthesis of Elastomers* 18, 19, 20*: PEG* 5 *(400g·mol^{-1})-functional networks crosslinked with PDMS* 4 *(16,200 g·mol^{-1})

See Supporting Information for details.

Synthesis of Elastomers* 21, 22*: PEG* 6 *(800 g·mol^{-1})-functional networks crosslinked with PDMS 3 (7800 g·mol^{-1})

See Supporting Information for details.

Synthesis of Elastomers* 23, 24 *PEG 6 (800 g·mol^{-1})-functional networks crosslinked with PDMS 4 (16200 g·mol^{-1})

See Supporting Information for details.

Synthesis of Elastomers* 25, 26, 27*: PEG 5 (400 g·mol^{-1})-functional networks crosslinked with PDMS* 2 *(3600 g·mol^{-1})

A representative procedure for the synthesis of PEG and azide functional PDMS networks, **25-27**, is illustrated by the synthesis of **25**. **8** (1.94 g, 0.81 mmol of alkynyl PEG, 2.19 mmol of azido groups) and **2** (2.02 g, 1.12 mmol of alkyne) were mixed with 2 mL of $CHCl_3$ and stirred vigorously to homogenize the mixture. The mixture was poured into a 5 cm Pyrex Petri dish, covered and placed in a 60 °C oven for 18 h. The temperature was

increased to 90 °C for an additional hour to ensure that the rubber was fully cured and then removed from the heat and allowed to cool.

26: **9** (2.58 g, 1.76 mmol alkynyl PEG, 1.70 mmol azido groups) and **2** (1.55 g, 0.86 mmol) were mixed (6 mL $CHCl_3$) to produce elastomer **26** (4.13g).

27: **10** (3.38 g, 3.01 mmol alkynyl PEG, 1.00 mmol azido groups) and **2** (0.96 g, 0.53 mmol) were mixed (7 mL $CHCl_3$) to produce elastomer **27** (4.34 g).

A similar process was used to make rubber **28** from PEG **6** (813 $g \cdot mol^{-1}$) and PDMS **2** (3600 $g \cdot mol^{-1}$) and rubber **29** from PEG **7** (2060 $g \cdot mol^{-1}$) and PDMS **2** (3600 $g \cdot mol^{-1}$)

See Supporting Information for details.

Synthesis of α,ω-PEG propiolates, **30**, and example elastomer with α,ω-Silicone and α,ω-PEG propiolates, **31**

See Supporting Information for details.

Table 5.1 Amounts of reagents used

Azide **1** g: mmol per azide	PEG- g: mmol	Azide-PEG	Stoichio-metry (azide: PEG)	PDMS Alkyne- g: mmol per alkyne	Product number
0.73: 1.36	**5**-0.14: 0.34	**8**	1:0.25	**3**-3.98: 1.02	**15**
1.09: 2.03	**5**-0.42/1.03	**9**	1:0.5	**3**-4.02: 1.03	**16**

1.62: 3.02	**5**-0.92: 2.25	**10**	1:0.75	**3**-2.99: 0.77	**17**
0.41: 0.76	**5**-0.07: 0.17	**8**	1:0.25	**4**-4.76: 0.59	**18**
0.54: 1.00	**5**-0.20: 0.49	**9**	1:0.5	**4**-4.00: 0.49	**19**
1.10: 2.05	**5**-0.62: 1.52	**10**	1:0.75	**4**-4.26: 0.53	**20**
0.68: 1.27	**6**-0.25: 0.31	**11**	1:0.25	**3**-3.76: 0.96	**21**
0.87: 1.62	**6**-0.68: 0.84	**12**	1:0.5	**3**-3.13: 0.80	**22**
0.37: 0.69	**6**-0.14: 0.17	**11**	1:0.25	**4**-3.94: 0.51	**23**
0.49: 0.91	**6**-0.36: 0.44	**12**	1:0.5	**4**-3.52: 0.47	**24**
1.61: 3.00	**5**-0.33: 0.81	**8**	1:0.25	**2**-2.02: 1.12	**25**
1.86: 3.46	**5**-0.72: 1.76	**9**	1:0.5	**2**-1.55: 0.86	**26**
2.15: 4.00	**5**-1.23: 3.01	**10**	1:0.75	**2**-0.96: 0.53	**27**
1.50: 3.03	**6**-0.62: 0.76	**11**	1:0.25	**2**-2.08: 1.15	**28**
1.21: 2.25	**7**-1.27: 0.62	**14**	1:0.25	**2**-1.71: 0.83	**29**

5.4. Results and Discussions

5.4.1. Starting Materials

Three distinct constituents were used to create PEG-modified silicone elastomers: pendant azidoalkylsilicones; dialkyne-terminated silicone chains; and monoalkyne-terminated PEG (Figure 5.1A). Polyfunctional poly(dimethylsiloxane)-co-(methyl(azidopropyl)siloxane) **1** was prepared from commercially available starting materials according to the procedure by Rambarran et al.[31]; the average molecular weight of 537 g·mol^{-1} per azide monomer unit was determined by ^{1}H NMR (i.e., $(Me(N_3(CH_2)_3)SiO)_1(Me_2SiO)_5$). Alkyne (propiolate)-terminated PDMS was synthesized using activated esters in three different molecular

weights as previously described[31]; **2** (M_n=3,600 g·mol^{-1}, 93% yield), **3** (M_n=7,800 g·mol^{-1}, 90% yield), and **4** (M_n=16,200 g·mol^{-1}, 88% yield) were obtained as colorless oils. Monoalkyne (propiolate)-functional PEG was also synthesized in three different molecular weights from commercially available starting materials as previously described;[33] the average molecular weights of **5** (408 g·mol^{-1}), **6** (813 g·mol^{-1}), and **7** (2060 g·mol^{-1}) were determined by ^{1}H NMR using end group analysis. α,ω-Propiolate PEG was prepared following a modified method of Rambarran et al.[31]

5.4.2. Pendant PEG-PDMS polymers

The azide-functional silicones were first modified with monofunctional PEG to create reactive silicone-PEG graft copolymers (**8-14,** Figure 5.1B). Propiolate-functional PEGs of three different MW were attached onto the PDMS backbone in three different ratios, leaving residual reactive groups (Figure 5.1B).

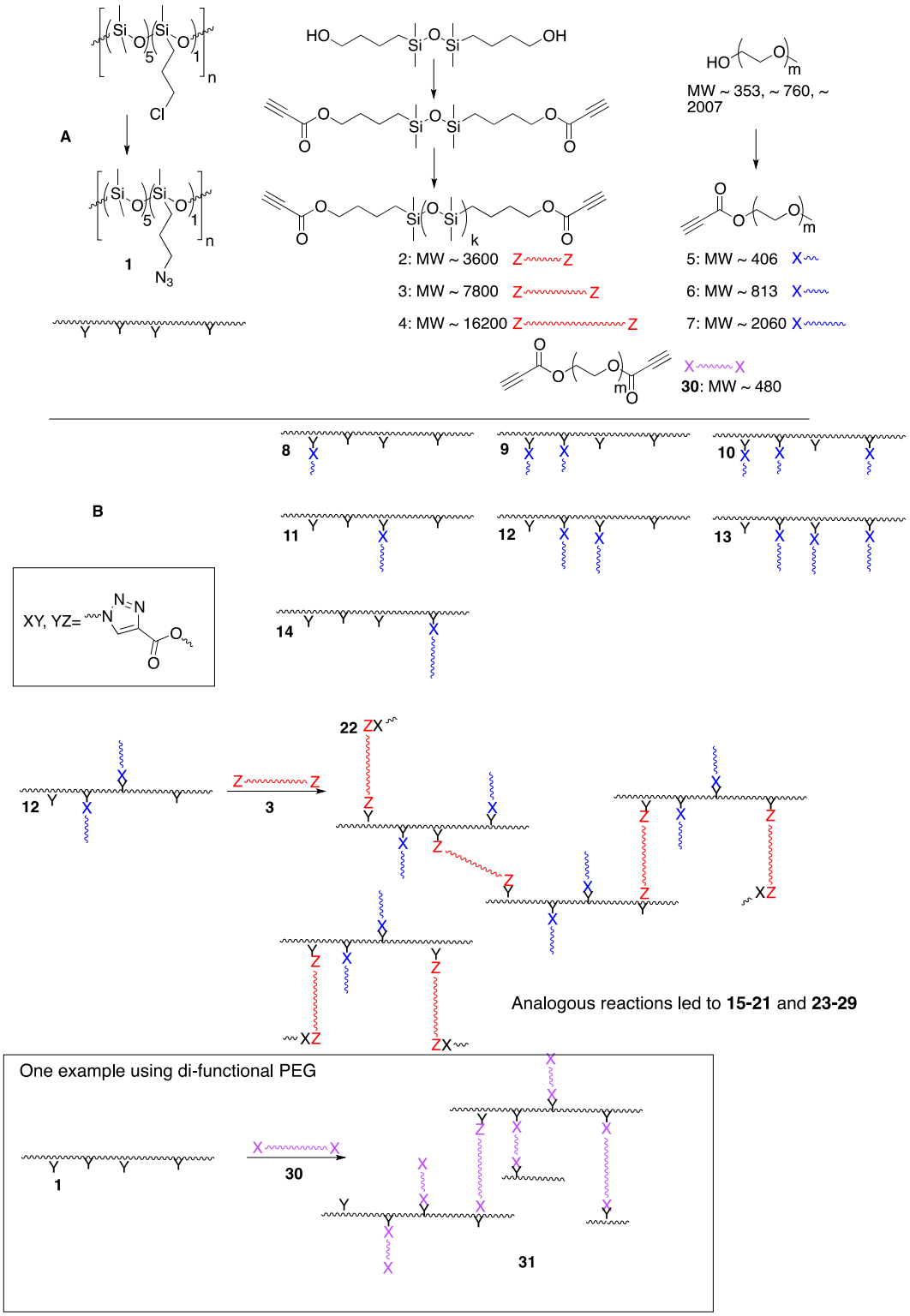

Figure 5.1 Functionalizing and crosslinking PEG-PDMS

For example, PEG monopropiolate, **5** (408 g·mol^{-1}) was grafted onto polymer **1** (azido-PDMS) at a 25, 50 or 75% molar equivalent of the available azido groups by mixing the appropriate amount of each reagent (see Supporting Information) with a small amount of solvent (chloroform or toluene) and heating them to 60 °C for 18 - 24 hours, at which time the reactions were found to be complete by ^{1}H NMR, giving **8**, **9** or **10**. Analogous reactions were performed with longer PEG **6** (813 g·mol^{-1}), yielding polymers **11**, **12** or **13**. In these cases slightly longer reaction times (~12 hours) and additional solvent was required to homogenize the mixtures. (Note that in the absence of a small amount of solvent inconsistent and irreproducible mixing led to lower yields and more complex product mixtures). In a single example, **1** was functionalized with a 25% equivalent of the higher molecular weight PEG **7** (2060 g·mol^{-1}) in $CHCl_3$ and toluene at 60 °C for 24 h with stirring to yield polymer **14**. The products were pure (uncontaminated with reagent polymers) after removal of the solvent by evaporation: the thermal reaction between pendant azido groups on the reactive polysiloxane backbone and PEG occurred in near quantitative yields (Supporting Information).

This process constitutes a simple strategy to synthesize a variety of rake style silicone polyethers with differing molecular weights and PEG content. Such polymers are used in a variety of applications, including stabilization of polyurethane foams. The residual azide groups can be used in a subsequent Huisgen reaction for further functionalization. This was demonstrated in a previous investigation by modifying a polymer analogous to **11** with acetylene dicarboxylic acid, where an examination of the surfactancy of these intermediates is reported.[32]

5.4.3. Amphiphilic silicone elastomers

The same synthetic strategy was used to create 15 amphiphilic thermoset elastomers that differed in composition and structure (**15-29**, Figure 5.1C). Shorter propiolate-terminated PDMS **3** (~8,000 g·mol^{-1}) was used to bridge crosslinkers **8**, **9** or **10** at a ratio sufficient to consume the available azido groups. The pre-polymer mixtures were homogenized with a small amount of $CHCl_3$ and/or toluene, cast in a glass Petri dish and allowed to cure in a 60 °C oven for 24 hours, followed by 1 hour at 90 °C to ensure complete cure, yielding **15**, **16**, or **17**, respectively. IR data confirmed the complete disappearance of the 2097 cm^{-1} that arises from unreacted azide moieties (Supporting Information). Analogous elastomers were prepared from the reaction of **8**, **9** or **10** with higher molecular weight PDMS, **4** (~16,200 g·mol^{-1}) to yield elastomers **18**, **19**, or **20**, respectively. Polymers with medium molecular weight PEG side chains **11** or **12** (25 and 50% equiv. of PEG **6**, 813 g·mol^{-1}) were also crosslinked with an equivalent amount of **3** (~8,000 g·mol^{-1}) to yield **21** or **22**, or crosslinked with **4** (~16,200 g·mol^{-1}) to yield **23** or **24**, respectively. In a single example, an elastomer was formed from crosslinking **1** with a telechelic PEG with propiolate termini, **30**, using the same reaction conditions to create an elastomer, **31**.

It was also possible to prepare elastomers with residual reactive azide groups: shorter propiolate terminated PDMS **2** (~3,600 g·mol^{-1}) was used to bridge crosslinkers. For example, compounds **8**, **9**, or **10** were homogenized in a small amount of solvent with **2** and thermally cured to produce elastomers **25**, **26** or **27**. In these elastomers approximately half of the remaining azide groups (i.e., 37.5, 25 and 12.5 % of the original amount, respectively) were used for crosslinking and the other half remained free in the

network, as confirmed by ATR-IR. The resultant materials were transparent, easy to manipulate, firm, neither tacky nor brittle, and had smooth surfaces. This procedure was repeated by crosslinking the more PEG-rich **11** with **2** to give **28**. Because of the longer PEG chain, this material was softer and more water absorbent than its lower molecular weight PEG counterpart, **25**. Finally, one functional elastomer was prepared that contained nearly 30% PEG by weight by reacting **7** with PDMS **2** in a mixture of toluene and chloroform and allowing partial cure with stirring for several hours prior to the final cure in the oven (see next section). The resultant material was hard, somewhat brittle, opaque and waxy. A summary of the materials is contained in Table 5.2. Amounts of the reagents used and the IR spectra can be found in the Supporting Information. As previously shown, the networks can be further functionalized by performing a Huisgen reaction with either the surface bound or all the azides.[31]

Two competing processes were observed during cure: crosslinking due to azide-alkyne cycloaddition, and phase separation between the alkynyl-PDMS and the graft copolymers. Different network morphologies could result depending on the relative kinetics of the two processes. Therefore, to enhance the reproducibility of the outcomes, small amounts of solvents were used to homogenize the polymers to avoid phase separation during cure. For each pre-elastomer, the volume of solvent was adjusted until clear mixtures and a clear crosslinked gel was obtained. In some instances, it was necessary to partly 'pre-cure' the material with stirring for some time and then finish the curing process in the oven.

Table 5.2 PDMS-g-PEG elastomers and properties.

This utilization of solvent allowed some chemical bonds to form during mixing, which kept

PEG	Azide -PEG	Ratio (azide: PEG)	PDMS Alkyne	Product number	Tan □ 0.1 Hz/ 100Hz	G'(kPa) 0.1Hz/ 100Hz	PEG Wt %	Description	Contact Angle (@300s)	Shore OO
5	**8**	1:0.25	**3**	**15**	0.067/ 0.07	93.6/ 96.8	2.8	Slightly opaque, flexible, not tacky	101±3	77±2
5	**9**	1:0.5	**3**	**16**	NA/ 0.03	95.9/ 110.5	7.6	Transparent, flexible, not tacky	92±5	71±2
5	**10**	1:0.75	**3**	**17**	0.009/ 0.296	12.7/ 24.1	16. 6	Transparent, gel, very tacky	-	45±4
5	**8**	1:0.25	**4**	**18**	0.011/ 0.073	53.9/ 68.7	1.4	Slightly opaque, flexible, slightly tacky	109±3	66±1
5	**9**	1:0.5	**4**	**19**	0.009/ 0.094	34.0/ 44.7	4.6	Transparent and mildly white, very tacky, prone to cracks, flexible	101±6	57±1
5	**10**	1:0.75	**4**	**20**	0.070/ 0.078	67.8/ 100.0	10. 4	Transparent, soft, very tacky	87±6	67±4
6	**11**	1:0.25	**3**	**21**	0.004/ 0.124	115.3/ 115.8	5.4	Slightly opaque, flexible, not tacky	107±1	74±2
6	**12**	1:0.5	**3**	**22**	0.026/ 0.223	95.8/ 98.2	14. 4	Transparent (over time turned very slightly opaque), flexible, not tacky	76±6	70±2
6	**11**	1:0.25	**4**	**23**	0.045/ 0.156	64.8/ 74.2	3.1	Opaque, flexible, not tacky	45±4	70±2
6	**12**	1:0.5	**4**	**24**	0.212/ 0.476	48.6/ 74.7	9.3	Transparent, uneven, very tacky	67±2	59±1
5	**8**	1:0.25	**2**	**25**	0.073/ 0.606	63.2/ 67.2	8.4	Transparent, firm, not tacky	50±2	68±1
5	**9**	1:0.5	**2**	**26**	0.020/ 0.170	84.0/ 81.1	17. 6	Transparent, flexible	68	65±1
5	**10**	1:0.75	**2**	**27**	0.044/ 0.232	30.0/ 38.2	28	Transparent, flexible, tacky	60±5	55±2
6	**11**	1:0.25	**2**	**28**	0.000/ 0.061	5.3/ 22.7	14. 6	Slightly opaque, very flexible, stretchy, a little tacky	57±2	36±4
7	**14**	1:0.25	**2**	**29**	n/a	n/a	30. 4	Opaque, waxy	57±2	83±3

the dispersion homogenous, before finally curing the polymers (without agitation) under

conditions where phase separation could not compete kinetically with the cure. The resultant materials ranged from colorless to pale yellow and transparent to hazy depending on the PEG/silicone ratio (Table 5.2, Supporting Information).

5.4.4. Characterization

5.4.4.a. Shore OO Hardness

Durometer (resistance to indentation) is a common way to characterize elastomeric materials. Shore OO measurements, which are particularly useful for the characterization of the viscoelastic properties of soft materials, demonstrated that the Huisgen process allows for customizable silicone materials. Unsurprisingly, for elastomers in which the monofunctional PEG and difunctional PDMS lengths are held constant, the hardness was observed to decrease with decreasing crosslink density and increase with backbone-grafted PEG (Figure 5.2a). The use of shorter difunctional PDMS while holding the PEG concentration fixed led to harder materials as the longer PDMS spacers imparted more flexibility into the network (Figure 5.2b).

More subtle changes were observed when the PEG molecular weight was changed while holding the number of crosslinks constant (25, 50, 75%). With ~8,000 g/mol difunctional PDMS spacers, formulations with 400 MW PEG, **15** and **16**, were slightly harder than those with 800 MW PEG, **21** and **22**; the opposite was true with ~16,000 g/mol difunctional PDMS spacers, where 400 MW PEG **18** and

19 were slightly softer than 800 MW PEG **23** and **24** (Figure 5.2c). PEG can help to reinforce the network via crystallization of the PEG segments,[18] which could explain the change in hardness with increasing PEG length within the network.

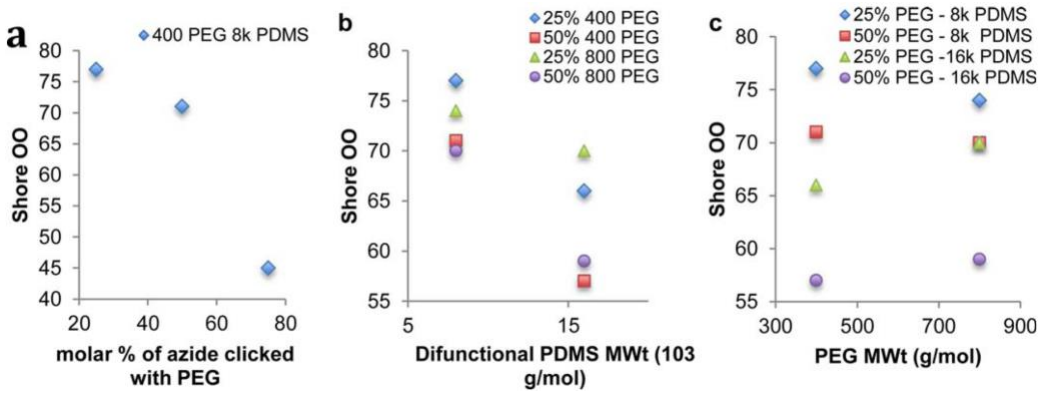

Figure 5.2 Changes in elastomer hardness: a) as a function of the quantity of grafted PEG, b) with increasing difunctional PDMS molecular weight, c) with increased PEG molecular weight.

These materials, such as **20** and **24**, possess enhanced hardness when compared to analogous unfilled silicone elastomers that do not contain PEG. In a previous investigation, an elastomer analogous to **20** in terms of PDMS spacer length and amount of crosslinks but without PEG in the network, possessed a Shore OO value of 35±4,[31] which is nearly half the hardness of its PEG containing counterpart described above (Shore OO for **20** = 67±4). This supports the assertion that the PEG contained in the network can enhance the physical hardness. With shorter PEG as with materials **18** and **19**, there may be insufficient PEG chain length for enhanced crystallization, but sufficient length to facilitate repulsion between silicone and PEG in the network, leading to a softer gel-like network. Note that the quantity of polar extractables (using water) within the network was low (<2%), confirming that the PEG is efficiently grafted onto the PDMS backbone prior to crosslinking (Supporting Information). Very small amounts of organic extractables (less than 15%) were observed for the majority of the elastomers (Supporting Information). Compounds **17**, **19** and **28** demonstrated higher amounts of organic extractables.

5.4.4.b. Rheology

The ability to tune properties of these elastomers was also shown from rheological experiments. The linear viscoelastic (LVE) region was determined by performing a dynamic strain sweep at constant frequency. Dynamic frequency sweeps were then performed choosing a strain within the LVE regions. The storage modulus (G') of the elastomers generated varied over a wide range – 5,000-115,000 Pa: both flat and responsive effects of frequency were observed (Figure 5.3a, Table 5.2 and Supporting Information). Many of the elastomers displayed a frequency-independent G' during the frequency sweep at constant strain (in the LVE range) and had essentially the same elastic response independent of the changing frequency, which is the characteristic behavior of an ideal elastomer or gel.[34,35]

Some networks displayed a frequency-dependent G' (the modulus increased with increasing frequency), a property typical of highly branched polymers or of gels containing polymers that are not bound into the network.[34] The materials with higher amount of organic extractables demonstrated low G'; **17** and **28** also had significant frequency dependent moduli, suggesting there may have been incomplete curing of these materials. Sequestered monografted α,ω-silicone propiolates can contribute to this effect. At low frequencies, the gel network and sol fractions can rearrange to accommodate stress: the observed properties resemble the equilibrium elastic deformation of the network because polymer entanglement lifetimes are shorter than the oscillation period.[36] As the frequencies

increase, the oscillation becomes faster than the time it takes for physical entanglements to rearrange resulting in stored elastic energy, which leads to an observable increase in the storage modulus.

Rheological properties (G') of unfilled silicone elastomers made using traditional platinum-catalyzed addition cure (hydrosilylation of Si-H and Si-vinyl functional PDMS) exhibited comparable elastic properties to the 'click' silicones described above. Robert et al. has demonstrated that unmatched ratios of functional groups yield elastomers with lower storage modulus resulting from a less cross-linked network, similar to our thermoset elastomer structures.[37] A 20% - 90% excess of a functional groups within the PDMS network produced G' values between 900 and 9 kPa. The authors noted that dangling chains connected to the network at only one end could act as plasticizers of the silicone network.[37] Larsen et al. also investigated the elastic properties of non-stoichiometrically cured PDMS rubbers (from hydrosilylation) and found G' values between 158 – 30 kPa for elastomers with 15 – 50% excess of one type of functional group.[38]

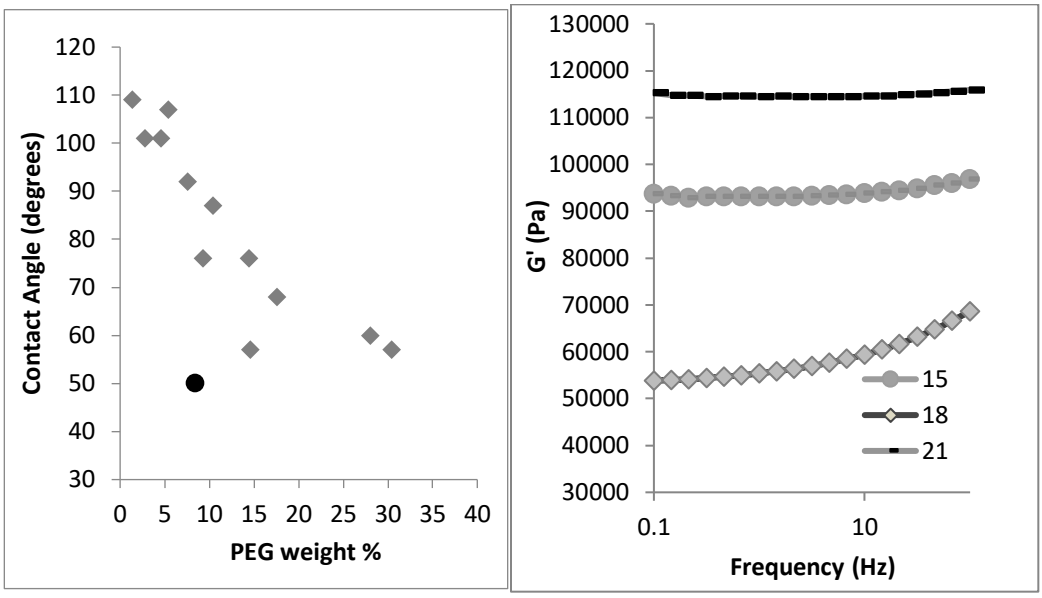

Figure 5.3 A Left: Contact angle vs. PEG weight percent (The outlier (•) represents the wettable elastomer 25) B Right: Example storage modulus of elastomers/gels.

5.4.4.c. Water Uptake

One of the objectives of this work was to make materials that had potential utility in biomaterials' applications. In light of this objective it was important to characterize the response of the materials to water as hydrogels are used in biomedical applications ranging from contact lenses to wound dressings. The amount of water uptake into the networks was measured at two time points, 24 hours and 14 days. While most of the elastomers remained relatively unchanged during the water equilibration stage, others took up significant amounts of water (from 1 – 61 wt% over 24 hours, Supporting Information Figure 4S). After 2 weeks, the water uptake increased significantly in several of the elastomers, ranging from 3 – 113 wt%. Surprisingly, the water uptake was not directly proportional to the PEG content in the network. Instead, networks that were more gel like, with longer PEG chains and had increasing G' with frequency in the rheological experiments, tended to swell more

with water. This observation is likely a reflection of the network structure; for example, **28** (made with PEG 750 $g \cdot mol^{-1}$), swelled substantially more than **25** (made with PEG 350 $g \cdot mol^{-1}$), its lower PEG counterpart. From these data it is clear that these reactions permit the design of silicone-PEG hydrogels.

5.4.4.d. Contact Angle

Static water contact angles were measured to analyze how the incorporation of PEGs (of various chain length and grafting density) in the elastomer body affected wettability, compared to pure silicone elastomers that have contact angles >100°.[39] When PEG is grafted using the Huisgen reaction onto the surface of elastomers containing excess azido groups, enhanced surface wettability was observed, with decreases in contact angle ranging from 41 – 87° at 30 minutes).[31] Prior to measuring contact angles on the rubbers described above, they were soaked in deionized water for several days to ensure the PEG chains were fully hydrated. In the absence of this conditioning, surface effects involving hydration and adsorption/absorption of water can affect the observed angles. The contact angles were measured at time = 300 s, in triplicate for each rubber (see Table 5.2). It was anticipated that all of the elastomers would display a decrease in contact angle arising from the quantity of PEG found within the network.

The results varied across the different elastomers and gels, contact angles ranging between 45±4° (elastomer **25**) and 109±3° (elastomer **18**), with the majority falling under 70°. These changes were not the result of changes in surface roughness, which were small (Supporting Information). There is a rough correlation between the amount of PEG in the network and the decrease in the contact angel (Figure 5.3B). Compound **25** was exceptional, exhibiting

both rapid and significant decrease in contact angle to ~35° in air after 5 minutes (Figure 5.4). This high wettability is apparently a consequence both of the molecular weight of the PEG and its mobility. A network analogous to **25** but incorporating α,ω-propiolate-PEG (i.e., tethered at both ends) of low molecular weight **30** was created for comparison (Supporting Information); this elastomer was found to have a water contact angle from air of 62±2° at 300s.

Lin et al. have previously created silicone networks using the Sn-catalyzed room temperature condensation of silanols and alkoxy silanes (RTV), separately incorporating two different molecular weight dangling PEG chains within the network. They found that elastomers made with ~ 6 – 9 PEG units had water contact angles that decreased down to 40°, while those made with 4 – 6 PEG units decreased only to 80°.[19] Ding and coworkers made analogous networks using platinum-catalyzed hydrosilylation, similarly incorporating ~ 300 $g \cdot mol^{-1}$ dangling PEG chains into the network at loadings from 11 – 25 wt% and found decreases in contact angle to 55 – 95°, respectively.[20] Taken with our previous finding that PDMS modified with 750 $g \cdot mol^{-1}$ PEG created more wettable surfaces than those modified with 2000 $g \cdot mol^{-1}$ PEG, the data suggests that shorter, but not shorter than about 300 MW molecular weight PEG, incorporated into or on silicone elastomers yields more wettable surfaces. Similar effects have been observed with so-called superwetting surfactants that exhibit maximum surface activity at 6-8 PEG units.[40]

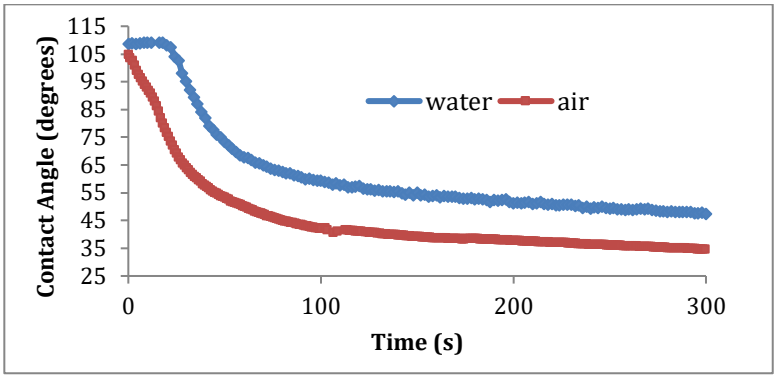

Figure 5.4 Contact angle of 25 **before (air) and after soaking in water for 24 hours**

The results suggest that not only does the amount and length of PEG incorporated into the network influence the wettability, but the crosslink density of the material also plays a key role. For example, **25** and **15**, which vary in the amount of crosslinks and the length of difunctional PDMS, have contact angle values of ~50° and ~100°, demonstrating how relatively subtle changes in the crosslinking can drastically impact the wettability of the surface.

As previously noted, silicones surfaces with enhanced hydrophilicity are necessary in some biomaterials applications to minimize lipid and protein adsorption and subsequent conformational changes. Exemplar materials were selected to confirm the assertion that higher wettability surfaces correlates with decreased protein adsorption, a key step in surface fouling. Figure 5.5 depicts the hen egg lysozyme (HEL) and bovine serum albumin (BSA) adsorption results of four materials, as determined by radiolabeling: Sylgard 184, click elastomer with no PEG, material **22** (low wettability), and material **25** (high wettability). The control materials, Sylgard 184 and the 'click' elastomer with no PEG, showed similar amounts of protein adsorption; it is expected these levels correspond to a

protein monolayer forming on the surface during the 3 hour incubation time. The elastomer with low wettability, **22**, showed similar adsorption to the controls for BSA but higher protein deposition levels for HEL. Given that this material showed greater swelling than the control materials, and that HEL is smaller than BSA, it is likely that some of this smaller HEL protein penetrated into the material to account for higher HEL loading.

The highly wettable elastomer **25** substantially reduced the adsorption of both HEL and BSA relative to the control materials, as expected. This is likely due to the mobile nature of these PEG chains creating a large, hydrated, protective layer on the silicone surface. These results are promising and demonstrate that these amphiphilic 'click' materials can yield silicone surfaces that have improved interfaces in biological environments.

The azide/alkyne click reaction offers significant advantages for the creation of modified silicone networks over traditional technologies. As demonstrated herein, without the need for a catalyst, metal based or not, and with no byproducts, it is possible to efficiently functionalize and sequentially crosslink silicone elastomers to create amphiphilic networks that, at high PEG content, are hydrogels.

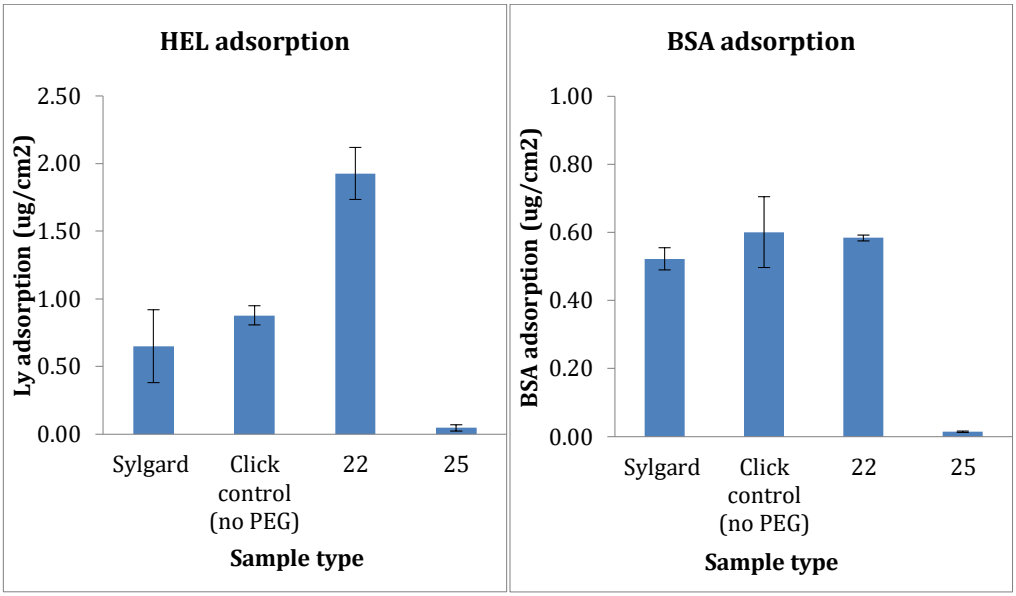

Figure 5.5 HEL and BSA Adsorption of different silicone surfaces (n=4 for each material)

The properties of the elastomers can be controlled by simply varying the ratio and composition of the azido and alkyne functional building blocks. The network structure, surface chemistry and wettability, crosslink density, length and amount of PEG functional groups can be easily manipulated.

Elastomers for biomaterials applications are frequently made in "one off" processes, which is inherently inefficient when one is trying to identify the optimal hardness, wettability, water content and, in the case of ophthalmic materials, oxygen permeability. As seen from the range of materials described above, it is trivial to make elastomers that traverse the hard/soft, wettable/water repellent surfaces, hydrogel/dehydrated silicone spectrum using thermal linking of PEG and silicone. Importantly, the system permits

additional functionalization on the surface or thorough the body of the object in subsequent Huisgen reactions.

5.5. Conclusions

The catalyst-free (metal-free) Huisgen reaction can be used for the creation of amphiphilic silicone networks containing PEG (1.4 – 46 wt%). The mild and efficient reaction can be used to both PEG-functionalize and crosslink azide- and alkyne-modified silicones to create novel amphiphilic materials. The metal-free synthesis is simple and high yielding, with no by-products or work up required and represents a highly efficient method for preparing silicone-PEG networks. Silicone surfactants containing dangling (pendant) PEG throughout the bulk of the network were created by first grafting monoalkynyl-PEG on an azido-functional PDMS backbone to give PDMS-g-PEG polymers, while preserving unreacted azido groups. Subsequent crosslinking with α□ω-alkynyl-PDMS permitted control over the weight% PEG in the final material, the crosslink density of the network and, consequently, a variety of physical properties of the materials, including viscoelastic properties and wetting. The residual azide groups are also available for further functionalization if desired. One highly wettable material with an advancing contact angle of 35° relies on a balance of mobile PEG chains at relatively low concentration and a median crosslink density for this behavior. The simple synthetic platform can create materials with antifouling properties as a result of the pendant PEG within the network as demonstrated by the low protein adsorption in demonstrated for the most wettable materials.

5.6. Acknowledgements

We thank the Natural Sciences and Engineering Research Council of Canada and the 20/20 NSERC Ophthalmic Materials Network for financial support of this research. T.R. also thanks NSERC for the award of the Julie Payette Research Scholarship and the Alexander Graham Bell Canada Graduate Scholarship D Level. We would like to thank Prof. M. Howlader for use of the contact angle machine and Mrs. Fangfang Zhang for help with the AFM imaging.

5.7. Supporting Information

Synthesis and characterization of PEG dipropiolate **30**, functional polymers **1** – **14**, and elastomers **15** – **29**, **31** (including contact angles, images, IR data. Details of protein adsorption, AFM, and rheological data.

5.8. References and Notes

1. P. N. Nge, C. I. Rogers, A. T. Woolley, *Chem. Rev.*, **2013**, 113, 2550-2583.
2. H. Chen, Z. Zhang, Y. Chen, M. A. Brook, H. Sheardown, *Biomaterials*, **2005**, 2391-2399.
3. M. A. Brook, *Silicon in Organic, Organometallic, and Polymer Chemistry*, John Wiley & Sons, Inc.: New York, NY, **2000**.
4. H. Chen, M. A. Brook, H. Sheardown, *Biomaterials*, **2004**, 25, 2273-2282.
5. D. Rana, T. Matsuura, *Chem. Rev.* **2010**, 110, 2448-2471.
6. L. Jones, M. Senchyna, M. A. Glasier, J. Schickler, I. Forbes, D. Louie, C. May, *Eye & Contact Lens* **2003**, 29 (1 Suppl), S75-9, discussion S83-4, S192-4.
7. H. Hillborg, U. W. Gedde, *Polymer*, **1998**, 39, 1991–1998.
8. H. Hillborg, M. Sandelin, U. W. Gedde, *Polymer*, **2001**, 42, 7349–7362.
9. D. J. Heiler, S. F. Groemminger, J. J. Denick, L. C. Simpson, *Surface treatment of silicone hydrogel contact lenses*. US Patent 6,348,507 (to Bausch & Lomb Inc.) February 19, 2002.
10. R. I. Williams, D. J. Wilsone, N. P. Rhodes, *Biomaterials*, **2004**, 25, 4659–4673.
11. P. Kingshott, H. Thissen, H. J. Griesser, *Biomaterials*, **2002**, 23, 2043-2056.
12. G. Erdodi, J. P. Kennedy, *Prog. Polym. Sci*., **2006**, 31, 1-18.
13. H. Chen, M. A. Brook, H. Sheardown, *Biomaterials*, **2004**, 25, 2273-2282.
14. J. Wang, X. Li, *J. Appl. Polym. Sci.*, **2010**, 116, 2749–2757.
15. F. Abbasi, H. Mirzadeh, M. J. Simjoo, *Biomater. Sci. Polym. Ed.*, **2006**, 17, 341–355.

16. Q. Tang, J. R. Yu, L. Chen, J. Zhu, Z. M. Hu, *Curr. Appl. Phys.*, **2011**, 11, 945-950.
17. R. Bischoff, S. E. Cray, *Prog. Polym. Sci.*, **1999**, 24, 185–219.
18. E. L. Chaikof, E. W. Merrill, *Net Polym. Mater*., **1990**, 2, 125-147.
19. G. Lin, X. Zhang, S. R. Kumar, J. E. Mark, *Molec. Cryst. Liq. Cryst.*, **2010**, 521, 56 – 71.
20. Y. Ding, Z. S. Jiao, D. J. Guo, S. J. Xiao, W. Tan, Z. Dai, *Colloids and Surfaces A: Physicochem. Eng. Aspects*, **2012**, 395, 199 -206.
21. H. C. Kolb, M. G. Finn, K. B. Sharpless, *Angew. Chem. Int. Edit.*, **2001**, 40, 2004-2021
22. V. V. Rostovtsev, L. G. Green, V. V. Fokin, K. B. Sharpless, *Angew. Chem. Int. Ed.*, **2002**, 41, 2596-2599.
23. A. K. Feldman, B. Colasson, V. V. Fokin, *Org. Lett.*, **2004**, 6, 3897-3899.
24. S. Chittaboina, F. Xie, Q. Wang, *Tetrahedron Lett.*, **2005**, 4, 2331-2336.
25. L. A. Canalle, S. S. van Berkel, L. T. de Haan, J. C. T. van Hest, *Adv. Funct. Mater*., **2009**, *19*, 3464-3470.
26. V. Truong, I. Blakey, A. K. Whittaker, *Biomacromolecules*, **2012**, 13, 4012–4021
27. C. R. Bertozzi, *Accounts Chem. Res.*, **2011**, *44*, 651-653.
28. J. C. Jewett, C. R. Bertozzi, *Chem. Soc. Rev.*, **2010**, *39*, 1272-1279.
29. R. Huisgen. *Proc. Chem. Soc. London*, **1961**, 357.
30. F. Gonzaga, G. Yu, M. A. Brook, *Macromolecules* **2009**, 42, 9220-9224.
31. T. Rambarran, F. Gonzaga, M. A. Brook, *Macromolecules*, **2012**, 45, 2276–2285.
32. T. Rambarran, F. Gonzaga, M. A. Brook, *J. Polym. Sci. Part A: Polym. Chem.*, **2012,** 51, 855-864.
33. F. Gonzaga, J. B. Grande, M. A. Brook. *Chem. Eur. J.*, **2012**, 18, 1536-1541.
34. S. K. Patel, S. Malone, C. Cohen, J. R. Gillmor, R. H. Colby, *Macromolecules*, **1992**, 25, 5241-5251.
35. A. M. Grillet, N. B. Wyatt, L. M. Gloe, *Polymer Gel Rheology and Adhesion*, *Rheology*, De Vicente, J. (Ed.). Rijeka, Croatia. **2012**. ISBN: 978-953-51-0187-1, InTech Available from: http://www.intechopen.com/books/rheology/rheology-and-adhesion-of-polymer-gels
36. R. A. Mrozek, P. J. Cole, K. J. Otim, K. R. Shull, J. L. Lenhart, *Polymer*, **2011**, 52, 3422-3430.
37. C. Robert, A. Crespy, S. Bastide, J. M. Lopez-Cuesta, S. Kerboeuf, C. Artigue, E. Grard, *J. Appl. Polym. Sci.*, **2003**, 87, 1152–1160.
38. A. L. Larsen, K. Hansen, P. Sommer-Larsen, O. Hassager, A. Bach, S. Ndoni, M. Jørgensen. *Macromolecules*, **2003**, 36, 10063-10070.
39. V. Roucoules, A. Ponche, A. Geissler, F. Siffer, L. Vidal, S. Ollivier, M. F. Vallat, P. Marie, J. C. Voegel, P. Schaaf, J. Hemmerle. *Langmuir*, **2007**, 23, 13136-13145.
40. R. M. Hill, Siloxane Surfactants. In *Silicone Surfactants*, R. M. Hill, Ed. Marcel Dekker, Inc.: New York, **1999**.

6. PEG-Containing Siloxane Materials by Metal-Free Click-Chemistry for Ocular Drug Delivery Applications

Frances Lasowski[1], Talena Rambarran[2], Vida Rahmani[1], Michael A. Brook[2], Heather Sheardown[1*]

[1]Department of Chemical Engineering, McMaster University, 1280 Main Street West, Hamilton ON L8S 4L7, Canada

[2]Department of Chemistry and Chemical Biology, McMaster University, 1280 Main Street West, Hamilton ON L8S 4M1, Canada

* Corresponding author: sheardow@mcmaster.ca

Objectives:
This work sought to build off the previous work which saw PEG-silicone materials created that had greatly reduced protein fouling. After identifying the materials which had the greatest potential for use as biomaterials, alterations were made to determine how the amount of PEG incorporation, the crosslinking and the length of PEG used influenced their fouling and drug release properties.

Main Scientific Contributions:
- Preparation of PEG-silicone elastomers at various PEG loadings, PEG molecular weights and crosslinking densities.
- Preparation of drug loaded elastomers at various loading levels by soaking.
- Property measurements of the materials, including water content and swelling.
- Investigating drug release from the various materials, noting the differences in kinetics particularly as they relate to the different material modifications.
- Investigating protein fouling from the various materials, noting the differences as they relate to the different material modifications.

Author Contribution:
Frances was responsible for all experimental planning and design, interpretation of the results and paper write up. The material compositions used were chosen iteratively by Frances and Dr. Talena Rambarran. Dr. Talena Rambarran synthesized the polymers and materials. Frances conducted the radiolabeling experiments, with assistance from Lina Liu and Myrto Korogiannaki when required. The swelling experiments and drug release experiments were conducted according to the experimental design by Aakash Shaw and Dr. Vida Rahmani. The work was done in consultation with and under the supervision of Dr. Michael Brook (synthesis) and Dr. Heather Sheardown (material characterization). Dr. Heather Sheardown revised the draft to the final version.

6.1. Abstract

Metal-free click-chemistry can be used to create silicone hydrogels for ocular drug delivery applications, imparting the benefits of silicones without catalyst contamination. Previous work has demonstrated the capacity for these materials to significantly reduce protein adsorption. Building upon this success, the current work examines different materials in terms of their protein adsorption and drug release capabilities. Specifically, lower molecular weight PEGs are better able to reduce protein adsorption. However, with higher molecular weight PEGs the materials exhibit excellent water content and better drug release profiles. The lower molecular weight PEGs are also able to deliver the drug in excess of 4 months, with the amount of crosslinking having the greatest impact on the amount of drug release. Overall, these materials show great promise for ocular applications.

6.2. Introduction

Silicone elastomers are frequently used as biomaterials, as they are stable, have high oxygen permeability and are easy to process; but they are limited by their high hydrophobicity in some applications. Hydrophobic surfaces can adsorb greater amounts of protein and lipid, [Brook 2000] such as in contact lens applications, and this fouling can result in the failure of the biomaterial and problems on the eye. [Jones 2003] Introducing hydrophilic moieties, such as poly-ethylene glycol (PEG), could increase the utility of these polydimethylsiloxane (PDMS) materials, but passivating the surface with these compounds often result in hydrophobic recovery, rendering the surface hydrophobic over time. [Kingshott 2002] While silicone hydrogels, which are copolymer networks with improved hydrophilic character both on the surface and in the interior of the material, are promising, [Chen 2004, Wang 2010] they also suffer from limitations. Incompatibilities can make the crosslinking of these materials difficult or leave potentially harmful metal catalysts trapped within the materials. [Lin 2010]

Recently, it has been shown that a metal-free click reaction can be used to create various PDMS-PEG copolymers. [Rambarran 2015] Specifically, PDMS-g-PEG surfactants are created which contain reactive azido groups that can subsequently be used to crosslink alkyne-terminated PDMS, and these materials circumvent the possibility of hydrophobic recovery over time as it is a bulk modification. Previous studies have shown that some of these materials exhibit excellent wettability and have greatly reduced protein adsorption characteristics. [Rambarran 2015] Based on these properties, it was desirable to continue development of these materials to determine which parameters could yield a material best suited for ocular biomedical applications.

Sustained ocular drug delivery remains a challenge. While topical treatments are preferred, they suffer from many limitations including low penetration and short residence

times. [Kim 2008] This can lead to poor patience compliance and outcomes, particularly in pediatric populations. [Hsu 2014] However, injections are highly invasive and for certain conditions, such as retinoblastoma, must be used cautiously to avoid tumor seeding. [Munier 2013] Given that CdK inhibitors, such as roscovitine, have been suggested as chemo-preventative agents for the treatment of retinoblastoma, [Sangwan 2012] it is desirable to create a non-invasive, transscleral delivery system that could be used in this vulnerable population. A silicone hydrogel with low protein fouling and sustained release kinetics could provide an ideal material. The purpose of this study is to examine how modifications to the material composition and formulation alter the hydrophilicity of these PDMS-PEG materials, and how this subsequently influences important biomaterial characteristics, such as water content, protein adhesion, drug release and cell viability.

6.3. Experimental

6.3.1. Materials and Methods

(Chloropropyl)methylsiloxane-dimethylsiloxane copolymer (14–16 mol% (chloropropyl)methylsiloxanes, MW 7500–10,000 g/mol, trimethylsiloxy-terminated), octamethylcyclotetrasiloxane (D4), and 1,3-bis(hydroxybutyl)tetramethyldisiloxane were obtained from Gelest. Propiolic acid (95%), monomethoxy poly(ethylene oxide) (average MW: 750), monomethoxy poly(ethylene oxide) (average MW: 350), poly(ethylene oxide) (average MW: 400), propiolic acid (95%), sodium azide (99.5%), (dimethylamino)pyridine (DMAP, 99%), and tetra-n-butylammonium azide were obtained from Sigma-Aldrich. All other materials were purchased form Sigma-Aldrich unless otherwise noted. Roscovitine was purchased from Selleck (Houston, TX). All materials were used as received.

^{1}H NMR were recorded at room temperature on a Bruker AV 600 spectrometer (at 600 MHz for ^{1}H) using deuterated solvents ($CDCl_3$). Contact angle measurements were performed using a Kruss DSA Contact Angle Apparatus using 18.1 mΩ·cm (MilliQ) water.

6.3.2. Elastomer Synthesis

Poly(azidopropylmethyl)-co-(dimethylsiloxane) (Y, 525 g/mol per azide group), α-ω(propiolatobutyl)polydimethylsiloxne (Z, 3600, 4200, 8100 g/mol) and monopropiolate-terminated monomethoxy poly(ethylene oxide) (X, 393 and 813 g/mol) were synthesized according to the procedure of Rambarran et al. [2012] to create PEG-modified silicone elastomers. The average polymer molecular weight per reactive azide group (Y) was determined by ^{1}H NMR. The average polymer molecular weight for Z and X were determined by ^{1}H NMR using end group analysis. To create the PEG-silicone elastomers, the same procedure by Rambarran et al was followed [2015]. Briefly, propiolate-functional PEGs of different molecular weights were grafted onto the PDMS backbone in different ratios by mixing the polymers in $CHCl_3$, leaving residual reactive azide groups. Complete consumption of the alkyne was confirmed by ^{1}H NMR. Propiolate-terminated PDMS was subsequently added to consume some of the available azido groups and bridge the PEG functional crosslinker to create elastomeric materials in amounts given in Table 6.1 (Iteration 1). The pre-polymer mixtures were homogenized with a small amount of $CHCl_3$ or toluene, cast in a glass Petri dish and allowed to cure in a 60°C oven for 24 hours. Some materials (those noted in iteration 1 and all materials in iterations 2 and 3) were purified by Soxhlet extraction using DCM at 40°C for 2 hours and dried slowly a room temperature for 8 hours. The materials were then placed in a vacuum oven at 40 degrees for 24 hours (as noted for materials in iteration 1, all materials in iterations 2 and 3).

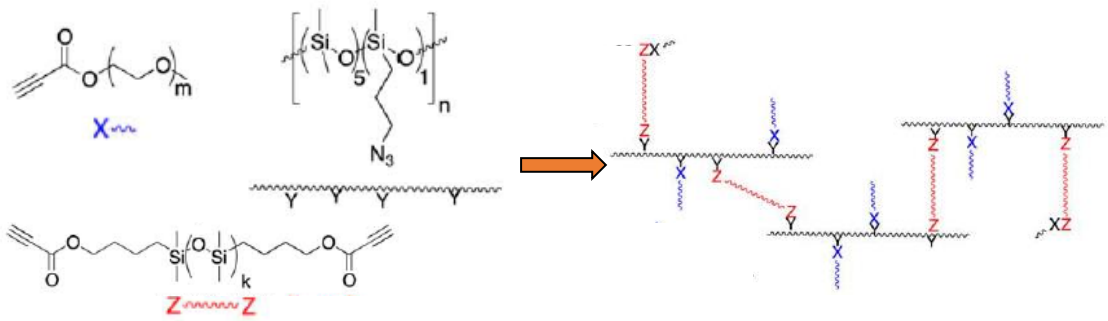

Figure 6.1 Functionalizing and crosslinking PEG-PDMS.

Table 6.1 Material compositions for Iteration 1.

Material No.	Material	PEG (g/mol)	Stoichiometry (Azide:PEG)	PDMS Alkyne	Stoichiometry (Azide: PDMS)	PEG Wt%
1	Sylgard Control	0	0	0	N/A	0
2	Click Control	0	N/A	N/A	1 : 0.5	0
3	50-750-8	813	1 : 0.5	7800 g/mol	1 : 0.5	14.4
4	25-350-4	406	1 : 0.25	3600 g/mol	1 : 0.37	8.4
5	25-350-4	406	1 : 0.25	3600 g/mol	1 : 0.50	6.8

Table 6.2 Material compositions for Iteration 2.

Material No.	Material	PEG (g/mol)	Stoichiometry (Azide:PEG)	PDMS Alkyne	Stoichiometry (Azide:PDMS)	PEG Wt%
1	Sylgard Control	0	0	0	N/A	0
2	350 MW PEG	393	1 : 0.25	4200 g/mol	1 : 0.37	6.9
3	750 MW PEG	813	1 : 0.25	4200 g/mol	1 : 0.5	11.2

Table 6.3 Material compositions for Iteration 3.

Material No.	Material	PEG (g/mol)	Stoichiometry (Azide:PEG)	PDMS Alkyne	Stoichiometry (Azide:PDMS)	PEG Wt%
1	25% PEG, 37% Xlink	393	1 : 0.25	4200 g/mol	1 : 0.37	6.9
2	25% PEG, 50% Xlink	393	1 : 0.25	4200 g/mol	1 : 0.5	5.8
3	25% PEG, 75% Xlink	393	1 : 0.25	4200 g/mol	1 : 0.75	4.4
4	20% PEG, 50% Xlink	393	1 : 0.20	4200 g/mol	1 : 0.50	6.7
5	30% PEG, 50% Xlink	393	1 : 0.30	4200 g/mol	1 : 0.50	6.8
6	Sylgard Control	0	0	0	N/A	0

6.3.3. Swelling and Equilibrium Water Content

The equilibrium water content (EWC) of the samples was determined by mass balance. The mass of each sample was measured after soaking in 1 mL of Milli Q water for at least 48 hours (wet mass, m_w). Each sample was then dried at 70°C for 24 h and the mass was measured (dry mass, m_d). The EWC is shown in Figure 6.1. The reported values are the average of triplicate experiments. To determine the extent of swelling in isopropyl alcohol (IPA), the same protocol was followed using 1 mL of IPA.

$$EWC\% = \frac{M_H - M_D}{M_H} \cdot 100\% \qquad (1)$$

6.3.4. Protein Adsorption

The adsorption of hen egg lysozyme (HEL; Sigma-Aldrich, St. Louis, MO) and bovine serum albumin (BSA; Sigma-Aldrich), respectively on silicone elastomers, were investigated by radiolabeling. HEL and BSA were conjugated to I^{125} using the iodine monochloride method, as previously described. [Luensmann 2010, Vyner 2013] Briefly, radiolabeled protein solution was passed through two columns packed with AG 1-X4 (Bio-Rad, Hercules, CA) to remove unbound I^{125}; the columns were subsequently rinsed with phosphate buffered saline (PBS) to ensure all of the labeled protein was removed. Free iodide, determined using trichloroacetic acid precipitation, was low for both proteins. The materials, having a surface area of 0.633 cm^2, were then incubated for 3 h in a 1 mg/mL or 0.1 mg/mL solution of either HEL or BSA, which were comprised of 10% radiolabeled protein and 90% unlabeled protein. Surfaces were subsequently rinsed in PBS three times, for 5 minutes each time, and counted using an automated gamma counter (1470 Wallac Wizard; PerkinElmer, Woodbridge, ON). Adsorption of protein was measured using 4 discs for each protein solution. The radioactivity on each material was converted into micrograms of protein per cm^2 for quantification.

6.3.5. Cell Viability

30,000 human ARPE19 cells were plated into a 48 well plate for 24 and 72 hour studies and left for one hour to adhere. Discs were then added to the media for 24 or 72 hours. The control had no disc. Discs were removed and a MTT Assay performed with a 2 hour incubation time. Results were read at 540 nm.

6.3.6. Drug Loading & Release

To load the drug, the samples were placed in 50:50 mixture of Ethanol:Water which contained either 1 mg/mL or 2 mg/mL of roscovitine. The samples were soaked for 72 hours to load the drug into the materials. Excess drug loading solution was then wiped off the samples and they were placed in 1 mL of PBS (pH 7.4) at 37°C; to ensure sink conditions, the samples were transferred to fresh PBS at regular intervals, initially at 0.5, 1.5, 2.5, 3.5, 5, 7, 24 and 30 hours and then at least 24 hours apart. The drug release was measured by UV-spectrophotometry (Spectramax Plus 384, Molecular Devices, Corp, Sunnyvale, CA, USA) at 293 nm. The amount of roscovitine released was normalized to the weight of the sample. When the release profiles appeared to plateau and no additional drug was being released, the samples were placed into 1 mL of ethanol for 2 weeks to determine the amount of drug which remained in the samples. This, added to the amount of drug released, was used to calculate the initial loading from soaking. The percent drug release was calculated as the average amount of drug released at that time point divided by the total amount of drug loaded into the material.

6.4. Results and Discussion

6.4.1. Material Iteration 1

6.4.1.a. Material Characterization

The material properties varied based on the composition of the materials, [Rambarran 2015] with some properties given in Table 6.4. For example, material 3 was flexible and not tacky while material 4 was firm. They showed similar mechanical properties for Shore OO hardness (70 ± 2 and 68 ± 1 respectively) [Rambarran 2015] but

differed in their wettability based on the type and amount and molecular weight of PEG incorporated.

Table 6.4 Properties of various materials. Note EWC is after 24 hours.

Material No.	Transparency	Contact Angle	EWC (%)
1	Transparent	>100 °	2 ± 1
2	Transparent	83 ± 5°	
3	Slight Cloud	76 ± 6°	12 ± 1
4	Transparent	50 ± 2°	5 ± 1
5	Transparent	51 ± 7°	

6.4.1.b. Protein Adsorption

The protein adsorption for materials 4 and 5, which were highly wettable, is greatly reduced relative to the control materials for both proteins examined. This is likely due to the mobile PEG chains, which create a large protecting area, and also give the material its high wettability. Conversely, material 3, which had low wettability, shows similar adsorption for BSA to the sylgard control, but increased deposition for HEL relative to the control. Given the greater swelling of this material, it is likely this smaller HEL protein was able to penetrate into the material, resulting in protein levels greater than a monolayer.

Given the large reduction in protein adsorption, materials 3 and 4 were also examined at a lower protein concentration. This lower protein load showed lower adsorption for the materials, though this more apparent with BSA, as seen in Figure 6.4 compared to the HEL in Figure 6.6. Material 4 was extracted to determine if extraction improved cell viability, though it did not appear to have an effect on the adsorption of either protein.

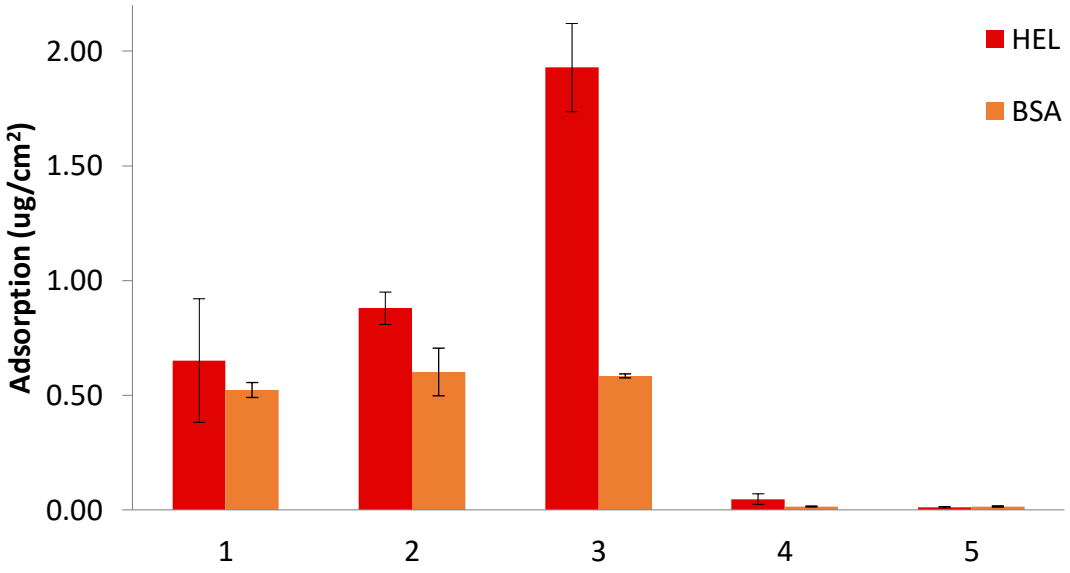

Figure 6.2 Protein adsorption for all materials with both HEL (red) and BSA (orange) soaked in a 1 mg/mL solution.

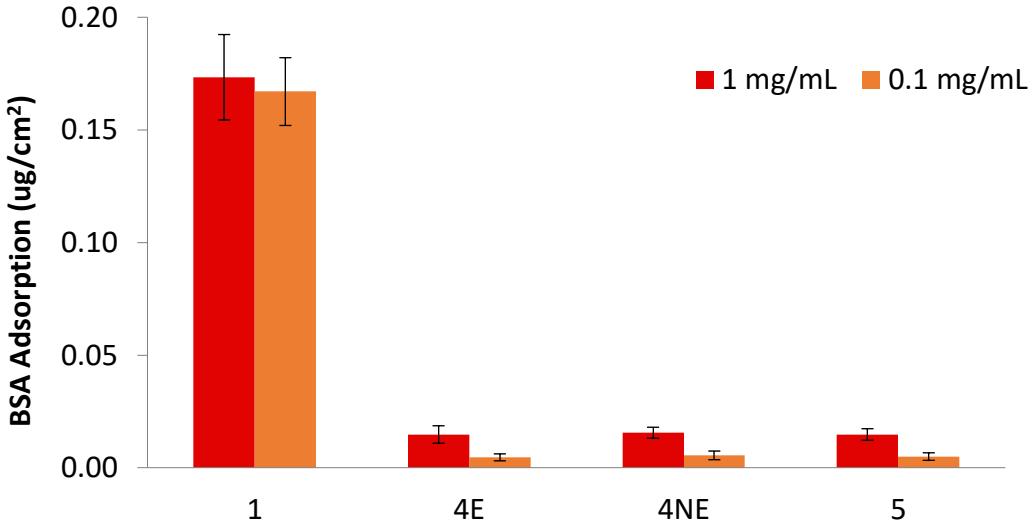

Figure 6.3 Protein adsorption for select materials with BSA soaked in a 1 mg/mL (red) or 0.1 mg/mL (orange) solution. E is extracted and NE is non-extracted materials.

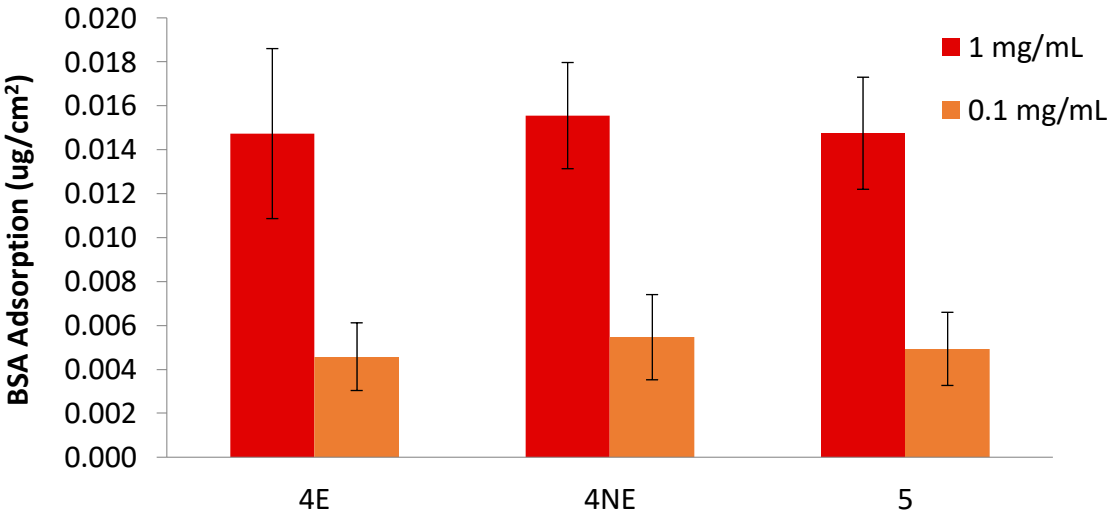

Figure 6.4 Protein adsorption for Materials 4 and 5 with BSA soaked in a 1 mg/mL (red) or 0.1 mg/mL (orange) solution. E is extracted and NE is non-extracted materials.

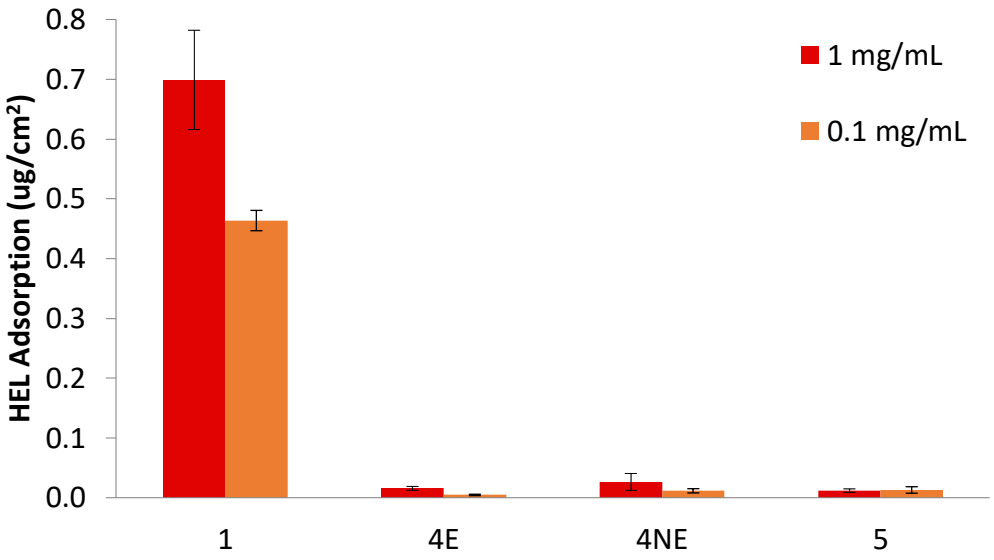

Figure 6.5 Protein adsorption for select materials with HEL soaked in a 1 mg/mL (red) or 0.1 mg/mL (orange) solution. E is extracted and NE is non-extracted materials.

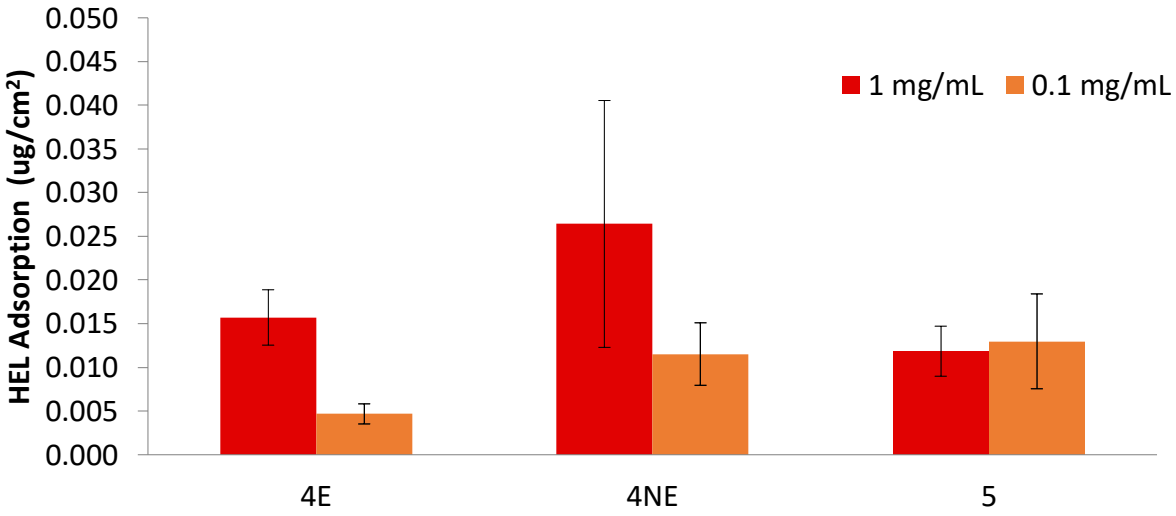

Figure 6.6 Protein adsorption for Materials 4 and 5 with HEL soaked in a 1 mg/mL (red) or 0.1 mg/mL (orange) solution. E is extracted and NE is non-extracted materials.

6.4.1.c. Cell Viability

After 24 hours, all materials showed above 85% viability. Material 4 showed high viability after 72 hours, regardless of whether it is extracted. This suggests that the materials have little leaching of unreacted material and could make them easier to process. Material 5 showed reduced cell viability after 72 hours. Since it is more loosely crosslinked than material 4, it could have more leaching, and thus an extraction will be done to determine if this improves the cell viability.

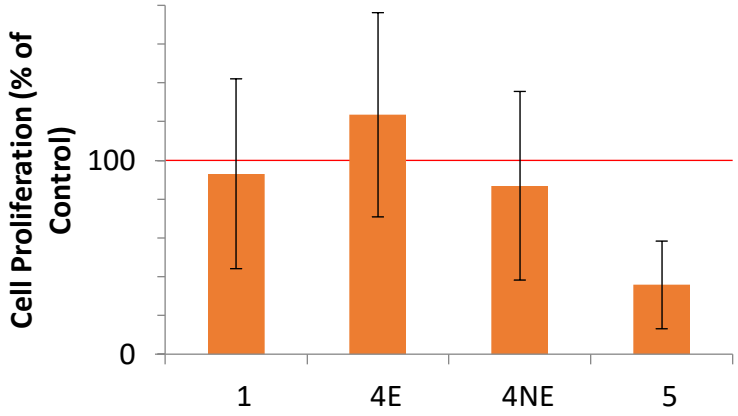

Figure 6.7 Cell viability after 72 hour material incubation with ARPE19 cells seeded at 30,000 per well.

6.4.2. Material Iteration 2

Given the difference in behaviour of the 350 MW PEG and the 750 MW PEG samples from the first study, it was desirable to learn more about these materials. Therefore, these materials were created which altered the molecular weight of the PEG, incorporating either a 350 MW PEG or a 750 MW PEG in the same ratio (25%) of functionalization on the PDMS backbone, crosslinking 4,200 g/mol PDMS, leaving 37%

and 25% residual azide groups respectively. While it would have been ideal to have used the same residual azide groups, the higher MW PEG material with only 37% crosslinking was too tacky to use in these applications. It is worth noting that Material 3 in Table 6.2 in analogous to Material 5 in Table 6.1, but using 750 MW PEG instead of 350 MW PEG. These materials were chosen to see if the small changes could improve the behaviour of the materials in the biological system.

6.4.2.a. Equilibrium Water Content and Swelling

The water content and alcohol swelling values were determined for these materials, as this is typically an important consideration for the drug loading and subsequent release. It can also influence protein adsorption. From Table 6.5, it is clear that the 750 MW PEG materials have a significantly greater water content than the 350 MW PEG materials or the control materials (no PEG). This is expected, as previous studies had indicated that the longer PEGs showed greater swelling, even when the overall PEG incorporation (as determined by wt%) was the same, likely owing to differences in the network structure. [Rambarran 2015] It is worth noting, however, that these materials still exhibit relatively low water contents when compared to silicone hydrogels that are used as contact lenses, likely owing to the much lower overall hydrophilic content. However, that does not negate them from being used as an implant in the anterior segment of the eye, particularly as silicones are soft and could be comfortable in the fornix of the eye for example. Both materials showed good swelling in alcohol, suggesting they would be able to readily take up drug from the loading mixtures.

Table 6.5 EWC and IPA swelling values (n=3).

Material	EWC (%)	IPA Swelling (%)
Sylgard Control	2.0 ± 1.2	9.2 ± 0.3
350 MW PEG	4.0 ± 2.0	85 ± 10
750 MW PEG	17.7 ± 5.0	113 ± 10

6.4.2.b. Protein Adsorption

The protein adsorption for these materials is shown in Figure 6.8. Similar to what was seen in previous studies [Rambarran 2015] and the first iteration of materials in this work, there is not a significant protein reduction for either type of protein with the 750 MW PEG material compared to the Sylgard control. This indicates that while the material has good swelling characteristics, this is not a determining factor in its protein adsorption characteristic. Given that the PEG chains are longer, it is possible that they are less mobile and thus cannot create the same water barrier on the surface of the material that the 350 MW PEG is capable of. Conversely, as expected, the 350 MW PEG materials showed a reduction in both protein adsorption levels relative to the control.

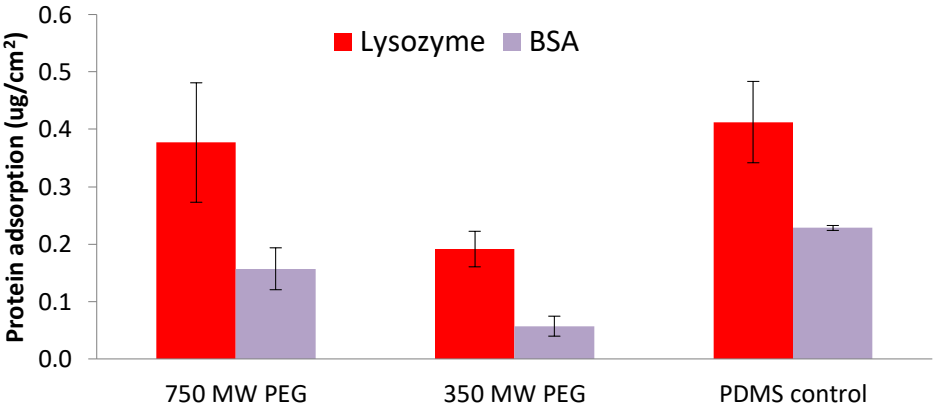

Figure 6.8 Protein adsorption for all materials with both HEL (red) and BSA (purple) soaked in a 1 mg/mL solution (n=4).

6.4.2.c. Drug Release

Given the relatively high water content of the 750 MW PEG materials, the drug release was explored for roscovitine at two different loadings. As seen in Figure 6.9, the materials release for a very long time, exceeding 4 months of release at either loading level. Both loading levels exhibit an initial burst over the first few days, which is expected given that the materials are already swollen when placed in the initial loading solutions. Furthermore, while we know only a small amount of roscovitine is needed to exhibit its therapeutic effect [Sangwan 2012], a burst may be beneficial, as it will result in tissue drug levels increasing more rapidly, and then the material can steadily replace the levels with its lower release rate. It is also clear that the amount of drug eluting can be tailored based on the loading, as there is almost double amounts of the drug being released from the materials loaded at the higher concentration of 2 mg/mL compared to the lower loading level of 1 mg/mL. The sustained release capabilities of this material are not surprising, as the high swelling in alcohol would have allowed for ample drug to enter the material during loading, and its relatively high water content would allow easy access for the drug to migrate out of the materials through the water channels and into the sink media. It should be noted that the control material was also loaded, but it did not show any release beyond the first time point, suggesting that it had poor loading, owing to its small swelling in alcohol, and poor release kinetics, owing to its low EWC.

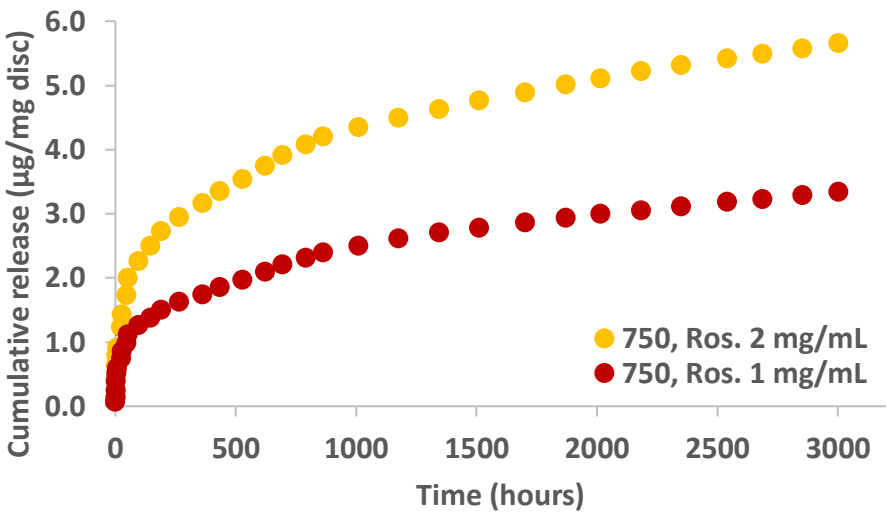

Figure 6.9 Roscovitine release from the 750 MW PEG materials at 2 mg/mL loading (yellow) and 1 mg/mL loading (red) (n=4).

6.4.3. Material Iteration 3

Given the excellent reduction in protein adsorption seen with the 350 MW PEG material, more work was done to explore which of the properties are critical to this behaviour and how they may influence the bulk properties and the drug release capabilities of the materials. Therefore, materials with various amounts of PEG substitutions and various crosslinking amounts were created.

6.4.3.a. Material Characterization

From Table 6.6, it is clear that the EWC of all materials is less than that seen with the 750 MW PEG from the second iteration. While there are some general trends within the EWC values, there is not a statistically significant difference along the material groups (i.e. the 20-25-30% PEG substitution or the 37-50-75% crosslinking). However, it does appear that increasing the amount of crosslinking in the material decreases its water content, which is expected as the network loses the ability to easily

swell. Interestingly, there does not seem to be much difference at all based on the PEG substitution levels. This is likely because the overall PEG content of the material (Table 6.3) is quite similar and the variation (20-30%) is relatively small. It is worth noting that the EWC of all of the materials is higher than the control, owing to their hydrophilic content relative to Sylgard. The same trends are apparent when looking at the IPA swelling. There is no difference between the materials with the varied amount of PEG substitution. However, there is a significant variation as the crosslinking amounts change, with the lowest crosslinking giving the greatest swelling. Since all of the levels are quite high, it is expected that there should be good drug loading for all materials.

Table 6.6 EWC and IPA swelling values (n=3).

Material	EWC (%)	IPA Swelling (%)
1	10.5 ± 3.0	103 ± 3.5
2	7.9 ± 4.0	81.7 ± 2.8
3	5.3 ± 1.6	67.3 ± 1.5
4	4.1 ± 1.4	78.0 ± 5.7
5	6.8 ± 2.2	82.9 ± 0.9
6 (Control)	2.0 ± 1.2	9.2 ± 0.3

6.4.3.b. Protein Adsorption

Protein adsorption was examined with the various 350 MW PEG materials. Material 3, which had the greatest amount of crosslinking, was not used for these studies, as the materials had a rough surface which could interfere with the results. Figure 6.10 shows lysozyme adsorption at both a high and low protein concentrations and Figure 6.11 shows albumin adsorption at both concentrations. Similar to the results seen in Iterations

1 and 2, there is a significant reduction in adsorption for all of the materials relative to the control. However, it does not appear that the crosslinking density or the PEG substitution levels, within the 20-30% range, impact the protein adsorption characteristics at either loading level or protein type. This suggests that the MW of the PEG used is the most influential factor for the protein adsorption. While it is difficult to determine without Material 3, as it had the fewest number of free azide groups, it is possible that these materials with greater azide substitution have reduced wettability, as the number of polar azide groups are reduced, and that this contributes to an increase in protein adsorption relative to less substituted materials. Also, while the lower protein loading generally appears to adsorb less protein, this difference is generally not statistically significant.

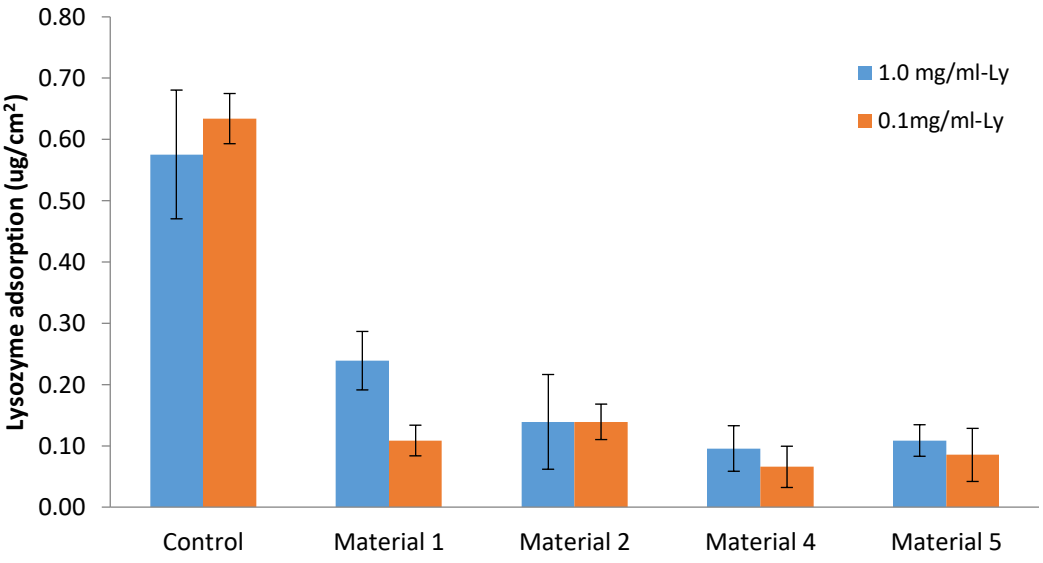

Figure 6.10 Lysozyme adsorption for 350 MW PEG materials soaked in a 1 mg/mL solution (blue) or a 0.1 mg/mL solution (orange) (n=4).

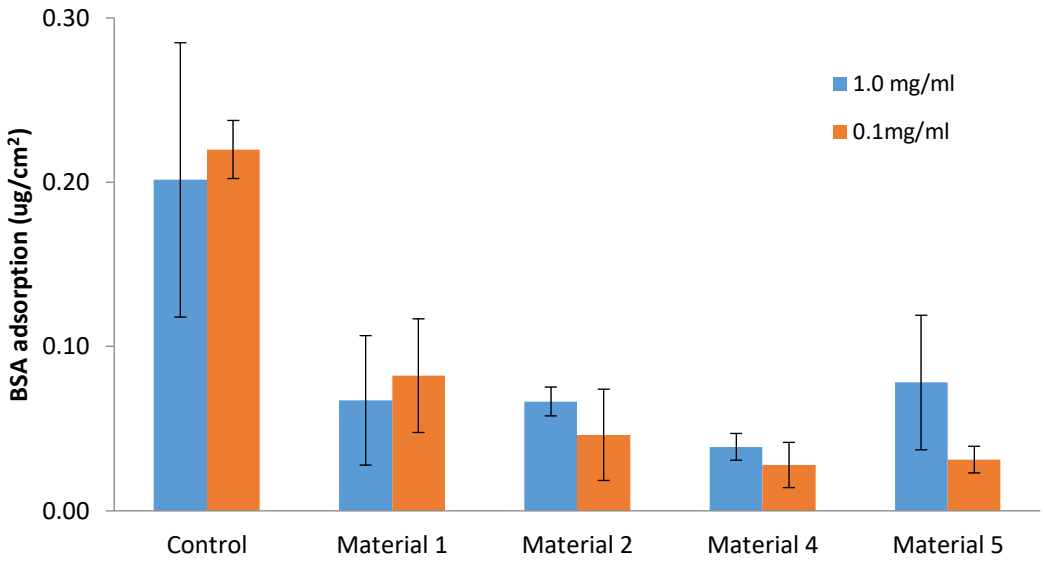

Figure 6.11 BSA adsorption for 350 MW PEG materials soaked in a 1 mg/mL solution (blue) or a 0.1 mg/mL solution (orange) (n=4).

6.4.3.c. Drug Release

Figure 6.12 shows the drug release from the various 350 MW PEG materials. Consistent with the swelling data, the variations with in the crosslinking has the greatest impact on the drug release. Specifically, the material with the lowest crosslinking (Material 1- blue), showed the greatest amount of drug release. The higher levels of crosslinking resulted in reduced release (Material 3- green). There was less variation between the materials with the varying amounts of PEG. It is worth noting that all of the materials displayed some burst release, lasting approximately 3 days, however substantial release continues for almost a month for all of the materials. Furthermore, many of the materials do not begin to show any plateau until nearly 2 months. These extended time frames are likely due to the moderate EWC exhibited by the materials. Again, it should be noted that the control material was also loaded, but it did not show any release beyond the

first time point, suggesting that it had poor loading, owing to its small swelling in alcohol, and poor release kinetics, owing to its low EWC.

Table 6.7 shows the total amount of drug loaded into each material. While there is a large amount of variability with the samples, likely owing in part to the differences in thickness of each material, the trends follow the swelling data, showing that both the higher crosslinked materials and the lower PEG substituted materials load less drug. However, these materials are also able to release more of their total drug loading, though all materials released nearly all of their payload. These release kinetics and loading properties suggest that an implant could be tailored based on its PEG content and crosslinking properties to deliver a certain amount of drug over a specific time interval, particularly as Iteration 2 demonstrated that the loading levels influence the total amount of drug released without substantially altering the timing of the burst and plateau periods.

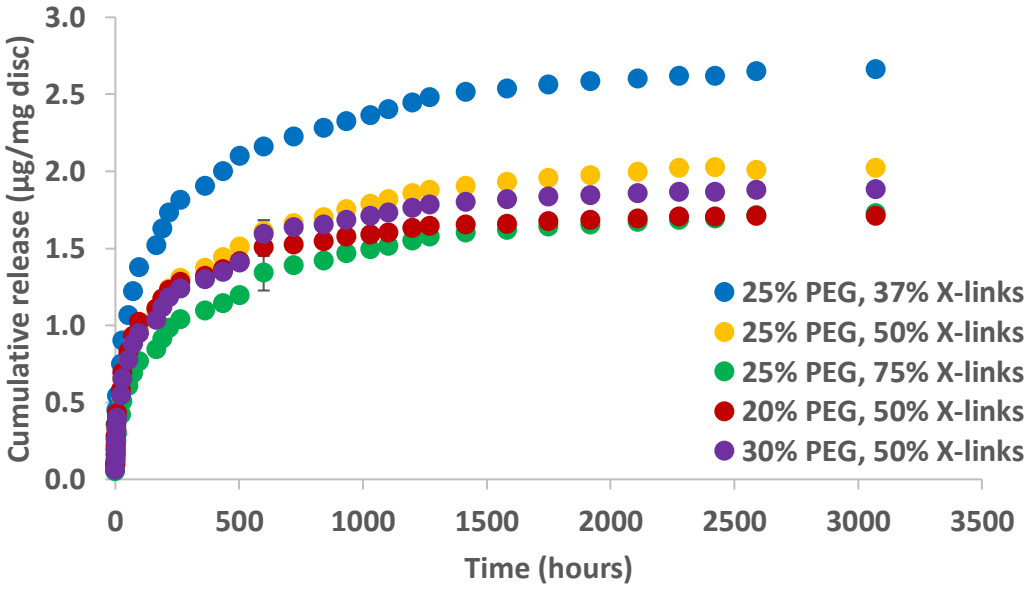

Figure 6.12 Roscovitine release from the various 350 MW PEG materials at 2 mg/mL loading (n=5).

Table 6.7 Drug amounts loaded (µg/mg) and total drug released (%) (n=5).

Material	Drug amounts loaded (µg/mg)	Total drug released (%)
1	2.76 ± 0.49	96.7 ± 0.2
2	2.16 ± 0.46	93.7 ± 0.3
3	1.81 ± 0.23	95.0 ± 0.1
4	1.75 ± 0.27	98.1 ± 0.4
5	2.04 ± 0.23	92.9 ± 0.5

6.5. Conclusions

Overall, materials which have good wettability, expressed through low contact angle measurements, showed significant reductions in both lysozyme and albumin protein adhesion and while maintaining cell viability. Based on the properties, it is clear that 350 MW PEG materials exhibit better anti-fouling properties than the 750 MW PEG, however both are capable of good drug release kinetics that can last up to 4 months. The amount of drug release can be tailored, with the strongest factors being the drug loading levels and the amount of crosslinking. This demonstrates that these silicone elastomers show great potential as improved ocular biomaterials, particularly for the possible treatment of retinoblastoma.

6.6. Acknowledgements

The authors would like to acknowledge the financial support of the C20/20 Ontario Research Fund. Thank you to Lina Liu and Myrto Korogiannaki who assisted with the radiolabeling studies and to Aakash Shaw who assisted with the swelling studies.

6.7. References

Brook MA. Silicon in Organic, Organometallic, and Polymer Chemistry; Wiley: New York, NY, 2000.

Chen H, Brook MA, Sheardown H. Biomaterials. 2004, 25:2273–2282.

Hsu KH, Gause S, Chauhan A. Journal of Drug Delivery Science and Technology. 2014, 24:123-35.

Jones L, Senchyna M, Glasier MA, Schickler J, Forbes I, Louie J, May C. Eye Contact Lens. 2003, 29: S75–S79, S83-S84, S192-S194.

Kingshott P, Thissen H, Griesser HJ. Biomaterials. 2002, 23:2043–2056.

Kim J, Conway A, Chauhan A. Biomaterials. 2008, 29:2259-69.

Lin G, Zhang X, Kumar SR, Mark JE. Molecular Crystals Liquid Crystals. 2010, 521:56–71.

Luensmann D, Heynen M, Liu L, Sheardown H, Jones L. Molecular Vision. 2010, 16:79-92.

Munier FL, Gaillard MC, Balmer A, Beck-Popovic M. Saudi J. Ophthalmol. 2013, 27,147–150.

Rambarran T, Gonzaga F, Brook MA. Macromolecules. 2012, 45:2276-2285.

Rambarran T, Gonzaga F, Brook MA, Lasowski F, Sheardown H. Polymer Chemistry. 2015, 53:1082-1093.

Sangwan M, McCurdy SR, Livne-Bar I, Ahmad M, Wrana JL, Chen D, Bremner R. Oncogene. 2012, 31:5019-28.

Vyner MC, Liu L, Sheardown HD, Amsden BG. Biomaterials. 2013, 34:9287–9294.

Wang J, Li X. J. Appl. Polym. Sci. 2010, 116:2749–2757.

7. Summary and Conclusions

This work set out to create an ocular drug delivery system that would be useful in the treatment of childhood conditions. Specifically, the goal was to deliver roscovitine and atropine primarily through non-invasive methods for periods of at least two weeks. It was envisioned that this could be accomplished with a transscleral delivery system. The hypothesis was that the hydrophilic/hydrophobic interface was critical to the creation of a sustained drug release system, so experiments were undertaken to determine which variables exerted the greatest impact on that interface and resulted in the best sustained drug release profiles.

The first aim of this work was to determine the ideal parameters of a silicone hydrogel material for drug delivery. Chapter 2 examined a silicone contact lens system for the delivery of both atropine and roscovitine. While this is presented as a contact lens, the material could be used anywhere on the ocular surface. Model lenses were created using DMA and TRIS or modified-TRIS materials, and their subsequent material properties were evaluated. As expected, increasing the hydrophilic character of the material, either through greater DMA incorporation or the use of a modified TRIS material, resulted in greater water content. However, these materials also exhibited a greater burst release profile. The drug type, the amount of drug loading and the method of loading influenced the burst amounts. This suggests that hydrophobic character of the drug determines where the drug locates in the material, confirming the hypothesis that these hydrophobic/hydrophilic interfaces are critical to sustained drug release. Importantly, it does not appear that low levels of drug loading influence the bulk

properties of the hydrogels, allowing the materials to retain their core features required for use as a contact lens (i.e. EWC, transparency). Despite these bursts, the 70:30 DMA/TRIS and 70/30 DMA/TRIS-OH lenses were generally able to deliver atropine and roscovitine over a two-week period, while both the 80/20 and 70/30 compositions were able to deliver roscovitine over a one-month period.

Chapter 3 extended this work, looking to covalently incorporate the drug into the silicone hydrogel lens material. The purpose of this was two-fold: first, by covalently incorporating the drug, there would be an additional step to release, and thus the bursts seen in the direct loading experiments previous could be more readily controlled. Second, given how silicone contact lenses are manufactured, the covalent incorporation would facilitate a greater drug retention in the final material. By incorporating a labile lactide tether, it was possible to control the rate of release based on the length of the tether, with a 10 unit tether releasing the drug faster than a 0 unit tether. Since the lactide tether is degraded through hydrolysis, the hydrophilic and hydrophobic content of the silicone hydrogels are critical to its release profile, as more swollen materials would allow quicker degradation. Furthermore, the second objective was confirmed, as greater amounts of drug remained in the material after an extraction period. The lactide tether was able to be incorporated without compromising any core lens properties.

The second aim of this work was to explore alternative materials whose properties would facilitate ocular drug delivery through a transscleral approach. To accomplish this, two materials were examined: amphiphilic molecules which self-assemble in water and PEG-PDMS materials. Chapter 4 examined the amphiphilic molecules, whose self-

assembly is driven by hydrophobic and hydrophilic interactions. Here, oleoylethanolamide and linoleoylethanolamide were combined to create new materials whose cubic phases, from which drug delivery is ideal, corresponded to physiological ocular conditions. It was clear that the drug loading amounts and the drug type influenced the phase formation of these materials, likely due to the localization of the drug within the material and its subsequent impact on the hydrophobic/hydrophilic interactions. Specifically, more hydrophilic drugs localize to the heads of the materials, putting them close to the interpenetrating water channels. While this can initially dehydrate the water channels, it allows for a more constant release profile, as the drugs are more limited by diffusion out of the material than diffusion into the water channels themselves. Conversely, the more hydrophobic drugs localize at the tail, resulting in minimal bursts and slow release profiles, as the drugs must diffuse into the water channels and then out of the materials, though the loading levels seem to influence this, likely as greater drug loading results in greater disruption to the self-assembly. For atropine, roscovitine and R547, these materials were able to sustain release for at least a month.

Chapter 5 introduces a new method of synthesizing PEG-PDMS materials. While silicones have been well used as biomaterials, their hydrophobic character limits their usefulness in some applications, particularly for drug delivery. While previous work has shown that PEG incorporation can improve this, utilizing a metal-free synthesis which may be beneficial to improve biocompatibility. By improving the hydrophilic character of the elastomer, drug delivery becomes feasible. Furthermore, as shown in this study, the greater hydrophilic character is able to reduce protein adsorption, as this is known to also

influence both the materials performance and drug delivery properties. Specifically, materials incorporating shorter length PEG showed the greatest protein adsorption.

Building off of these observations, iterations on the material composition were completed to better understand how different material properties, specifically PEG molecular weight, the extent of PEG substitution and the extent of crosslinking, would influence the material properties and drug release capabilities in Chapter 6. While these studies confirmed that higher MW PEG do not exhibit the reduce protein fouling, they do show excellent swelling and drug release profiles. This is due to the increased hydrophilic content in the material, which allows for greater amounts of drug to be loaded into the material and subsequently released over numerous months. The lower MW PEG materials show significantly reduced fouling, and also facilitate extended drug release. This release can be tailored based on the amount of crosslinking in the material, where more highly crosslinked materials release less drug. This is characteristic of a tighter network, as there are more barriers to diffusion. While varying the amount of PEG substitution did not seem to affect the drug release substantially, exploring a larger range of substitutions (i.e. 15-40%) may have had a greater impact, as this would likely influence the domain formation within the material and could alter where the drug localizes once loaded.

Overall, the various approaches to understand the impact of the hydrophilic/hydrophobic interface on drug delivery has yielded three feasible drug delivery systems for non-invasive applications in pediatric populations. While none of these materials are commercial-ready at the moment, further work could help determine which ones would be easiest and best received to clinically implement. Specifically, these

studies have yielded various ways to manipulate the materials to produce a desired drug delivery profile and amount. These systems could be modeled to fit a clinical dosing requirement using these different levers. While clinical development of a chemo-preventative therapy for retinoblastoma may be difficult due to ethical considerations, this work could be utilized in other areas where roscovitine is used as a chemotherapeutic agent. This includes glioblastoma, whose solid tumours are incurable with high relapse rates and definite mortality. [Pandey 2019] Much of this treatment is multi-targeted, [Sestito 2018] and the incorporation of this targeted, slow-release therapy could be beneficial. Furthermore, this work has reinforced that the nature of the drug itself plays a large role in how it interacts with the material, particularly due to the interaction of the drug at the hydrophilic/hydrophobic interfaces. Therefore, these delivery systems must be developed as drug-device combinations, and platform technologies must acknowledge that additional work is required to fit new therapeutics into their systems. However, the greater the understanding of the material properties and interface interactions, the easier these outcomes are to predict and test, and the faster any of these systems could move to market.

References:

Pandey V, Ranjan N, Narne P, Prakash Babu P. Roscovitine effectively enhances antitumor activity of temozolomide in vitro and in vivo mediated by increased autophagy and Caspase-3 dependent apoptosis. Nature Scientific Reports. 2019;9:5012.

Sestito S, Runfola M, Tonelli M, Ghiellini G, Rapposelli S. New Multitarget Approaches in the War Against Glioblastoma: A Mini-Perspective. Frontiers in Pharmacology. 2018;9:874.

8. Appendix 1: Partial Supporting Information for Chapter 4: Amphiphilic Elastomers from Metal-Free, Click Crosslinking of PEG-Grafted Silicone Surfactants

8.1. Experimental Synthesis

8.1.1. α,ω-Silicone propiolates

Propiolate-terminated disiloxane was synthesized from 1,3-bis(hydroxybutyl)tetramethyldisiloxane and propiolic acid. **2** (MW of 3,600 g·mol^{-1}), **3** (MW 7,800 g·mol^{-1}) and **4** (MW of 16,200 g·mol^{-1}, MW determined by ^{1}H NMR), respectively. **2**: ^{1}H NMR ($CDCl_3$, 200 MHz, δ): 0.07 (s, 273H, SiC*H*$_3$); 0.56 (t, 4H, *J*=8.3 Hz, SiC*H*$_2$CH$_2$CH$_2$CH$_2$); 1.37 (m, 4H, SiCH$_2$C*H*$_2$CH$_2$CH$_2$); 1.68 (m, 4H, SiCH$_2$CH$_2$C*H*$_2$CH$_2$); 2.86 (s, 2H, C≡C*H*); 4.20 (t, 4H, *J*=6.5 Hz, SiCH$_2$CH$_2$CH$_2$C*H*$_2$). **3**: ^{1}H NMR ($CDCl_3$, 200 MHz, δ): 0.07 (s, 605H, SiC*H*$_3$); 0.56 (t, 4H, *J*=8.3 Hz, SiC*H*$_2$CH$_2$CH$_2$CH$_2$); 1.37 (m, 4H, SiCH$_2$C*H*$_2$CH$_2$CH$_2$); 1.68 (m, 4H, SiCH$_2$CH$_2$C*H*$_2$CH$_2$); 2.86 (s, 2H, C≡C*H*); 4.20 (t, 4H, *J*=6.5 Hz, SiCH$_2$CH$_2$CH$_2$C*H*$_2$). **4**: ^{1}H NMR ($CDCl_3$, 200 MHz, δ): 0.07 (s, 1295H, SiC*H*$_3$); 0.56 (t, 4H, *J*=8.3 Hz, SiC*H*$_2$CH$_2$CH$_2$CH$_2$); 1.37 (m, 4H, SiCH$_2$C*H*$_2$CH$_2$CH$_2$); 1.68 (m, 4H, SiCH$_2$CH$_2$C*H*$_2$CH$_2$); 2.86 (s, 2H, C≡C*H*); 4.20 (t, 4H, *J*=6.5 Hz, SiCH$_2$CH$_2$CH$_2$C*H*$_2$).

8.1.2. PEG-monopropiolates

PEG mono-propiolate **5** (MW of 406 g·mol^{-1}, determined by ^{1}H NMR), **6** (MW of 813 g·mol^{-1}), and **7** (MW of 2060 g·mol^{-1})(MW determined by ^{1}H NMR) were prepared from monomethoxy poly(ethylene oxide) according to a previously

described procedure.[i] **5**: ^{1}H NMR ($CDCl_3$, 600 MHz): δ 4.34 (t, 2 H's, -COOC**H$_2$**-, *J* = 6.0 Hz), 3.74 to 3.55 (m, ~ 29 H's, -OC**H$_2$**C**H$_2$**O-), 3.37 (s, 3 H's, OCH_3), 2.89 (s, broad, 1H, **H**CCCOO). **6**: ^{1}H NMR ($CDCl_3$, 600 MHz): δ 4.34 (t, 2 H's, -COOC**H$_2$**-, *J* = 6.0 Hz), 3.74 to 3.55 (m, ~ 66 H's, -OC**H$_2$**C**H$_2$**O-), 3.37 (s, 3 H's, OCH_3), 2.89 (s, broad, 1H, **H**CCCOO). **7**: ^{1}H NMR ($CDCl_3$, 600 MHz): δ 4.34 (t, 2 H's, -COOC**H$_2$**-, *J* = 6.0 Hz), 3.74 to 3.55 (m, ~ 180 H's, -OC**H$_2$**C**H$_2$**O-), 3.37 (s, 3 H's, OCH_3), 2.89 (s, broad, 1H, **H**CCCOO).

8.1.3. Medium molecular weight 6 PEG-modified (PEG-800 g·mol^{-1}) functional silicones *11*, *12* and *13*

1 (1.07 g, 1.99 mmol of azide) and **6** (0.41 g, 0.50 mmol of alkyne, 0.25 eq.) were homogenized with 2 mL of chloroform to produce **11** (1.48 g, quant.).

1 (0.87 g, 1.62 mmol of azide) and **6** (0.68 g, 0.84 mmol of alkyne, ~0.50 eq.) were reacted in 5 mL of toluene to yield **12** (1.55 g, quant.).

1 (1.48 g, 3.00 mmol of azide) and **6** (1.83 g, 2.25 mmol of alkyne, ~0.75 eq.) were reacted in 5 mL of toluene to yield **13** (3.31 g, quant.; reaction required additional 12 h).

11 *(Major isomer 1,4 (A ~ 80%), Minor isomer 1,5 (B ~20%):* ^{1}H NMR ($CDCl_3$, 600 MHz, δ): 0.05 to 0.09 (s, 31.9H, SiC*H*$_3$, *11*), 0.47-0.51 (m, 0.5H, SiC*H*$_2$CH$_2$CH$_2$triazole, *1*), 0.53-0.59 (m, 1.5H, C*H*$_2$CH$_2$CH$_2$N$_3$, *1'*), 1.61-1.67 (m, 1.5H, SiCH$_2$C*H*$_2$CH$_2$N$_3$, *13*), 1.91-1.99 (m, 0.5H, SiCH$_2$C*H*$_2$CH$_2$triazole, *2*), 3.22 (t, *J*=6.0 Hz, 1.5H, C*H*$_2$N$_3$, *14*), 3.37 (s, 0.75H, -OCH_3, *9*), 3.55 (t, *J*=6.0 Hz, 1H, C*H*$_2$$OCH_3$, *8*), 3.64-3.65 (m, ~15H, -OC*H*$_2$C*H*$_2$O-, *10*), 3.68 (m, 0.5H,

C*H*$_2$CH$_2$OCH$_3$, *7*), 3.79-3.84 (m, 0.5H, -COOCH$_2$C*H*$_2$, *6*), 4.35,4.66 (m, 0.5H total, SiCH$_2$CH$_2$C*H*$_2$triazole, *3A, 3B*), 4.45, 4.48 (0.5H total, -COOC*H*$_2$ -, *5A, 5B*), 8.07-8.15 (multiple singlets, 0.25H, *H*CCCOO,*4A, 4B*).

12 *(Major isomer 1,4 (A ~ 80%), Minor isomer 1,5 (B ~20%):* ^{1}H NMR (CDCl$_3$, 600 MHz, δ): 0.05 to 0.09 (s, 31.9H, SiC*H*$_3$, *11*), 0.47-0.51 (m, 1H, SiC*H*$_2$CH$_2$CH$_2$triazole, *1*), 0.53-0.59 (m, 1H, C*H*$_2$CH$_2$CH$_2$N$_3$, *1'*), 1.61-1.67 (m, 1H, SiCH$_2$C*H*$_2$CH$_2$N$_3$, *13*), 1.91-1.99 (m, 1H, SiCH$_2$C*H*$_2$CH$_2$triazole, *2*), 3.22 (t , *J*=6.0 Hz, 1H, C*H*$_2$N$_3$, *14*), 3.37 (s, 1.5H, -OCH$_3$, *9*), 3.55 (t, *J*=6.0 Hz, 1H, C*H*$_2$OCH$_3$, *8*), 3.64-3.65 (m, ~29H, -OC*H*$_2$C*H*$_2$O-, *10*), 3.68 (m, 1H, C*H*$_2$CH$_2$OCH$_3$, *7*), 3.79-3.84 (m, 1H, -COOCH$_2$C*H*$_2$, *6*), 4.35,4.66 (m, 1H total, SiCH$_2$CH$_2$C*H*$_2$triazole, *3A, 3B*), 4.45, 4.48 (1H total, -COOC*H*$_2$-, *5A, 5B*), 8.07-8.15 (multiple singlets, 0.5H, *H*CCCOO,*4A, 4B*).

13 *(Major isomer 1,4 (A ~ 80%), Minor isomer 1,5 (B ~20%):* ^{1}H NMR (CDCl$_3$, 600 MHz, δ): 0.05 to 0.09 (s, 31.9H, SiC*H*$_3$, *11*), 0.47-0.51 (m, 1.5H, SiC*H*$_2$CH$_2$CH$_2$triazole, *1*), 0.53-0.59 (m, 0.5H, C*H*$_2$CH$_2$CH$_2$N$_3$, *1'*), 1.61-1.67 (m, 0.5H, SiCH$_2$C*H*$_2$CH$_2$N$_3$, *13*), 1.91-1.99 (m, 1.5H, SiCH$_2$C*H*$_2$CH$_2$triazole, *2*), 3.22 (t, *J*=6.0 Hz, 0.5H, C*H*$_2$N$_3$, *14*), 3.37 (s, 2.25H, -OCH$_3$, *9*), 3.55 (t, *J*=6.0 Hz, 1.5H, C*H*$_2$OCH$_3$, *8*), 3.64-3.65 (m, ~34H, -OC*H*$_2$C*H*$_2$O-, *10*), 3.68 (m, 1.5H, C*H*$_2$CH$_2$OCH$_3$, *7*), 3.79-3.84 (m, 1.5H, -COOCH$_2$C*H*$_2$, *6*), 4.35,4.66 (m, 1.5H total, SiCH$_2$CH$_2$C*H*$_2$triazole, *3A, 3B*), 4.45, 4.48 (1.5H total, -COOC*H*$_2$ -, *5A, 5B*), 8.07-8.15 (multiple singlets, 0.75H, *H*CCCOO,*4A, 4B*).

The same procedure was used to make reactive functional silicone **14** from higher molecular weight PEG **7**, PEG 2060 g·mol^{-1}) functional silicones polymers **1** (1.21 g, 2.44 mmol) and **7** (1.27 g, 0.62 mmol, 0.25 eq.) yielding **14** (2.48 g, quant.).

14 *(Major isomer 1,4 (A ~ 80%), Minor isomer 1,5 (B ~20%):* ^{1}H NMR ($CDCl_3$, 600 MHz, δ): 0.05 to 0.09 (s, 31.9H, SiC*H*$_3$, *11*), 0.47-0.51 (m, 0.5H, SiC*H*$_2$CH$_2$CH$_2$triazole, *1*), 0.53-0.59 (m, 1.5H, C*H*$_2$CH$_2$CH$_2$N$_3$, *1'*), 1.61-1.67 (m, 1.5H, SiCH$_2$C*H*$_2$CH$_2$N$_3$, *13*), 1.91-1.99 (m, 0.5H, SiCH$_2$C*H*$_2$CH$_2$triazole, *2*), 3.22 (t, *J*=6.0 Hz, 1.5H, C*H*$_2$N$_3$, *14*), 3.37 (s, 0.75H, -OCH$_3$, *9*), 3.55 (t, *J*=6.0 Hz, 1H, C*H*$_2$OCH$_3$, *8*), 3.64-3.65 (m, ~43H, -OC*H*$_2$C*H*$_2$O-, *10*), 3.68 (m, 0.5H, C*H*$_2$CH$_2$OCH$_3$, *7*), 3.79-3.84 (m, 0.5H, -COOCH$_2$C*H*$_2$, *6*), 4.35,4.66 (m, 0.5H total, SiCH$_2$CH$_2$C*H*$_2$triazole, *3A*, *3B*), 4.45, 4.48 (0.5H total, -COOC*H*$_2$ -, *5A*, *5B*), 8.07-8.15 (multiple singlets, 0.25H, *H*CCCOO,*4A*, *4B*).

8.1.4. Synthesis of Elastomers *15*, *16*, *17*: PEG *5* (400 g·mol^{-1}) functional networks crosslinked with PDMS *3* (7,800 g·mol^{-1})

The materials were characterized by; Shore OO hardness, IR, rheology; **15** and **16** were additionally characterized by water contact angle and swellability in water.

8.1.5. Synthesis of Elastomers *18*, *19*, *20*: PEG 5 (400g·mol^{-1}) functional networks crosslinked with PDMS 4 (16,200 g·mol^{-1})

18: **8** (0.48 g, 0.17 mmol of alkynyl PEG, 0.59 mmol of azido groups) and **4** (4.76 g, 0.59 mmol of alkyne) were reacted (6 mL of toluene and 3 mL $CHCl_3$) to produce elastomer **18** (5.24 g).

19: **9** (0.74 g, 0.49 mmol of alkynyl PEG, 0.51 mmol of azido groups) and **4** (4.00 g, 0.49 mmol of alkyne) were reacted (5 mL of toluene and 5 mL $CHCl_3$) to produce elastomer **19** (4.74 g).

20: **10** (1.72 g, 1.52 mmol of alkynyl PEG, 0.53 mmol of azido groups) and **4** (4.26 g, 0.53 mmol of alkyne) were reacted (5 mL of toluene and 5 mL $CHCl_3$) to produce elastomer **20** (5.98 g).

The materials were characterized by Shore OO hardness, IR, rheology, water contact angle and swellability in water.

8.1.6. Synthesis of PEG 6 (800 $g \cdot mol^{-1}$)-based functional networks

The polymeric/solvent mixtures were sealed, and allowed to pre-cure with stirring at 60 °C for 2 h prior to being cured at 70 °C for 24 h, and 90 °C for 1 h.

Crosslinked with PDMS* 3 *(7800 $g \cdot mol^{-1}$)

21: **11** (0.93 g, 0.31 mmol alkynyl PEG, 0.96 mmol azido groups) and **3** (3.76 g, 0.96 mmol alkynyl groups) were reacted (3 mL of toluene and 5 mL $CHCl_3$) to produce **21** (4.69 g).

22: **12** (1.55 g, 0.84 mmol alkynyl PEG, 0.78 mmol azido groups) and **3** (3.13 g, 0.80 mmol alkynyl groups) were reacted (10 mL of toluene) to produce **22** (4.68 g).

Crosslinked with PDMS 4 (16200 $g \cdot mol^{-1}$)

23: **11** (0.51 g, 0.17 mmol alkynyl PEG, 0.51 mmol azido groups) and **4** (3.94 g, 0.51 mmol alkynyl groups) were reacted (10 mL of toluene and 2 mL $CHCl_3$) to produce **23** (4.45 g).

24: **12** (0.85 g, 0.44 mmol alkynyl PEG, 0.47 mmol azido groups) and **4** (3.52 g, 0.47 mmol alkynyl groups) were reacted (6 mL of toluene) to produce **24** (4.37 g). The materials were characterized by Shore OO hardness, IR, water contact angle and swellability in water.

8.1.7. Synthesis of Elastomers *25*, *26*, *27*: PEG *5* (400 g·mol^{-1})- functional networks crosslinked with PDMS *2* (3600 g·mol^{-1})

28: **11** (2.12 g, 0.76 mmol alkynyl PEG, 2.27 mmol azido groups) and **2** (2.08 g, 1.15 mmol) were mixed (1 mL toluene + 3 mL $CHCl_3$) to produce elastomer **28** (4.20 g).

29: **14** (2.48 g, 0.62 mmol of alkynyl PEG, 1.63 mmol of azido groups) and **2** (1.71 g, 0.83 mmol of alkyne) were mixed (6 mL toluene + 5 mL $CHCl_3$) to produce **29**, 4.19 g).

The materials were characterized by Shore OO hardness, IR, rheology, water contact angle and swellability in water.

8.1.8. Example Elastomer with α,ω- PEG

8.1.9. Synthesis of α,ω-PEG propiolates, 30

The synthetic process for dipropiolate terminated poly(ethylene glycol) was modified from Gonzaga et al.[i] Propiolic acid (14.52 g, 207 mmol), toluene (25 mL), and a catalytic amount of *p*-toluenesulfonic acid (0.05 g, 2.6 mmol) were successively added in a round-bottomed flask containing poly(ethylene glycol) (aver. mol wt: 370, 10.27 g, 55 mmol of -OH). The flask, equipped with a Dean Stark apparatus, was heated with azeotropic removal of water. Completion of the

reaction was monitored by ^{1}H NMR spectroscopy (about 40 h). The solution was then cooled to room temperature, and washed three times with an aqueous potassium carbonate solution (50 mL). The PEG formed a separate phase and the crude brown product was directly loaded onto a chromatography column packed with silica gel. Elution started with pure dichloromethane, then increasing amounts of methanol were added to the eluent (up to 5% v:v). The fractions containing the propiolate ester were combined, evaporated under reduced pressure to afford pure propiolate-terminated poly(ethylene oxide) (7.91 g, 60% yield) as a yellow oil.

^{1}H NMR ($CDCl_3$, 600 MHz): δ = 4.23 (t, J = 6.0 Hz, 4H; COOC**H**$_2$-), 3.63 (t, J = 6.0 Hz, 4H; COOCH$_2$C**H**$_2$-), 3.57 to 3.54 (m, ≈ 25H; -C**H**$_2$C**H**$_2$-), 3.05 to 3.02 (s, broad, 2H; **H**CCCOO).

8.1.10. Elastomer with α□ω-Silicone and α,ω-PEG propiolates, 31

Compounds **1** (1.02 g, 2.00 mmol azide), **30** (0.24 g, 1.01 mmol alkyne) and **2** (0.73 g, 0.36 mmol alkyne) were homogenized with 1000 μL of $CHCl_3$ and 400 μL of toluene in a glass scintillation vial and placed to cure in a 60 °C oven. After 2 h, the polymers were mixed again and left to cure for another 18 h. At this time, the polymers had cured into a firm, slightly opaque yellow elastomer; the temperature was increased to 90 °C for an additional 12 h to ensure complete crosslinking. The elastomer was cooled to room temperature and removed from the curing vessel and ¼ inch diameter circular disks were punched for contact angle measurements. Water contact angles were measured in triplicate for the elastomer from air (62±2°) and after soaking in deionized water for 24 h (60±2°).

8.1.11. Protein Adsorption

The adsorption on silicone elastomers of hen egg lysozyme (HEL; Sigma-Aldrich, St. Louis, MO) and bovine serum albumin (BSA; Sigma-Aldrich), respectively, were investigated by radiolabeling. HEL and BSA were conjugated to I^{125} using the iodine monochloride method, as previously described.[ii,iii] Briefly, radiolabeled protein solution was passed through two columns packed with AG 1-X4 (Bio-Rad, Hercules, CA) to remove unbound I^{125}; the columns were subsequently rinsed with phosphate buffered saline (PBS) to ensure all labeled protein was removed. Free iodide was determined using trichloroacetic acid precipitation, and was found to be less than 1.1% for both proteins. The materials, having a surface area of 0.633 cm^2, were then incubated for 3 h in a 1 mg/mL solution of either HEL or BSA, which were comprised of 10% radiolabeled protein and 90% unlabeled protein. They were subsequently rinsed in PBS three times, for 5 minutes each time, and counted using an automated gamma counter (1470 Wallac Wizard; PerkinElmer, Woodbridge, ON). Adsorption of protein was measured using 4 discs for each protein solution. The radioactivity on each material was converted into micrograms of protein per cm^2 for quantification.

8.2. Additional Results

8.2.1. Atomic Force Microscopy

Increased surface roughness as a result of water sorption to the surface of the silicone elastomers can influence observed contact angle values (rough surfaces tend to have higher contact angles).[iv] The elastomers/gels were soaked in water for

several days, and some did have appreciable water uptake, which could contribute to the to the higher than anticipated contact angles. Even soaking normal silicone elastomers in water can lead to enhanced roughness.[v] The elastomers described herein, synthesized from fluid polymer precursors, had smooth surfaces and low surface roughness in air. However, after swelling in water, atomic force microscopy demonstrated small increases in surface roughness, but not enough to significantly affect the contact angle. Elastomer **22** had a surface roughness (R_q) = 6.7 and elastomer **25** R_q = 1.9 dry; after soaking in water the R_q values increased to 12.5 and 15.1, respectively. The water contact angles for dry **22** and **25** changed from 78±4° and 34±3° at 300 s, respectively, while the water soaked samples exhibited values of 76±6° and 50 ±2°.

Compound **25** is of particular interest because of its highly responsive nature. The compound was made by reacting 25% of the available azido groups with PEG **5** (350 g/mol) and crosslinking with the shorter PDMS **2** (3,600 g/mol), leaving residual azide groups. The change in contact angle over time was rapid and greater than any of the other compounds prepared, both from a dry and wet state. This result was initially counterintuitive because many of the other materials, **22** for example, have more PEG, both with respect to graft density and PEG chain length and were expected to be more highly wettability. However, we and others have observed analogous outcomes for PEG-containing networks: the key is PEG chain length.

8.2.2. Rheology

Generally, G' decreased with increasing alkynyl-PDMS chain length. As anticipated, a more flexible network resulted, reducing the stored elastic energy: e.g., **15** with the PDMS length ~8,000 g·mol^{-1} had a G' of 94 kPa compared to elastomer **18** with the PDMS length ~16,000 g·mol^{-1} whose G' was 54 kPa at 0.1 Hz.

When increasing the PEG length for elastomers/gels created with the same crosslink density (i.e., 25, 50 or 75% of the azido groups reacted) while maintaining the same alkynyl-PDMS linker length, an increase in the storage modulus was observed: e.g., going from **15** made with ~400 g·mol^{-1} PEG to **21** made with ~800 g·mol^{-1} PEG, the modulus increased from 94 kPa to 115 kPa, suggesting the PEG interactions (crystallization) adds to the elastic energy in the material.

A B

Figure 8.1 Photographs of PEG/silicone elastomers produced using the Huisgen reaction: A: 22 (left), B: 23 (right)

8.2.1. Aqueous Extractables

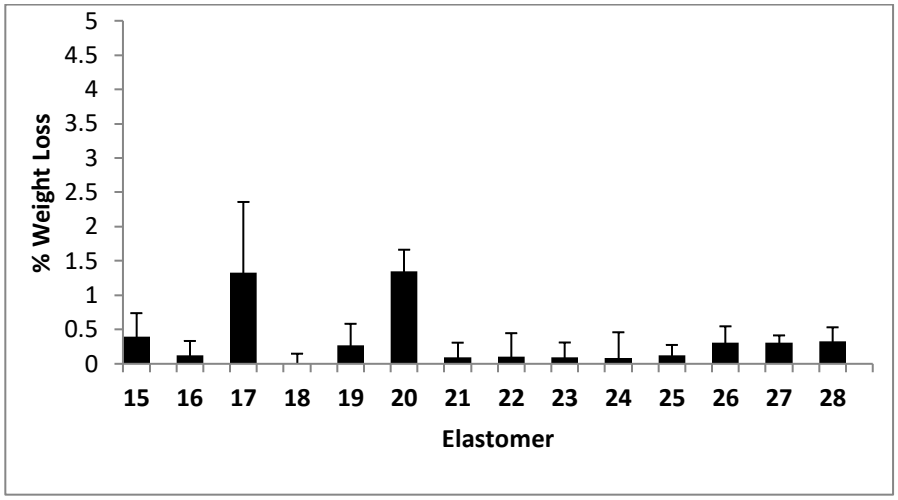

Figure 8.2 Aqueous extractables from the elastomers.

8.2.1. Organic Extractables

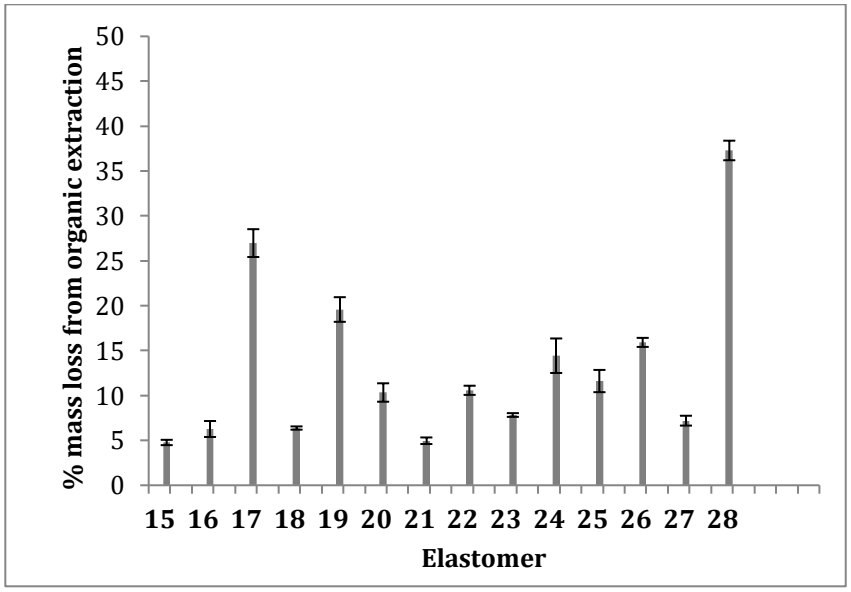

Figure 8.3 Organic extractables from the elastomers.

8.2.2. Water Uptake

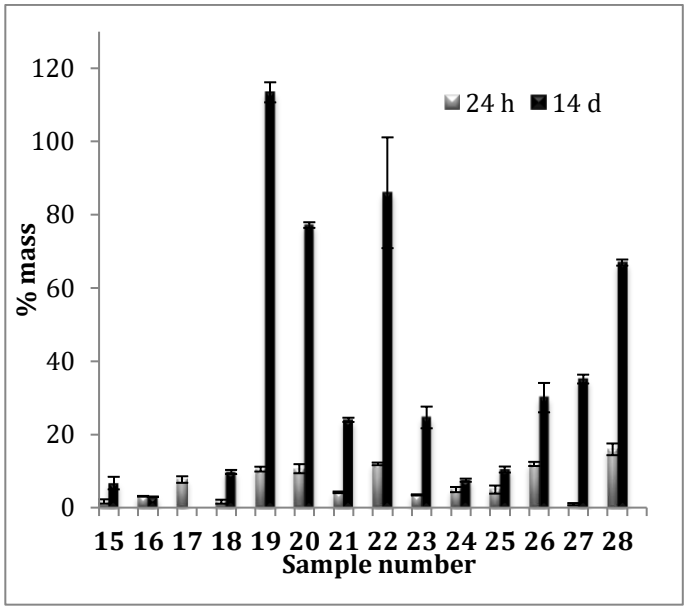

Figure 8.4 Water uptake (wt%) at 24 hours and 14 days

8.2.3. AFM of Select Elastomers

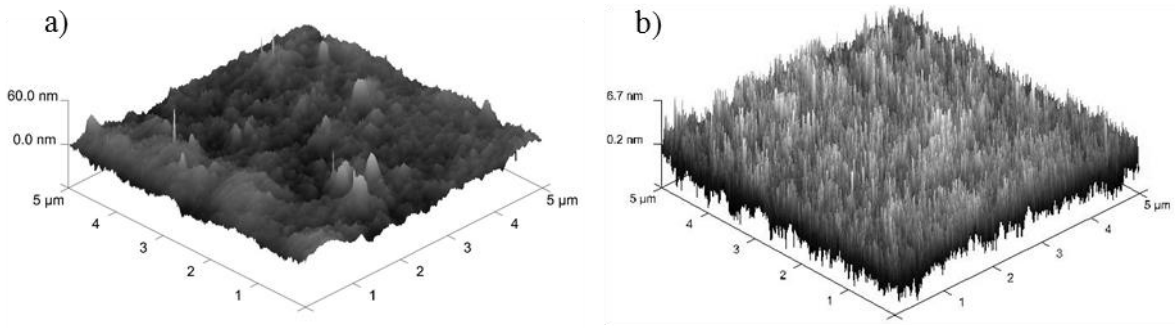

Figure 8.5 AFM of rubbers 22 (a) R_q = 6.7 and 25 (b) R_q = 1.9

8.2.4. Rheological Data

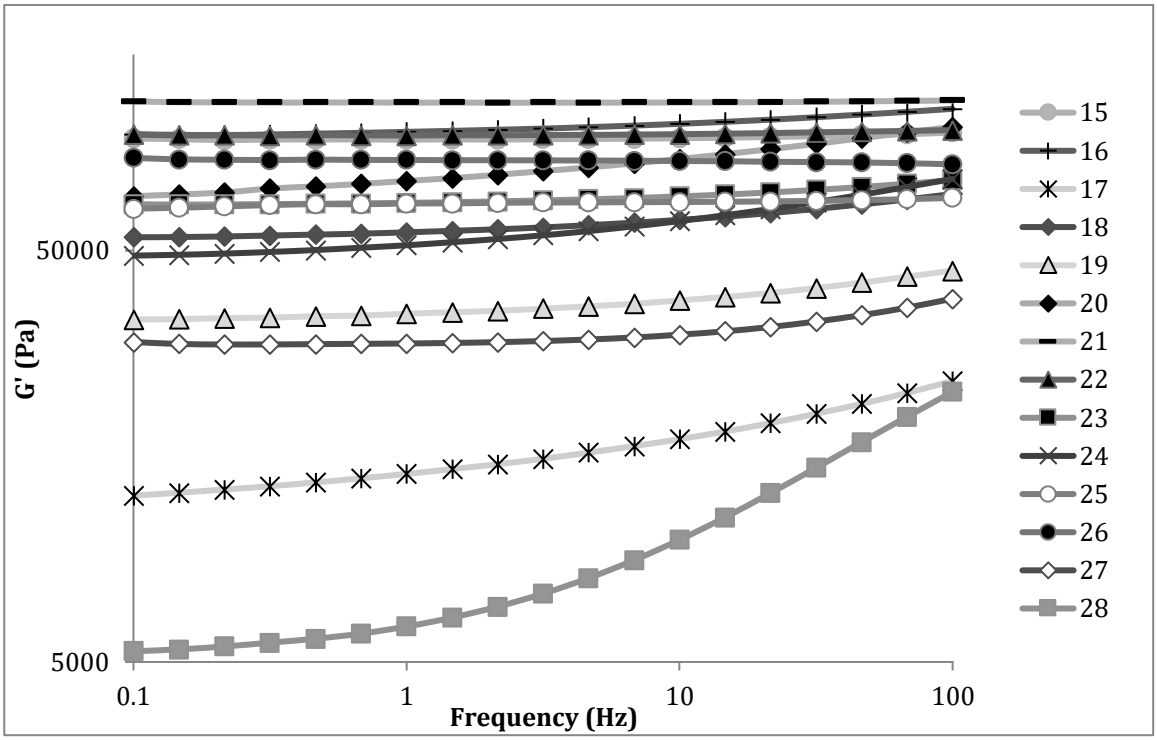

Figure 8.6 Storage modulus of elastomers/gels

[i] F. Gonzaga, J. B. Grande, M. A. Brook, *Chem. Eur. J.*, **2012**, 18, 1536-1541.
[ii] D. Luensmann, M. Heynen, L. Liu, H. Sheardown, L. Jones, *Molecular Vision*, **2010**, 16, 79-92.
[iii] M. C. Vyner, L. Liu, H. D. Sheardown, B. G. Amsden, *Biomaterials*, **2013**, 34, 9287–9294.
[iv] W. Fortuniak, U. Mizerska, J. Chojnowski, T. Basinska, S. Slomkowski, M. M. Chehimi, A. Konopacka, K. Turecka, W. Werel, *J. Inorg. Organomet. Polym*. **2011**, 21, 576−589.
[v] A. Beigbeder, C. Labruyere, P. Viville, M. E. Pettitt, M. E. Callow, J. A. Callow, L. Bonnaud, R. Lazzaroni, P. Dubois, *J. Adhes. Sci. Technol.* **2011,** 25, 1689-1700.